ILLUMINATING THE HETEROTROPIC COMMUNICATION OF THE PAIR-WISE INTERACTIONS IN PHOSPHOFRUCTOKINASE FROM BACILLUS STEAROTHERMOPHILUS

A Dissertation

By

STEPHANIE ANN PEREZ

Submitted to the Office of Graduate Studies of
Texas A&M University
In partial fulfillment of the requirements for the degree of

DOCTOR OF PHILOSOPHY

Approved by:

Chair of Committee,	Gregory Reinhart
Committee Members,	Nick Pace
	Dorothy Shippen
	Tatyana Igumenova
Head of Department,	Gregory Reinhart

December 2012

Major Subject: Biochemistry

ABSTRACT

The number of allosteric sites and active sites in phosphofructokinase from *Bacillus stearothermophilus* create an intricate network of communication within the enzyme. With thermodynamic linkage analysis, the overall allosteric communication can be quantified. This value, however, represents an average contribution for all the interactions involved. The recent development of a hybrid strategy has allowed for the quantification of single interactions, both heterotropic and homotropic. Focusing on the heterotropic interactions whose inhibition is entropy-driven, residues and regions within the enzyme can now be identified to further characterize each specific interaction using the hybrid strategy. Among the many components of entropy, the hybrid strategy has now allowed for the strategic placement of a reporter of side chain dynamics to identify conformational differences between the four ligand bound enzyme species of a single heterotropic interaction. In this study, a combination of these approaches was used in the methodology including constructing hybrids to isolate a single heterotropic interaction along with single tryptophan reporter. Site directed mutagenesis combined with the hybrid strategy was also implemented to directly assess the role of a single residue in the communication path of a single interaction. The region surrounding the allosteric site with the nearest active site has been implicated to be significant in transmitting the allosteric signal. In addition two single residues, T158 and D59, within this region have been identified to potentially contribute to the inhibition of this same interaction. An additional residue, G184, located outside this local region has also been identified as possibly having a significant role in the transmission of the inhibitory signal

of a unique heterotropic interaction. The implications of this study have led to the initial identification of residues involved in the 22Å route of allosteric communication of a single active site and allosteric site. This allosteric communication occurs to allow the enzyme to compensate for the binding of both ligands. With the location of these residues implicated to be involved in the communication of this isolated interaction, this compensation is not contained within a confined region but is however felt throughout the single subunit.

DEDICATION

I would like to dedicate this dissertation to my family, past and present. God has truly blessed me with a loving family. Even though my grandpa (we called him Welo) is no longer with us, I still hope I have made him proud of me. It wasn't easy, but I know in the end this achievement would only pave the road for greater achievements in the future. To my parents, thank you for always believing in me and helping me in every way possible. I could not have done this without my parental support and I only hope I can be as great a parent to my own kids. I want my children to know that this was all for them. I can't help you guys get to the top if I don't know the struggle it takes to get there. By the way, your fee is attached to the end of this document.

ACKNOWLEDGEMENTS

I would just like to acknowledge the people in my scientific world that helped me complete the Biochemistry program here at Texas A&M University. Coming from Texas Tech, I wasn't exactly excited about being an Aggie but everyone here in Biochemistry Department was really nice and welcoming.

The biggest thank you will go to my boss. He allowed me to join his lab (it took some convincing) and even gave me an awesome project that included scientific training in both areas of kinetics and fluorescence. He allowed me and my lab members to travel all over the United States to attend National scientific conferences. He taught me how to present my data through posters and platform talks. Anyone who knows me is well aware that these moments make me want to vomit on the shoes of my audience but Dr. Reinhart was always patient and encouraging. The writing process wasn't as glamorous, but a necessary learning experience none the less. He made sure we celebrated together afterwards and I will cherish those memories forever. I wouldn't trade this journey for the world and I'm truly grateful to have had him for my mentor.

To my committee members, Dr. Tatyana Igumenova, Dr. Dorothy Shippen, and Dr. Nick Pace, a huge thank you for all your encouraging words and scientific guidance. I also wanted to thank Dr. Michelle Lovingshimer and Dr. Mauricio Lasagna for sharing their expertise to ensure the success of the lab projects, especially mine. The rest of the lab members; Dr. Rockann Mosser, Dr. Scarlett Ferguson, Dr. Maria Shubina-McGresham, Amy Whitaker, David Holland, and Robert Koenig, I have much love and respect for you all. I hope science treats you well.

NOMENCLATURE

A	Substrate
[A]	Substrate concentration
AC	The signal amplitude at frequency ω
ADP	Adenosine 5'-diphosphate
BsPFK	Phosphofructokinase from *Bacillus stearothermophilus*
C	Single letter code for amino acid cysteine
D	Single letter code for amino acid aspartate
DC	The average signal at frequency ω
DTT	Dithiothreitol
ΔG_{ax}	Coupling free energy between the binding of substrate and inhibitor
ΔG_a	Binding Free Energy for Substrate
ΔG_x	Binding Free Energy for Inhibitor
ΔH_{ax}	Coupling enthalpy for the binding of the substrate and inhibitor
ΔS_{ax}	Coupling entropy for the binding of the substrate and inhibitor
E	Apo Enzyme
EcPFK	Phosphofructokinase from *Escherichia coli*
EDTA	Ethylenediamine Tetraacetic Acid
EPPS	N-[2-Hydroxyethyl] Piperazine-3-Propanesulfonic Acid
ES	Enzyme-Substrate Complex
F	Single letter for amino acid phenylalanine
F6P	Fructose-6-Phosphate

FBP	Fructose-1, 6-bisphosphate
FBPase	Fructose-1, 6-bisphosphatase
G	Single letter for amino acid glycine
H	Single letter for amino acid histidine
Hb	Hemoglobin
K_a	Apparent dissociation constant for substrate A
$K_{0.5}$	The concentration of ligand that produces half-maximal change
K_{ia}°	Dissociation constant for A in the absence of effector
K_{ia}^{∞}	Dissociation constant for A in the presence of a saturating concentration of effector
K_{ix}°	Dissociation constant for inhibitor in the absence of substrate
K_{ix}^{∞}	Dissociation constant for inhibitor in the presence of a saturating concentration of effector
KSCN	Potassium thiocyanate
LB	Luria Bertani broth
LbPFK	Phosphofructokinase from *Lactobacillus delbrueckii*
mM	Millimolar
MOPS	3-[N-Morpholino] Propanesulfonic acid
NADH	Nicotinamide Adenine Dinucleotide, reduced form
NAD+	Nicotinamide Adenine dinucleotide, oxidized form
n_H	Hill coefficient
NATA	N-acetyl-tryptophanamide
ns	nanosecond

p	polarization
P	Product
PAGE	Polyacrylamide gel electrophoresis
PEP	Phosphoenolpyruvate
PFK	Phosphofructokinase
Q_{ax}	Coupling constant between the binding of the substrate and inhibitor
r	Anisotropy
φ	Rotational Correlation Time
R	Gas constant
Tris	Tris [Hydroxymethyl] Aminomethane
T	Fluorescence lifetime
v	Initial velocity
W	Single letter code for tryptophan
X	Inhibitor
[X]	Concentration of Inhibitor

TABLE OF CONTENTS

LIST OF FIGURES

LIST OF TABLES

CHAPTER I

INTRODUCTION: ALLOSTERIC COMMUNICATION, FROM ONE BINDING SITE TO ANOTHER

Proteins such as enzymes can undergo multiple ligand binding. Ligands such as substrates can bind to the enzyme's active site, or effector molecules can bind to a site distinct from the active site. This ligand binding can be seen as an example of enzyme regulation within the cell. The binding of an effector molecule(s) can either activate or inhibit the binding of substrate to the enzyme, altering the enzyme's affinity for the substrate, known as a K-type effect, or altering the catalytic rate, known as a V-type effect. This form of enzyme regulation is characterized as allosterism. It is commonly seen in proteins with more than one subunit, containing more than one effector site and more than one active site resulting in multiple sites undergoing regulation.

Consider an allosteric enzyme with four identical subunits containing one active site and one allosteric site per subunit. This enzyme possesses a high degree of potential interactions between the binding sites, meaning the binding of ligand to one site has the potential to either enhance or antagonize the binding of ligand to a separate site. Interactions between the same types of binding sites are known as homotropic interactions. Interactions between unlike binding sites are classified as heterotropic interactions. With respect to the homotetramer, there are a total of 28 potential interactions. Six homotropic interactions exist between the active sites and six homotropic interactions exist between the allosteric sites. In addition, sixteen possible heterotropic interactions exist between the active and allosteric sites. Due to the

structural symmetry of the enzyme only a limited number of interactions are considered unique. These distinct interactions include three of the homotropic interactions between the allosteric sites, three homotropic interactions between the active sites, and four heterotropic interactions between the active and allosteric sites. The allosteric properties of this enzyme may be highly studied and characterized; however, the data is merely the average response of all these interactions combined. There is no direct assessment for each individual interaction but only an assumption for its individual contribution to the overall regulation of the enzyme. These assumptions have therefore lead to the formulation of inadequate models of allostery to predict the general behavior of regulated proteins.

Even with the currently accepted models for allostery, the molecular mechanism for this phenomenon is still not understood for a wide variety of enzymes. Although specific residues and regions have been predicted to be responsible for the allosteric communication of an enzyme, an outline of the allosteric signal transmitted through the protein from one effector site to its respective active site has never been defined. Thus, it has become a scientific quest as described in several examples below for researchers to strategically simplify complicated allosteric systems by the use of what is known as hybrid strategies to enable the isolation and direct examination of unique interactions involved in the system's overall communication pathway. By initially determining the respective contribution of single routes of communication, scientists can now formulate a more complete hypothesis of the overall allosteric communication of the enzyme.

Before I describe several cases where the hybrid strategy is used to aid in the development of the molecular mechanism for various allosteric systems, I will explain the two universally accepted models that many researchers still use to provide a structural basis for how an allosteric signal is transmitted throughout an enzyme. These models were developed in the 1960's and are still acknowledged today. They are commonly known as the concerted model (Monod-Wyman-Changeux model) and the sequential model (Koshland-Nemethy-Filmer model) (*1, 2*). For both models, the enzyme can shift between two conformational states. A high affinity state (R-state) binds substrate(s) or activator(s) with high affinity, and a low affinity state (T-state) capable of binding allosteric inhibitor(s) and binds substrate with low affinity. For the MWC model, the two states are in equilibrium and it is the binding of substrate to free enzyme that shifts the equilibrium to the R-state and the binding of inhibitor to the free enzyme that promotes the shift in equilibrium to the T-state. The MWC model predicts that the four allosteric sites are equally effective at influencing the binding of substrate. This is characterized by an allosteric concerted transition of all the subunits from the R-state to the inhibited T-state upon the binding of one equivalent of inhibitor to the free enzyme. The KNF model, however, predicts that the two states are not limited in equilibrium with each other, claiming that the ligand decides the conformation of the enzyme. It suggests that a specific allosteric site influences the binding of substrate to a single active site. Accordingly, the conversion of states occurs sequentially with each subunit since there is not an equal response to the ligation of each binding site. Once the effector binds, it can cause an enhancement in the binding of substrate identified as

positive cooperativity or repulsion in the binding of substrate identified as negative cooperativity. Since the allosteric transition is characterized sequentially, the enzyme is required to undergo full saturation to completely shift to one of the two conformational states. The first binding event of ligand seems to be the crucial distinction between the two models.

Oftentimes these models are not sufficient to describe the total allosteric properties of enzymes and the predicted enzyme behavior can actually conflict with the measured behavioral properties of the enzyme, thus adding confusion. Therefore scientists have attempted to dissect the complex nature of enzyme regulation by performing direct measurements on strategic hybrid forms of the enzyme to help delineate this confusion. The next section reviews allosteric systems that incorporate the use of hybrids to assist in the mechanistic study of allosteric communication as described using the MWC or KNF models or a variation of the two.

Part 1: Hybrid Systems

The Hybrid System of D-3-Phosphoglycerate Dehydrogenase (PGDH)

Our first example includes a V-type regulated enzyme with four effector sites. Here, the hybrid strategy revealed the percentage of enzyme inhibition is dependent upon specific effector sites bound with serine. The first committed step in the biosynthesis of L-serine is performed by D-3-Phosphoglycerate dehydrogenase. This enzyme converts 3-phosphoglycerate into 3-phosphohydroxypyruvate and is allosterically inhibited by a V-type effector, L-serine. The enzyme is a homotetramer

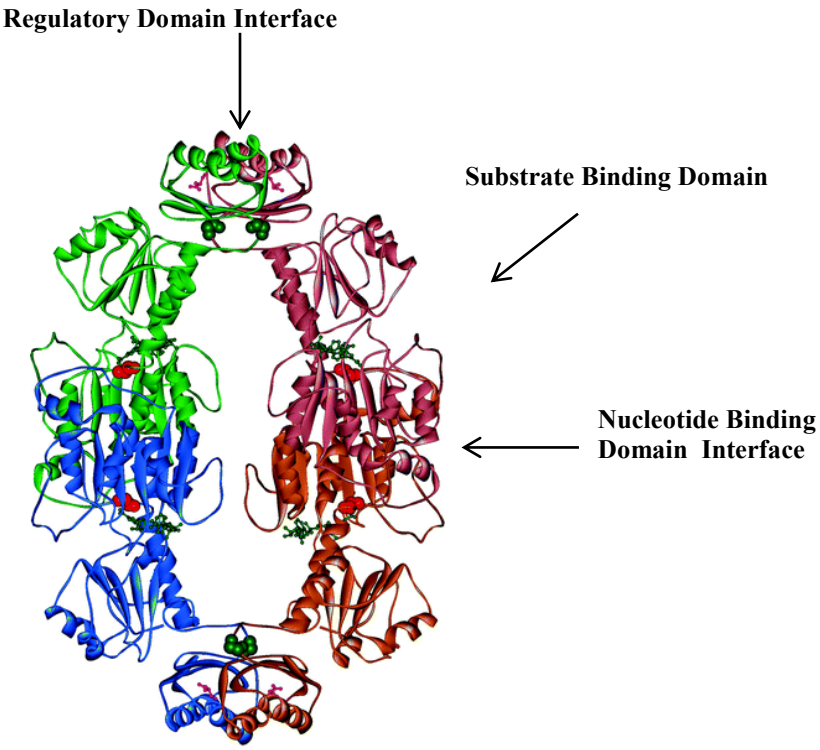

Figure 1-1. Ribbon Structure of *E. coli* D-3-Phosphoglycerate Dehydrogenase (adapted from Grant et. al. 2011). Each subunit is denoted by a different colored ribbon. The active sites are bound with NADH in green ball and stick. Serine molecules are shown in pink ball and stick located along the regulatory domains. The hinge regions of the enzyme are denoted by glycine residues in green and red space-filled atoms

A.

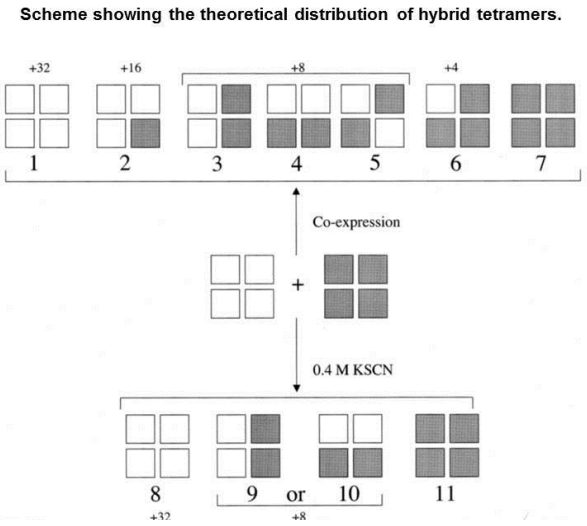

B.

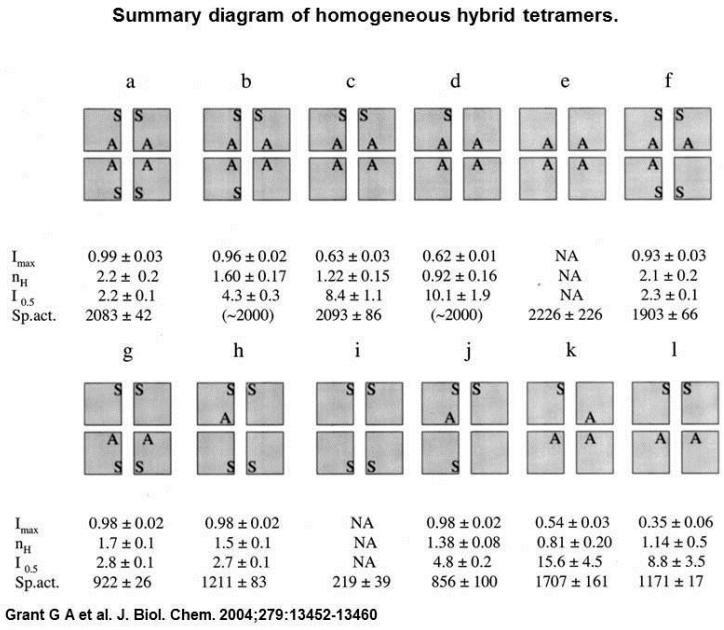

Figure 1-2 Hybrid Scheme of *In Vivo* and *In Vitro* Formation of all PGDH Species (adapted from Grant et. al. 2004). A. A co-expression system was developed for the formation of *in vivo* hybrids and a mild denaturant, KSCN, was used for subunit exchange *in vitro*. B. Summary of kinetic parameters defined for each hybrid tetramer that was isolated. The maximum inhibition of activity (I_{max}), the Hill coefficient for inhibition (n_H), the serine concentration at 50% of maximal inhibition of activity ($I_{0.5}$), and specific activity (Sp. act.) are defined below its respective hybrid.

with each subunit containing the substrate binding domain, the nucleotide binding domain, and the regulatory binding domain (Figure 1-1). PGDH is a dimer of dimers along the nucleotide binding domains with the regulatory domains at opposite ends. In 2004 Gregory Grant, et al., began to utilize these properties to create 12 possible hybrid forms of *Escherichia coli* PGDH using both *in vivo* and *in vitro* hybrid strategies to measure the kinetic properties and catalytic contribution of each active site and the regulatory participation of each effector site (Figure 1-2) (*3*).

The specific activity of 4 native active sites compared to 1 native active site only decreased by one-half revealing a "half-of-the-sites" activity for the enzyme where only half the sites are catalytically active at one time. Furthermore, the hybrid species with two native active sites located on opposite sides of the nucleotide binding interface in the trans position showed specific activity similar to the native enzyme. The I_{max} values representative of the degree of serine inhibition of PGDH, show the binding of the first serine molecule fully inhibits the binding of substrate within the same dimer and partially inhibits the opposite dimer suggesting an inter-subunit route of allosterism. The binding of the first serine molecule occurs with a 15º conformational change, as seen with crystal structure, resulting in positive cooperative binding of the second effector molecule to the trans site directly across the interface as shown by an increase in the Hill coefficient for inhibition (n_H) nearly completing the inhibition of enzyme activity, as shown by I_{max} fractional values near 1. The binding of additional serine molecules has no further inhibition of catalytic activity (*4*). These findings allowed the Grant group to propose a flip-flop mechanism as originally described in 1972 by M. Lazdunski (*5*). The

two dimers that interface the nucleotide binding domain are predicted to be conformationally distinct. One dimer, containing the two active sites, is in the "flipped" orientation and alternates with the other dimer comprised of the two remaining active sites in the opposite "flopped" direction.

The Hybrid Strategy for L-Lactate Dehydrogenase

Here the kinetic data obtained using a hybrid approach helped researchers define how activation at the allosteric site is transmitted to the active sites. L-Lactate dehydrogenase (LDH) is a homotetramer with pyruvate as a substrate and fructose 1,6-bisphosphate (FBP) as its allosteric K-type and V-type activator. The enzyme has four binding sites for pyruvate along the active site interface but only two sites for the activator to bind along the effector interface (Figure 1-3a). Using apo and substrate-bound crystal structures, H. Matsuzawa et. al., was able to predict the allosteric pathway of the *Bifidobacterium longum* LDH based on a model previously proposed by Monod-Wyman-Changeux of 1965 (*1*). It was hypothesized that in the T-state (tense), the binding of FBP neutralized the positive charge repulsion along the allosteric interface causing a conformational change. This change in conformation then induces a quaternary change to the protein, shifting the equilibrium to the R-state or active confirmation (*6*). A newly improved *in vivo* hybrid strategy was used to define the details of this transition between the R-(relaxed) and T-states as seen in the crystal structures.

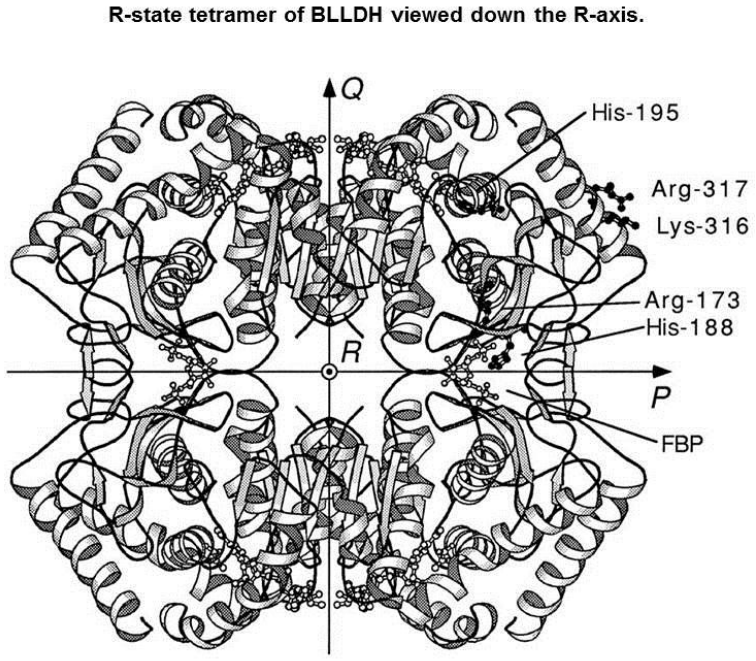

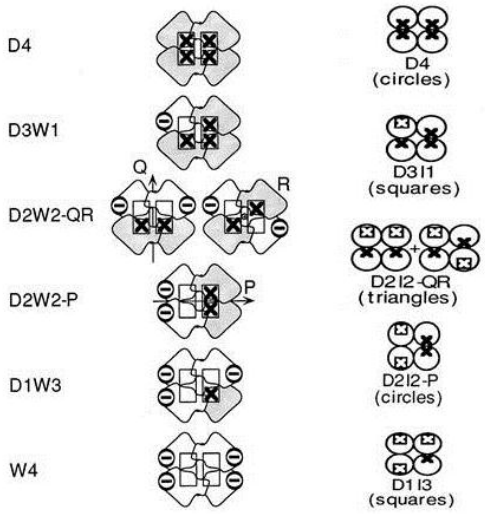

Figure 1-3 Structure and Hybrid Forms of *Bifidobacterium longum* L-Lactate Dehydrogenase. A. Each subunit is shown in ribbon form. The FBP binding site is located along the P-axis interface. Ball and stick molecules include NADH, oxamate, and FBP. B. Two-dimensional hybrid scheme of mutated allosteric sites alone (DW hybrids) and in combination with mutated active sites (DI hybrids, shown with circular subunits).

The Matsuzawa group developed two sets of hybrids. The D-W hybrid set used an activator-desensitized form of the enzyme mixed with wild-type enzyme and the D-I set included an activator-desensitized enzyme mixed with a catalytically inactive enzyme form (Figure 1-3b). In the D-W set that isolates one functional FBP site, the pyruvate saturation curve changed from hyperbolic to sigmoidal when no intact FBP binding sites are present, thus only partially neutralizing the allosteric interface resulting in the shift in equilibrium to an intermediate state between the T-state to the R-state. Next, the D-I hybrid with one native active and one native effector site on the opposite dimer 40Å away displayed an increase in substrate activity in the presence of FBP suggesting inter-subunit allosteric communication across the active site interface implying that a quaternary shift along this axis could be responsible for enzyme activation. Crystal studies suggest how this shift occurs, by sliding of helix α2F causing a replacement of His 68 by Arg-171 resulting the R-state conformation. The authors admit there are discrepancies with using a concerted model to fully describe the molecular mechanism of this enzyme and a shift in equilibrium may be a result of the mutations used in the hybrid strategy, but additional experiments are needed to confirm the effect of these changes (*7*).

The Hybrid Approach for Hemoglobin

Twenty years of extensive work with the use of hybrids, helped the Ackers group develop an alternative model known the Symmetry Rule to explain the positive cooperativity in oxygen binding to the protein. Human hemoglobin transports oxygen in the blood and is a tetrameric protein consisting of a dimer of αβ dimers (Figure 1-4a).

The molecular mechanism for hemoglobin has long been described using the two-state concerted model of Monod et. al., proposed in 1965. It was hypothesized that once oxygen binds to a single subunit of hemoglobin, this is transmitted to the other three subunits, thus weakening the dimer-dimer interface promoting a quaternary shift in equilibrium from the T-state to the R-state. A weakened dimer-dimer interface was supported by a 30-fold enhancement in the binding of the first oxygen molecule by breaking the hydrogen bond of a single mutated arginine located along the interface allowing the R-state to be highly favored.

Since 1992, Gary Ackers et. al., has predicted a new microstate model and formulated a new hybrid strategy replacing iron with zinc to help stabilize eight intermediate states, and applied a thermodynamic linkage analysis to calculate the binding constants (*8, 9*) (Figure 1-4b). After the stabilization of these microstates, the concerted model expanded into the Symmetry Rule Model in 2000 or the Global Allostery model in 2002 (*10, 11*). The Symmetry Rule model revealed that once oxygen binds, it is transmitted within the dimer, not across the interface. It is not until both dimers have at least one oxygen molecule each that there is a conversion between the T-state to the R-state. In addition two years later, Ackers calculated the binding constant of an asymmetric hybrid form after breaking the hydrogen bond of the previously studied arginine located along the dimer-dimer interface but this time, the mutation only exists within a single subunit. The breaking of hydrogen bonds along the interface was originally thought to weaken the dimer-dimer interface causing the quaternary shift to

A.

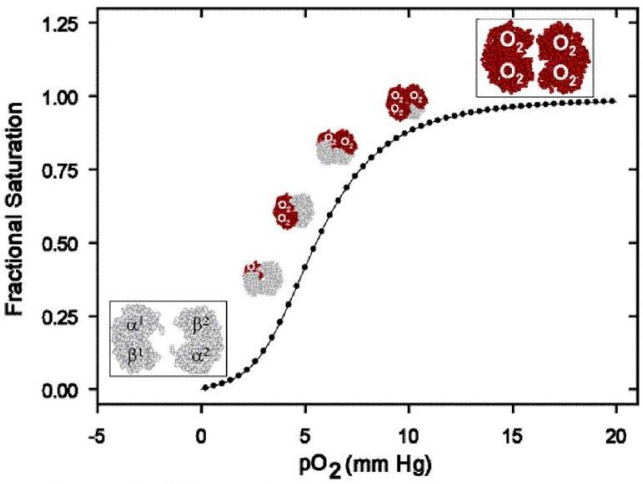

Ackers G K , Holt J M J. Biol. Chem. 2006;281:11441-11443

B.

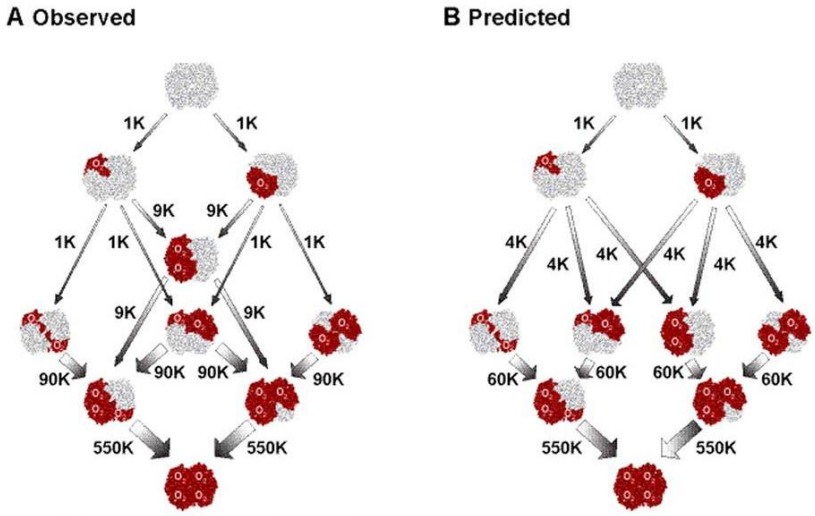

Ackers G K , Holt J M J. Biol. Chem. 2006;281:11441-11443

Figure 1-4 Oxygen Binding Steps to Saturate Hemoglobin. A. Saturation curve of oxygen molecules binding to each α or β subunit of the tetramer. B. Binding cascade of 16 ligation states were measured using thermodynamic linkage analysis vs. a two-state model. Positive cooperative binding of oxygen only occurs within the same dimer when the binding constants are calculated using thermodynamic linkage analysis. Under a simple two-state model, both dimers share the same binding constants at each ligation step.

the R-state. Since the binding constant for this asymmetric hybrid was surprisingly equal to the previously measured binding constant of the symmetric hybrid, then the original idea of coupling effects seen across the dimer-dimer interface now occurs within the αβ dimer (*12*). Ackers then postulated that using the Symmetry Rule to expand on the Sequential mechanism proposed by Koshland et al (*2*) may actually be a better fit for hemoglobin (*13*).

The Hybrid Scheme of Fructose1,6-Bisphosphatase

The use of a hybrid strategy allowed for the identification of a specific pathway with both cooperative binding of AMP and the strongest inhibition of FBPase activity. Fructose-1,6-bisphosphatase (FBPase) catalyzes the hydrolysis of fructose 1,6-bisphosphate to fructose 6-phosphate and inorganic phosphate. FBPase is a homotetramer that is allosterically inhibited by AMP (Figure 1-5a). This enzyme is also predicted to follow the MWC concerted model where the positive cooperative binding of AMP is thought to induce the transition from the R-state to the T-state. Structurally, both enzyme states have distinct conformations in loop 52-72 of an engaged, disengaged, or disordered loop. The binding of AMP is thought to stabilize the disengaged loop, and metals plus substrate stabilize the engaged loop needed for the active form. Changes in these loop conformations are assumed to be the conversion from the R-state (engaged and disordered loop) to the T-state (disengaged loop) and are confirmed by changes in emission spectra of AMP titrations using a tryptophan

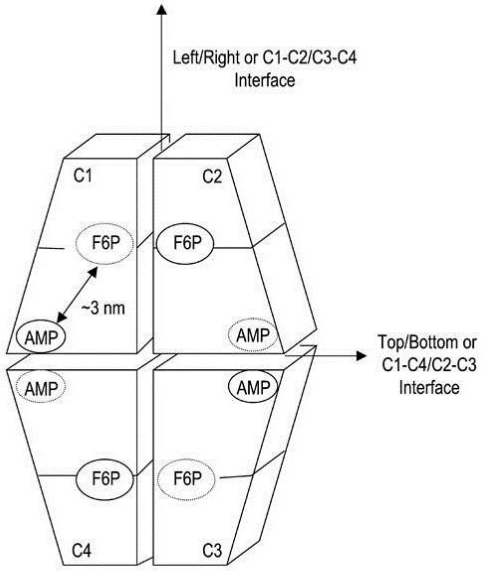

Nelson S W et al. J. Biol. Chem. 2002;277:15539-15545

Figure 1-5 2-D Schematic of FBPase Subunits and Interfaces. Active sites are labeled with substrate, F6P. The allosteric sites are labeled with AMP. The vertical interface is designated as C1-C2/C3-C4 and the horizontal interface is designated C1-C4/C2-C3.

fluorophore as a reporter in this area. How AMP cooperativity plays a part in the regulation of FBPase is still not understood.

Two different AMP communication pathways (C1 to C4 or C1 to C2 via the N-terminal segment) have previously been hypothesized. Yet several mutations have been made to the enzyme such as in the 52-72 loop, along both interfaces, all of which diminished AMP cooperativity making a definitive pathway difficult to map. One interesting mutation is an arginine at position 22 of subunit C1 that forms a hydrogen bond across the interface to a backbone carbonyl in the C4 subunit while in the T-state, but this interaction is absent in the R-state. When mutated to a methionine, the positive cooperative binding of AMP is diminished, thus implicating the horizontal interface (C1-C4/C2-C3) as key points for communication between the top and bottom halves necessary for AMP cooperativity. In 2002 Fromm et. al. used an *in vitro* hybrid strategy to define the molecular mechanism for the positive cooperative binding of AMP in the allosteric inhibition of FBPase (Figure 1-6a). The kinetic parameters and emission spectra for all hybrid species were measured for AMP, paying special attention to the three types of 2:2 hybrids. Kinetic parameters for all the hybrids were similar to wild-type except the IC_{50} values for AMP inhibition and the Hill coefficient measuring AMP cooperativity of binding. The IC_{50} of AMP for the 2:2q/2:2r was similar to the IC_{50} of a hybrid with three functional AMP sites, but the 2:2p hybrid species required a higher concentration to reach full inhibition of the enzyme with a Hill coefficient of 1. The inhibition seen with the 2:2p hybrid was accomplished without communication through the C1-C2 interface. So in order for AMP to bind cooperatively and strongly inhibit

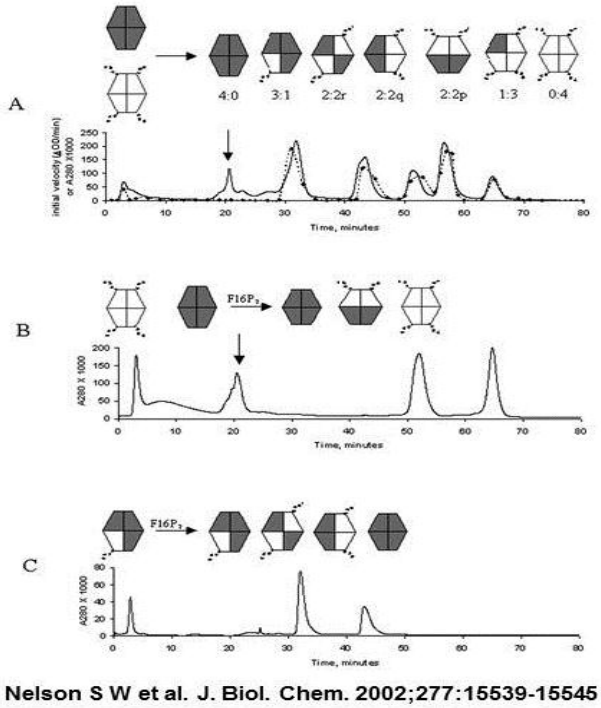

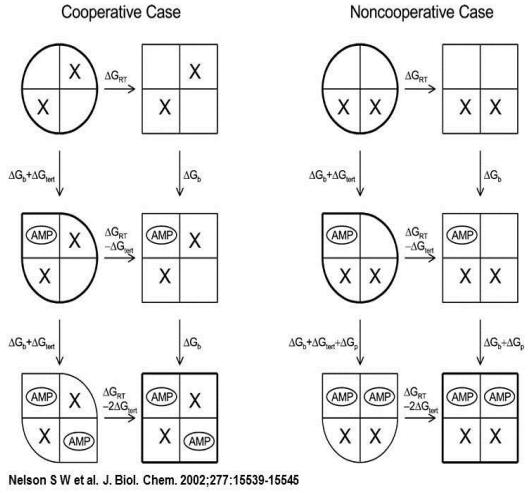

Figure 1-6. Hybrid Strategy and Two Allosteric Pathways for FBPase. A. Elution profile with assigned peaks for all possible hybrid species including different methodologies for the separation of 2:2 species. B. Cooperative vs. Noncooperative inhibition pathways of FBPase of 2:2 dimers by AMP in terms of free energy. Rounded-corner subunits represent R-state and subunits with a corner represent the T-state.

FBPase, then one AMP molecule must bind to each of the top and bottom half of the tetramer.

A tryptophan was strategically placed in the 52-72 loop and was combined with the inactive AMP subunit in the formation of hybrids. In this experiment, the native subunits bind ligand and any change in the emission spectra would be reported by the intrinsic tryptophan reporter located in the 52-72 loop of the inactive subunit indicative of a quaternary change. The 2:2 species were sensitive to titrations of AMP representing a shift in equilibrium from the R-state to the T-state; however the subunits with 1 or 0 native AMP sites were unresponsive as demonstrated with no change in their emission spectra. With the use of hybrids, two different pathways for allosteric inhibition were indicated (Figure 1-6b). The pathway with the highest affinity is the cooperative pathway, triggered when two AMP molecules bind to opposite sides of the top/bottom interface. However, a noncooperative pathway is initiated when AMP binds to the same side of the top/bottom interface. Both pathways shift the equilibrium from the R-state to the T-state (*14*).

The Hybrid Scheme for Aspartate Transcarbamoylase

This allosteric system has also been extensively studied for many years with the hybrid approach. The collection of kinetic and structural data is supported by the use of the two-state model. Aspartate transcarbamoylase (ATCase) catalyzes the first committed step in pyrimidine biosynthesis converting aspartate and carbamyl phosphate into N-carbamyl-L-aspartate and inorganic phosphate. This enzyme binds both of its

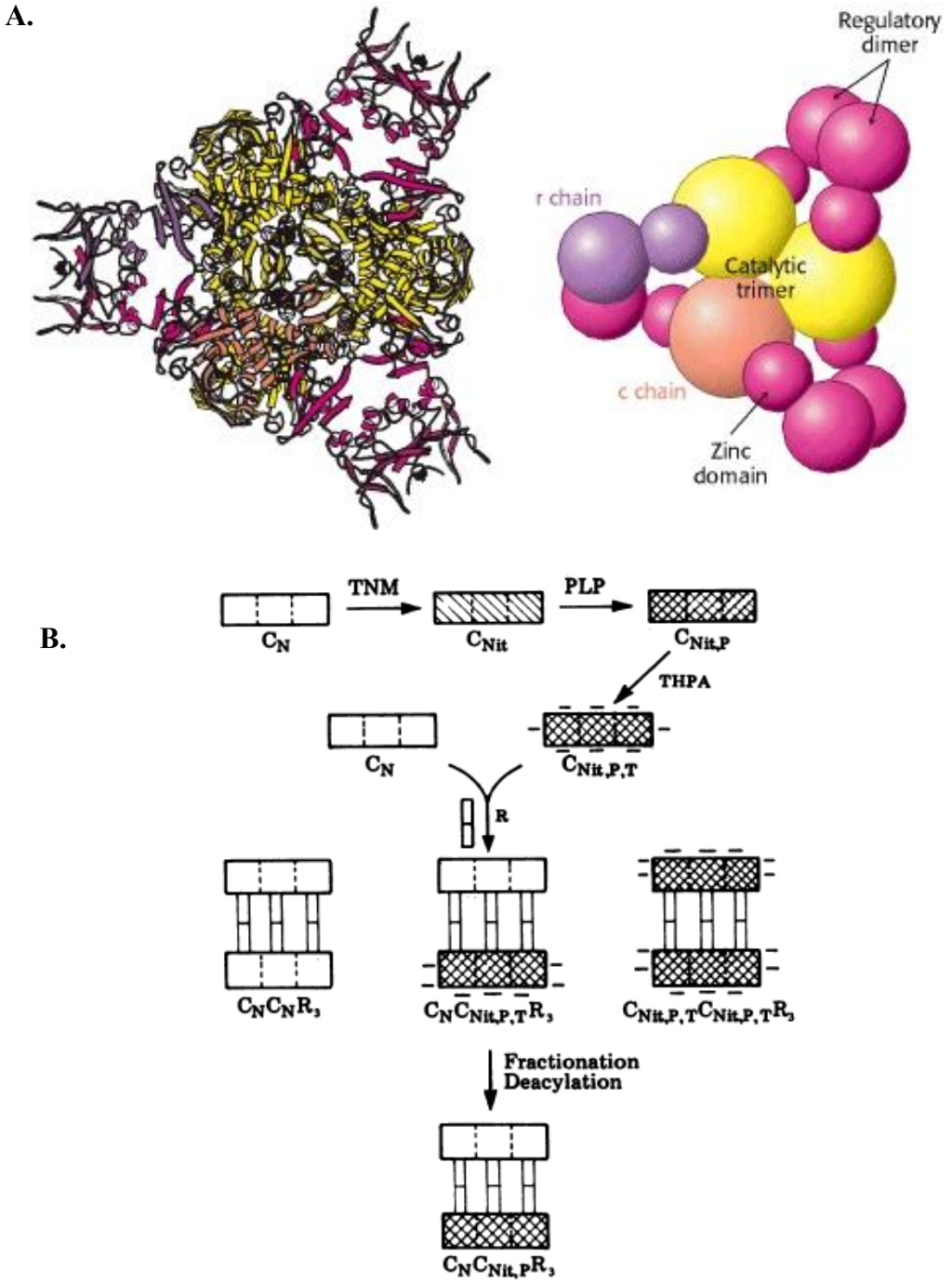

Figure 1-7: Crystal Structure and Hybrid Strategy of Aspartate Transcarbamoylase. A. Crystal structure and 2-D schematic of ATCase. Each of the two catalytic subunits are composed of trimers (the second subunit is not shown). The three regulatory subunits are composed of dimers. B. The hybrid strategy used to isolate a single catalytic subunit.

substrates cooperatively and is allosterically inhibited by CTP and activated by ATP. The MWC model is used to describe the allosteric transition from the CTP bound T-state to the activated, substrate bound R-state. Structurally it is made up of 12 subunits (C_2R_3) with two catalytic trimers (C subunits) connected by three regulatory dimers (R subunits) (Figure 1-7). A hybrid strategy for this enzyme was created by the Schachman group in the late 1970s, around the same time Ackers et. al., created a strategy for hemoglobin. In 1979, chemical modifications were used to produce hybrids that detected any conformational changes in the catalytic subunits upon effector binding to the regulatory subunits. Hybrid molecules were constructed by combining the 3 native regulatory subunits to active "nitrated" catalytic subunits having one sensitive nitrotyrosyl chromophore per catalytic chain. Upon binding of effectors, any change in the environment around these six chromophores can be detected by changes in their absorbance spectra, kinetic parameters, or sedimentation coefficients. Interestingly, a shift to the T-state can be characterized as a 10.5% decrease in absorbance when the inhibitor is present. In contrast, a shift to the R-state can be characterized by a 7.5% increase in absorbance in the presence of activator. In addition to the kinetic data and changes in sedimentation coefficients of the two ligated states, the Schachman group concluded the hybrids were able to differentiate between direct and indirect conformational effects to the catalytic subunits upon effector binding (*15*).

In 1980, the Schachman lab measured the transmission of communication to the regulatory subunits upon ligand binding to the catalytic subunits. Here, six metal ion binding sites important for structure were targeted. Normally these six zinc ions are

bound to a regulatory polypeptide chain by 4 cysteine residues and were strategically exchanged for 6 nickel ions that served as a monitor of conformational changes that occurred upon ligand binding to the catalytic subunits. Binding of co-substrates caused a spectral shift from the unligated absorption spectra suggesting that this hybrid strategy detected the predicted change in conformation consistent with the concerted model (*16*). The same year, hybrid enzymes were used to detect the propagation of allosteric signal from one catalytic subunit to the next upon binding of a substrate analog. This time the chromophores were placed on three inactive catalytic chains of one catalytic subunit, while leaving the other catalytic subunit active and connected by three regulatory subunits (Figure 1-7). A spectroscopic change was detectable in the inactive catalytic subunit upon binding of a bisubstrate analog to the active catalytic subunit, thus indicative of allosteric communication inducing not only a tertiary structural change, but a quaternary conformational change consistent with a shift to the R-state similar to the affects seen in hemoglobin (*17*). In 1986, the strategy was setup to detect conformational changes in a single inactive catalytic chain of the catalytic subunit that was spectroscopically active upon ligand binding. The Schachman group saw changes in the absorbance spectra and concluded that mapping the communication pathway for this enzyme would be difficult since tertiary and quaternary changes in conformation were seen throughout the protein (*18*). Hybrid experiments in 1992 and 2000 further explored the inter- and intra-subunit communication throughout the tetramer with the use of single point mutations (*19, 20*).

Part 2: The Hybrid Strategy for Phosphofructokinase

The Reinhart lab uses a glycolytic enzyme from various bacterial species as a model system to study the allosteric phenomenon. Phosphofructokinase (PFK) converts fructose 6-phosphate (F6P) to fructose-1,6-bisphosphate by a phosphoryl transfer from ATP. F6P is allosterically regulated by the K-type inhibitor, phosphoenolpyruvate (PEP), and the K-type activator, ADP. Structurally, bacterial PFK is a homotetramer with each subunit having an average molecular weight of 34,000 Da and is considered a dimer of dimers (*21, 22*). Subunit residues from either side of the dimer-dimer interface create four identical active sites and residues from the both subunits that make up the opposite dimer-dimer interface create four identical allosteric sites (Figure 1-8).

PFK is one of the original allosteric systems used to apply the MWC model, that specifically describes the allosteric response for both *Escherichia coli* PFK (EcPFK) and *Bacillus stearothermophilus* PFK (BsPFK) (*23*) (*24*). Initially, the kinetic parameters for EcPFK were measured and analyzed in order to define an equilibrium constant between the two hypothesized R and T-states. It was then concluded that no other sub-states were possible other than the inhibited state and the substrate/activator-bound state (*23*). Based on EcPFK, a mechanism for the structural transition between the two states of BsPFK was proposed by comparing the crystal structures of substrate/activator-bound enzyme to an inhibitor analog-bound enzyme form. Residue Arginine-162 was proposed to facilitate the binding of F6P, but it is replaced by Glutamate-161 when the inhibitor is bound. This glutamate provides repulsion for substrate binding, decreasing substrate affinity and stabilizing the T-state (*24*).

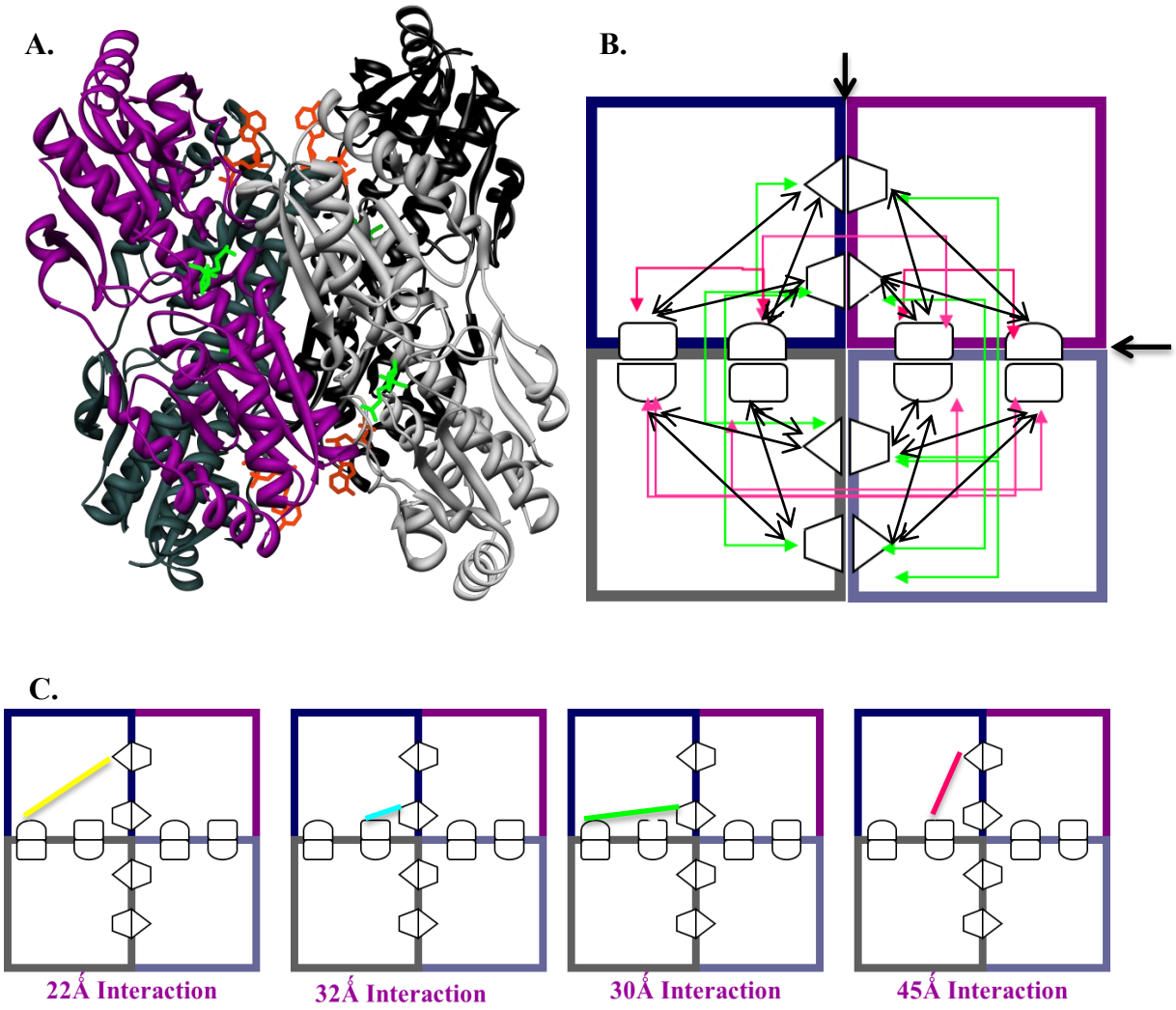

Figure 1-8. 3-D and 2-D Schematic of *Bacillus stearothermophilus* Phosphofructokinase (BsPFK). A. Crystal structure of BsPFK with F6P bound to the active sites as shown in orange ball and stick and ADP in the allosteric sites as shown in lime green ball and stick. B. 2-D schematic of the enzyme with all possible pair-wise interactions. The active site interface is depicted by the vertical black arrow and the allosteric site interface is depicted by the horizontal black arrow. C. The four unique heterotropic interactions within a single subunit and named according to the distance from the active site to its respective allosteric sites.

After close examination, the MWC model does not adequately describe the allosteric mechanism for PFK. First, the specific residue proposed to inhibit the binding of the negatively charged substrate at position 161 in BsPFK is not true for EcPFK. The residue at this position cannot provide the charge-charge repulsion that lowers the binding affinity of substrate. Second, in an examination of the two crystal forms, there is no structural indication of linkage. If the binding of effector to its effector site causes a conformational change in structure that affects the binding of substrate to its active site, then the binding of substrate to the active site should also cause a structural change that would affect the binding of effector to its effector site. However after examining the crystal structure of the T-state, there are no dramatic changes to the effector binding site. Third, in order to establish a structural basis of allosteric effects using crystal structure comparisons, it is necessary to include all four ligated states of the enzyme. In the crystal structure of the binary enzyme form, any structural changes observed are a result of ligand binding and these perturbations are not restricted to just their respective binding site. Evans et al. (*21*) did not include the crystal structure of the enzyme without ligands present, for structural reference nor the crystal structure with both the inhibitor and substrate bound, for structural changes due to allostery. This ternary species has been shown to exist experimentally for both EcPFK and BsPFK (*22-29*). The inadequacy of the MWC model to describe PFK has also been shown kinetically. Direct mutations to residues Arg-162 and Glu-161 did not drastically alter inhibition of the enzyme by PEP (*25, 30*).

Linked-function analysis (*31-34*) provides a different perspective to allosteric regulation using thermodynamic coupling free energies instead of crystal structures to describe changes upon ligand binding (*35*). Thermodynamic linkage analysis is the model currently used to describe the allosteric response of a single substrate single effector mechanism for PFK (Scheme 1). This model is for the simplest system consisting of substrate A, effector X, product P, and enzyme E. Linkage analysis considers all possible forms of the enzyme, applies to either inhibitor or activator, and describes a system where the consequence that an effector has on the binding of substrate to the enzyme should be equal to the consequence that substrate has on the binding of effector to the enzyme.

Scheme 1. Thermodynamic Linkage Analysis. This analysis represents changes in the binding affinity of a single substrate brought on by a single effector (*36, 37*). E represents enzyme, P represents product, A represents substrate and X represents effector.

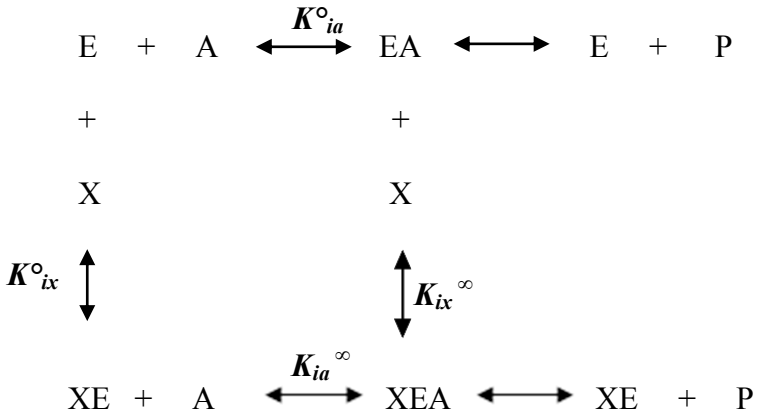

Thermodynamic dissociation constants defined by K's as shown below:

$$K^{\circ}_{ia} = \frac{[E][A]}{[EA]} \qquad K^{\circ}_{ix} = \frac{[E][X]}{[EX]} \tag{1-1}$$

$$K^{\infty}_{ia} = \frac{[XE][A]}{[XEA]} \qquad K^{\infty}_{ix} = \frac{[EA][X]}{[XEA]}$$

K°_{ia} and K^{∞}_{ia} represent the dissociation constants for the substrate in the absence and saturating presence of effector, respectively. K°_{ix} and K^{∞}_{ix} represent the dissociation constants for the effector in the absence and saturating presence of substrate, respectively. The consequence of the addition of X in the presence of A, or the addition of A in the presence of X should be equal and can be quantified by the coupling constant Q

$$Q_{ax} = \frac{K^{\circ}_{ia}}{K_{ia}{}^{\infty}} = \frac{K^{\circ}_{ix}}{K_{ix}{}^{\infty}} \tag{1-2}$$

This coupling parameter, Q_{ax}, defines the consequence of the second ligand binding in both nature and magnitude. If the above ratios are equal to 1, then the effector does not affect the binding of ligand. If the ratio is less than 1, then the effector is an inhibitor and if greater than 1, is an activator. Given the above definitions in equation 1-2, by simple rearrangement of these terms, we can define the coupling parameter using a ratio of the four different ligation states. This coupling constant, Q_{ax}, can also be further defined as an equilibrium constant that exists between the disproportionation reaction of the four ligation states.

$$Q_{ax} = \frac{[XEA][E]}{[XE][EA]} \tag{1-3}$$

$$\text{X-E + E-A} \overset{Q_{ax}}{\longleftrightarrow} \text{X-E-A + E} \tag{1-4}$$

This parameter can be quantified experimentally, by measuring the apparent dissociation constant for the substrate at increasing concentrations of effector. Graphically the data can be fit to the following equation where the dissociation constants for both A and X can be quantified along with the coupling parameter (*23, 24, 26-28*). Once the coupling parameter is measured, then it can be further defined, by the following equation with R as the gas constant and T as the absolute temperature in Kelvin. The coupling free energy term, ΔG_{ax} defines the nature and magnitude of the effector (*27*) with a positive coupling free energy represents an inhibitor, a negative value represents an activator, and no allosteric response is represented by a coupling free energy value of zero:

$$\Delta G_{ax} = -RT \ln Q_{ax} \tag{1-5}$$

With the replacement of the MWC model by thermodynamic linkage analysis, Reinhart et al., developed a hybrid strategy to dissect the molecular foundation of the allosteric pathway that exists for *Escherichia coli* and *Bacillus stearothermophilus* PFK (*38-42*). Out of 16 heterotropic interactions, four unique heterotropic interactions are manifested in one subunit, and are named by the distance between the active site and its respective allosteric site: 22Å (23Å in EcPFK), 32Å (33Å in EcPFK), 30Å, and 45Å. Their individual contribution to the allosteric inhibition, and activation for EcPFK, has been quantitatively determined using a linked-function analysis (Figure 1-9).

Each individual interaction has been shown to uniquely influence the overall heterotropic coupling with respect to PEP inhibition, and ADP activation for EcPFK (*41*). For both EcPFK and BsPFK, the strongest contribution of the inhibition of PEP is the shortest 22Å interaction. The 32Å interaction for BsPFK is the second greatest

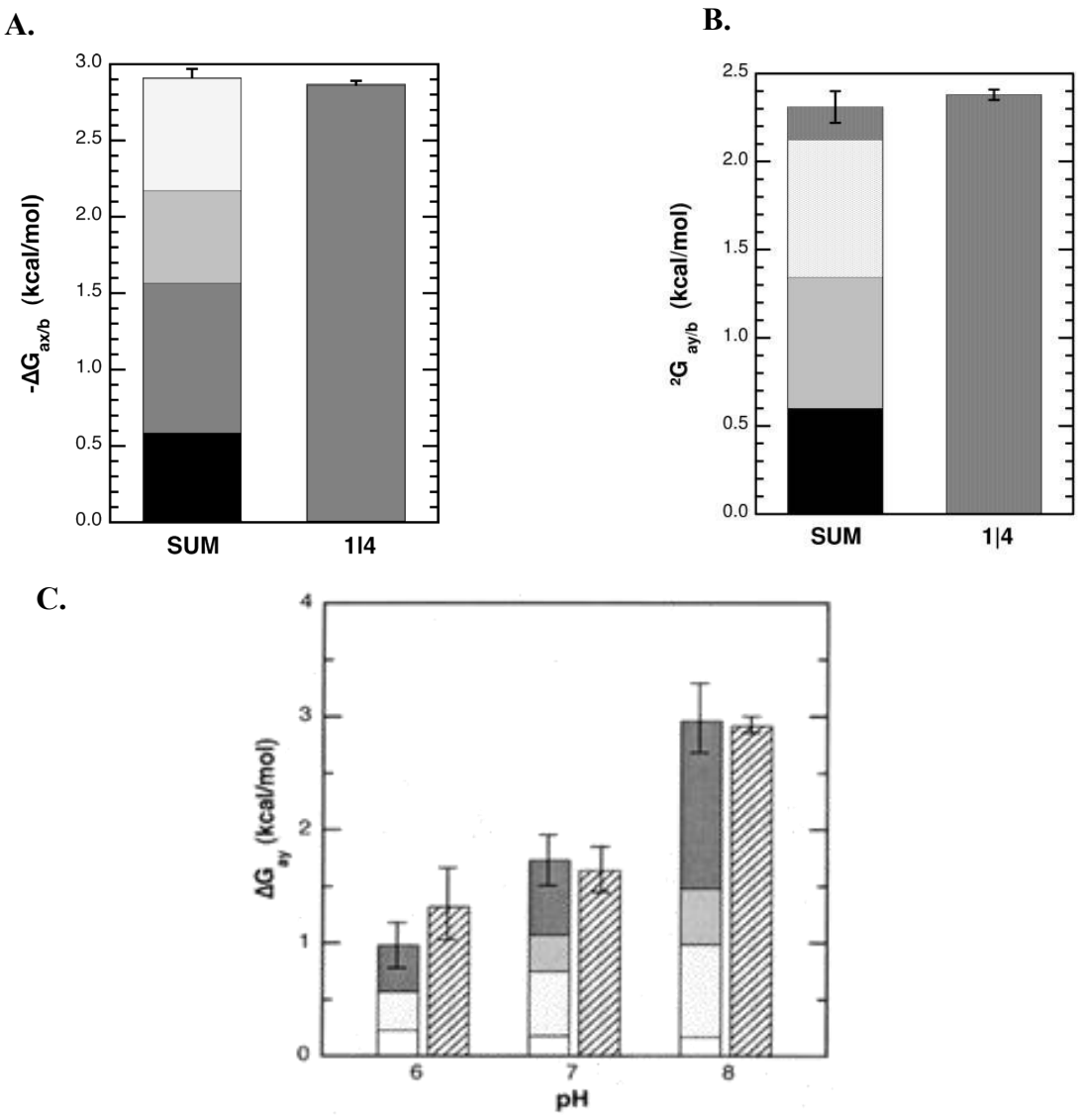

Figure 1-9. Coupling of the Four Individual Heterotropic Interactions for EcPFK and BsPFK. A. The sum of the 23Å interaction (light gray), the 33Å interaction (dark gray), the 30Å interaction (medium gray), and the 45Å interaction (black) equals the overall heterotropic coupling in EcPFK between ADP and F6P. B. The sum of the 23Å interaction (light gray), the 33Å interaction (dark gray), the 30Å interaction (medium gray), and the 45Å interaction (black) equals the total heterotropic coupling in EcPFK between PEP and F6P C. At each pH, the bar on the left is the sum of the 22Å interaction (black), the 32Å interaction (dark gray), the 30Å interaction (light gray), and the 45Å interaction (white). This sum is compared to the bar on the right which represents the total heterotropic coupling in BsPFK between PEP and F6P.

contributor, however in EcPFK the 33Å interaction actually contributes very little. The 45Å in BsPFK makes no significant contribution to inhibition, but inputs 25% of the total inhibition for EcPFK. The 30Å interaction for EcPFK is the second strongest contributor to the inhibition of the protein; however is the 3rd strongest contributor to the overall inhibition of the enzyme. In addition, the percent contribution of activation for the four interactions in EcPFK is not simply the opposite order for inhibition. These observations suggest the allosteric communication and structural pathways are distinct for each enzyme as well as within the enzyme between activation and inhibition for EcPFK. Furthermore, the heterotropic coupling observed in both of the species is derived from all four of these interactions and when combined represent the overall allosteric inhibition/activation of the monomer. Since it has been established that the BsPFK allosteric pathway is entropy-driven and the pathway for EcPFK is enthalpy-driven (*27*), the hybrid project has led to further evidence dissecting how the coupling is distributed throughout the enzyme for both species. The next step is then to identify specific residues or regions involved in each distinct communication pathway and assess if the residues within this region affect all the individual heterotropic interactions equally or are manifested in only specific heterotropic interactions. These next steps will help us to create the allosteric pathway transmitted from a single allosteric site to a single active site. We can then identify if these interactions share similar residues or regions in the network of the overall inhibition of the enzyme.

Overview

The overall goal of this study is to define how the inhibitory signal is transmitted throughout the phosphofructokinase from *Bacillus stearothermophilus*. With the disproval of the current models, the conclusions from this study will add to the formulation of a new model to describe the allosteric regulation for BsPFK and hopefully inspire the construction of new models for other allosteric systems. Chapter II describes general methodology including the general *in vitro* hybrid scheme used throughout the course of this study. Now that all ten of the unique interactions have been individually assessed and their contribution to the overall enzyme regulation has been quantified using the PFK hybrid strategy, the following step is to identify potential residues and regions necessary for the transmission of this inhibitory signal. Taking the previously established hybrid strategy a step further, the amount of influence a single residue possesses on a single interaction can now be directly quantified and is the focus of Chapter III. With the additional characterization of multiple residues we can distinguish the inhibitory pathways for each of the four heterotropic interactions as a distinct pathway, a duplicate pathway with the other three, or somewhere in between.

The hybrid species of PFK can also be further utilized to isolate single reporters in the form of a tryptophan placed in known proximity to a single interaction in order to detect hot spots within the native subunit involved the communication between these two specific binding sites. Chapter IV focuses on scanning the native subunit for the identification of these hot spot allosteric regions. Chapter V will be a summary of all the experiments combined and suggested experiments for the future.

CHAPTER II

GENERAL METHODS

Materials and Methods

All chemical reagents used in buffers, protein purifications, and enzymatic assays were of analytical grade purchased from Sigma Aldrich (St. Louis, MO) or Fisher Scientific (Fair Lawn, NJ). Ammonium sulfate suspension of glycerol 3-phosphate dehydrogenase and creatine kinase were purchased from Roche (Indianapolis, IN). Sodium salts of phosphocreatine, ATP, phospho(*enol*)pyruvate and the ammonium sulfate suspensions of aldolase and triose phosphate isomerase were purchased from Sigma Aldrich. Mimetic Blue 1 agarose resin purchased from Prometic Biosciences (Rockville, MD) and was used in all protein purifications. For use of the Fast Performance Liquid Chromatography (FPLC) system, a Mono Q HR10/10 anion exchange column was purchased from GE Lifescience (Charlottesville, VA). Before use in enzymatic assays, ammonium sulfate suspensions of coupling enzymes were extensively dialyzed against 50 mM MOPS-KOH, pH 7.0, 100 mM KCl, 5mM MgCl2 and 0.1 mM EDTA. Sodium salt of F6P was either purchased from Sigma Aldrich or USB Corporation (Cleveland, OH). NADH and DTT were purchased from Research Products International (Mt. Prospect, IL). Site-directed mutagenesis was performed using the QuickChange Site-Directed Mutagenesis System obtained from Stratagene (La Jolla, CA). Oligonucleotides were synthesized and purchased by Integrated DNA Technologies Inc. (Coralville, IA). Plasmid purifications were performed using Qiagen

(Hilden, Germany) Spin-column mini-prep kits. Deionized distilled water was used throughout.

Protein Purification

Plasmid pBR322/BsPFK was used for wild-type expression, containing the BsPFK gene under the control of the *Bacillus stearothermophilus* promoter and was received as a gift from Simon Chang (Louisiana State University) (*43*). Plasmid pGDR26 was used for mutant BsPFK expression, containing the BsPFK gene ligated into the pALTER vector (*28*). Plasmids were transformed into competent RL257 cells, an *E. coli* strain deficient in genes *PFK1* and *PFK2* (*44*).

All wild-type and mutant BsPFK proteins were purified as described previously (*45*) with a few alterations (*27, 38*). RL257 cells containing the plasmid of interest were grown for 16-18h at 37ºC in LB (Lysogeny Broth), ampicillin and when using pALTER, IPTG was also added (Tryptone 10 g/L, yeast extract 5 g/L, sodium chloride 10 g/L, ampicillin 100 µg/mL, and 2mM IPTG). Cells were then harvested by centrifugation and the pelleted cells were then frozen at -20ºC. The pellets were resuspended in 35 mL of Purification Buffer A (10mM Tris-HCl, 1mM EDTA, pH 7.5) and then lysed by sonication using a Fisher Sonic Dismembrator Model 550 at 0 ºC in 15 sec pulses for 10 minutes. Next, the crude lysate was centrifuged at 4 ºC for 1 hour at 22,500xg in a Beckman J2-21 centrifuge equipped with a JA-20 rotor. The supernatant was then heated in a 70 ºC water bath for 15 minutes, set on ice for 15 minutes, and centrifuged for an additional hour at 4 ºC at 22,500xg. The supernatant was diluted 5 -fold with Purification Buffer A and loaded onto a Mimetic Blue-A column equilibrated under the

same buffer conditions. After five bed-volumes of Buffer A were used to wash the Blue-A resin, the protein was then eluted using a 0 to1M NaCl linear gradient. PFK fractions were assessed for purity by SDS-PAGE, then collected and dialyzed against EPPS Buffer (50mM EPPS, 10mM $MgCl_2$, 100mM KCl, 0.1mM EDTA, pH 8.0) and stored at 4ºC. The total protein sample was concentrated and quantitated using the BCA protein assay reagent.

Enzymatic Activity Assay

The activity of wild-type and all mutant forms of PFK were measured by coupling the product formation of fructose-1,6-bisphospate to the oxidation of NADH (*46, 47*). The depletion of NADH was monitored over time as a decrease in absorbance at 340nm. Each assay contained 600µL of reaction sample containing 50mM EPPS Buffer (pH 8.0), 100mM KCl, 5mM $MgCl_2$, 0.1mM EDTA, 2mM DTT, 0.2mM NADH, 3mM ATP, 40µg/mL creatine kinase, 4mM phosphocreatine, 250µg aldolase, 50µg glycerol-3-phosphate dehydrogenase and 5µg triose phosphate isomerase. The reaction is kept at 25ºC and is initiated with the addition of 6µL of enzyme at the appropriate dilution. One unit of PFK activity is defined as the amount of enzyme needed to produce 1µmol of product, FBP. The rate of this reaction was measured using a Beckman series 600 spectrophotometer.

Hybrid Nomenclature

The hybrid strategy developed in the Reinhart lab uses a certain nomenclature for clarification of each hybrid species formed that makes up the total tetramer. The simplest notation used to describe each hybrid species is colon punctuation to define the

correct ratio of parent A monomers to parent B monomers respectively. In general, a total number of five hybrid species can be generated. As one example, to denote all parent A monomers and zero parent B monomers, a notation of 4:0 would be used to clarify this species. If a species contains one subunit of parent A and three subunits of parent B, then a notation of 1:3 hybrid enzyme would be used to specify the correct ratio of both parents present (*38*).

The second type of notation used to specify the number of native sites present in a hybrid tetramer is with a vertical bar notation (*41*). This vertical bar designates the number of native active sites to native allosteric sites respectively, within a specific hybrid species. This notation can also be used to describe a 4:0 species as 4|4 since it has four active sites and four native allosteric sites respectively. A 1:3 hybrid enzyme would be described as a 1|1 hybrid with one native active site and one native allosteric site. The vertical bar notation is commonly used to describe a hybrid species used as a control to account for the effect the mutated allosteric sites have on the coupling of a 1:3 hybrid species. The control hybrid is denoted 1|0 for one native active site and zero native allosteric sites.

In order to isolate each individual heterotropic interaction, parent B contains specific mutations within a subunit along the interface that were created to decrease the ligand binding affinity as shown in Figure 2-1 (*39*). The active site mutations are designated as either "a" or "b" mutations and the allosteric mutations are designated as either α or β mutations, depending on the interactions designed for isolation.

In Vitro Hybrid Tetramer Formation

The general *in vitro* method of forming BsPFK hybrids involves mixing parent A with parent B, dissociating these parents into monomer form, and then allowing the monomers to recombine in five possible configurations as shown in Figure 2-2. This technique (*38*) was adapted from previous work performed on the dissociation of EcPFK tetramers into monomers (*48, 49*). In order to favor the formation of the 1:3 hybrid species isolating a single heterotropic interaction, 10 mg of the 0|0 parent was added with 7 mg of the 4|4 parent. Potassium thiocyanate (KSCN), a mild denaturant, was added to a final concentration of 2M. To reach a final volume of 8mL, 20mM Tris-HCl (pH 8.5) was then added to the mixture if needed. After 30 minute incubation at room temperature, the monomer sample was dialyzed against 20mM Tris-HCl pH 8.5 for three hours replacing the buffer every hour. Before loading onto a Pharmacia HR 10/10 FPLC monoQ anion-exchange column, the hybrid mixture was filtered through a 0.22 μM membrane. The anion-exchange column was equilibrated with 20mM Tris-HCl (pH 8.5) before loading sample. Once the sample was loaded, the column was then washed with 3-5 bed volumes of buffer. A linear NaCl gradient was used to elute the hybrid samples in 1.0mL fraction volume. The absorbance for all eluted fractions was monitored at

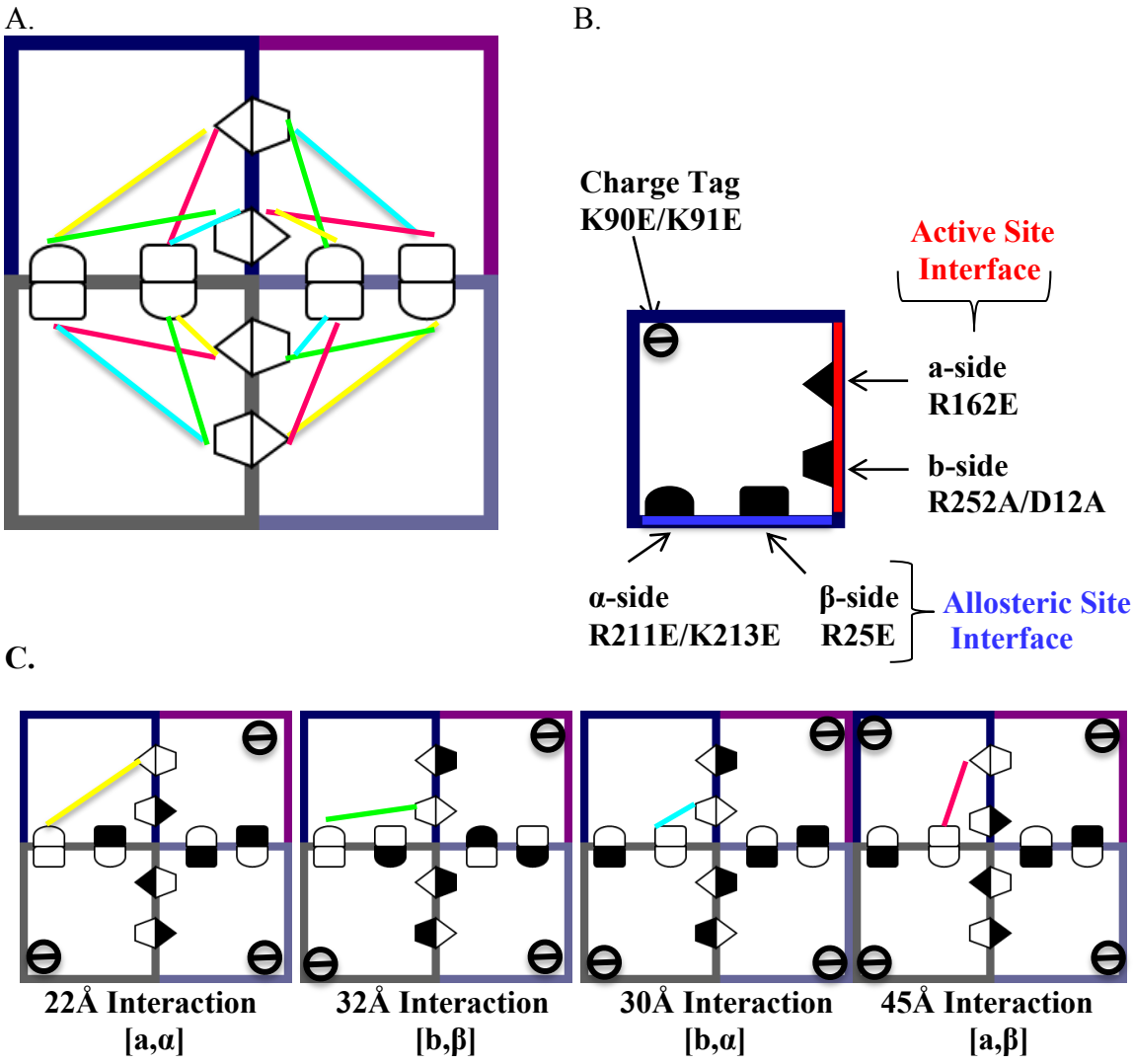

Figure 2-1 Strategy for Isolating the Four Individual Heterotropic Interactions. A. Sixteen possible heterotropic interactions of the 8 binding sites in BsPFK exist with four in each monomer as depicted with the four lines in cyan, pink, green, and yellow. B. A single subunit contains residues that make up one-half of a functional binding site as shown by the two different shapes of the site along its interface. As part of the hybrid strategy, residues along one side of the active site interface were mutated to diminish the binding affinity of substrate, as denoted by the color change from white to black. These mutated "sides" are defined as the a-side (R162E) and b-side (R252A/ D12A). Mutations that diminish the binding affinity of effector are located on one-half of the allosteric site interface and are known as the α-side (R211E/ K213E) and the β-side(R25E). The 22Å interaction contains the a-side and the α-side mutations. The 32Å interaction contains the b-side and the β-side mutations. The 30Å interaction contains the b-side and the α-side mutations. The 45Å interaction contains the a-side and the β-side mutations. All interactions contain the K90E/K91E charge mutation.

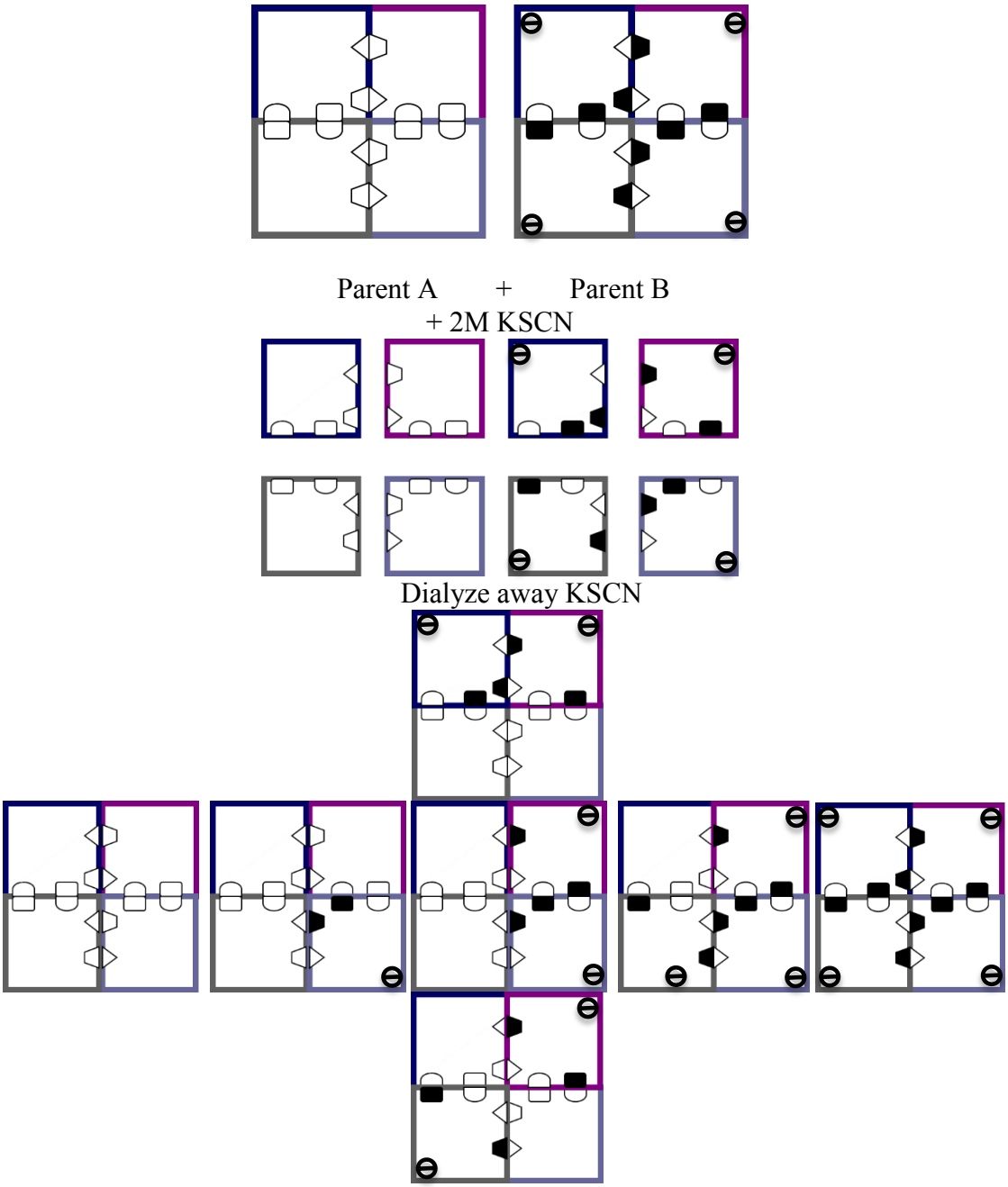

Figure 2-2 Schematic Graph of *In Vitro* Hybrid Formation. Two BsPFK parents are mixed with KSCN, a mild denaturant used to dissociate the tetramer forms. Parent A represents the wild-type form of the enzyme. Parent B contains mutations in the active site, the allosteric site, and the surface of the protein. Species from left to right are known as a 4:0, 3:1, 2:2, 1:3, and 0:4 respectively.

340nm and assayed for activity. Hybrid samples of interest were then run on a native PAGE gel to verify the purity of species (Figure 2-3). Species of interest were then dialyzed against 50mM EPPS Buffer (pH 8.0), 100mM KCl, 5mM $MgCl_2$, 0.1mM EDTA and stored in 4ºC to prevent rehybridization.

Data Analysis

All data analysis for enzymes with native binding sites was performed using Kaleidagraph software (Synergy). The Hill equation (*50*) was used to fit initial velocity kinetic activity of the enzyme as a function of F6P concentration:

$$v = \frac{\mathrm{Vmax[A]^{n_H}}}{\mathrm{K_{1/2}^{n_H}+[A]^{n_H}}} \qquad (2\text{-}1)$$

where v is the steady-state rate of turnover, V_{max} is the maximal rate, [A] is the concentration of F6P, $K_{1/2}$ is the concentration of F6P at half maximal specific activity, n_H is the Hill coefficient. Hybrid species, however, consist of active sites with both high and low binding affinities. Data for these constructs were fit to the equation:

$$v = \left[\left(\frac{V_{max}\,[\mathrm{A}]}{K_{1/2}+[\mathrm{A}]}\right) + \left(\frac{V\prime_{max}\,[\mathrm{A}]}{K\prime_{1/2}+[\mathrm{A}]}\right)\right] \qquad (2\text{-}2)$$

where V'_{max} and $K'_{1/2}$ are the kinetic parameters for the low-affinity binding site population due to the active site mutations of the hybrid strategy. Since PEP affects the binding affinity of substrate, the changes in $K_{1/2}$ were plotted as a function of PEP concentration and were fit to equation 2-3:

$$K_{1/2} = K^{\circ}_{ia}\left(\frac{K^{\circ}_{ix}+[\mathrm{X}]}{K^{\circ}_{ix}+Q_{ax}[\mathrm{X}]}\right) \qquad (2\text{-}3)$$

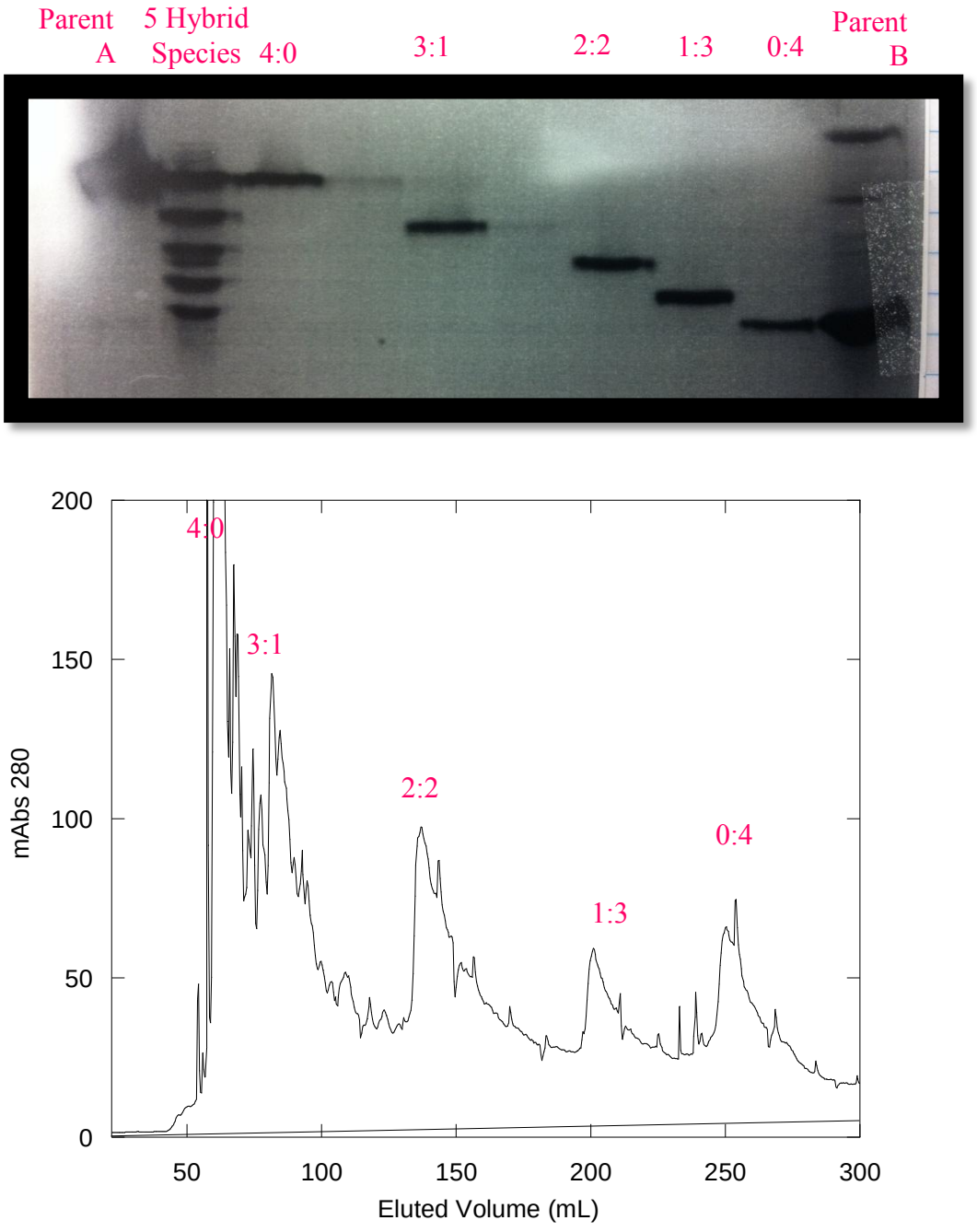

Figure 2-3 Strategy for the Purification and Isolation of the Hybrid Species for BsPFK. A. Native PAGE gel with species from left to right, parent A, after dialysis, parent A, 3:0 species, 2:2 species, 1:3 species, 0:4 species, parent B. B. Elution profile of all included species and their respective absorbance.

where $K_{1/2}$ represents the F6P concentration at one-half maximal specific activity. X represents the concentration of PEP. The apparent dissociation constant for F6P is defined by $K°_{ia}$ with no PEP present. The apparent dissociation constant for PEP is defined by $K°_{ix}$ in the absence of F6P. The coupling parameter that quantifies the allosteric response between both ligands is defined by Q_{ax}. This parameter describes the degree the binding of PEP has on the binding of F6P and the extent the binding of PEP has on the binding of F6P to the enzyme (*35*, *51*).

CHAPTER III

IDENTIFYING THE ALLOSTERIC RESIDUES INVOLVED IN THE HETEROTROPIC PATHWAY OF PHOSPHOFRUCTOKINASE IN *BACILLUS STEAROTHERMOPHILUS*

Introduction

The allosteric behavior of an oligomeric enzyme becomes highly intricate when the total possible interactions between active and allosteric sites are considered. The oligomer, phosphofructokinase of *Bacillus stearothermophilus* (BsPFK) is used as the allosteric model in this chapter, exemplified by its inhibition of substrate, fructose 6-phosphate (F6P) binding by phospho(enol)pyruvate (PEP). Structurally, the enzyme is comprised of four identical large subunits arranged as a dimer of dimers with four active sites located along the active site interface and four effector sites positioned along the allosteric site interface. Among all the possible interactions of binding sites, BsPFK contains four distinct interactions between the active and allosteric sites per subunit. A hybrid system has been implemented to analyze these four unique heterotropic interactions and their respective contribution to the overall allosteric communication of the enzyme has been measured individually (*39*). The next step is to identify key residues needed to propagate the heterotropic communication pathway within these same interactions. With an accumulation of residues, the use of the hybrid strategy will help to further outline the communication pathway for the overall enzyme.

Site-directed mutagenesis can be used to mutate candidate residues that are shown to moderately diminish coupling between F6P and PEP in the tetramer. The

hybrid strategy can then be employed to dissect which unique interactions heterotropic coupling has been perturbed as a result of the mutation. Three outcomes are possible: only one unique heterotropic interaction is affected, all four unique interactions are affected equally, or only specific interactions are affected. The results of this study will determine the degree of independence of the allosteric sites by examining how each candidate residue can distinctly affect each interaction. Combining the results of all the candidate residues will generate a route of allosteric communication between the active and allosteric sites of the enzyme.

Potential Residues

To identify residues necessary for the allosteric communication of BsPFK, various tactics were used in the selection process similar to previous tactics used with EcPFK (*52*). In that study, a sequence alignment was utilized containing phosphofructokinase from four species including two highly regulated species, *B. stearothermophilus* (BsPFK) and *E. coli* (EcPFK), plus two weakly regulated species, *Thermus thermophilus* (TtPFK), and *Lactobacillus delbrueckii* subspecies *bulgaricus* (LbPFK). The alignment with weaker regulated species was utilized to predict residues that would alter the coupling in EcPFK by focusing on a comparison of sequences between EcPFK and LbPFK. From the alignment, twenty-two EcPFK residues were chosen and mutated by altering these residues to the LbPFK counterpart and individually measuring the allosteric response of the enzyme as a result of each perturbation (*52*). Three of these twenty–two mutations were then further characterized using the hybrid strategy in EcPFK to further define the effect on the single heterotropic interactions (*53*).

Glycine 184 to a Cysteine

Of these three residues characterized in EcPFK, Glycine 184 is conserved in BsPFK and was therefore selected to be the first candidate to be examined. The LbPFK counterpart for residue 184 is a cysteine. For EcPFK, mutation G184C showed a twelve-fold decrease in PEP inhibition in the tetrameric form of the enzyme at 8.5ºC. Once the mutation was introduced in each of the four individual interactions, the greatest perturbation was seen in the 23Å interaction with a three-fold decrease in PEP inhibition. No effect as a result of the mutation was seen in the other three interactions (*53*).

Aspartic Acid 59 to a Glutamine

For EcPFK, aspartic acid 59 was mutated to an alanine. The *Lactobacillus* counterpart is a histidine; however the initial chimeric mutation from an aspartic acid to a histidine at residue 59 completely diminished the coupling between F6P and PEP for EcPFK. The alanine mutation at residue 59 showed a 38-fold decrease in PEP inhibition for EcPFK at 8.5ºC. Once the mutation was introduced into the individual heterotropic interactions, the greatest effect was seen in the 23Å interaction with a five-fold decrease in PEP inhibition, however possessed an enhancement in the 33Å interaction. Additionally the mutation expressed in the 30Å interaction had a three-fold decrease in PEP inhibition and had no effect on the 45Å interaction (*53*). For BsPFK, an asparagine stemming from *Thermus thermophilus* PFK (TtPFK) will be utilized at this position to characterize the role of this residue.

Threonine 158 to an Alanine

The last target residue for BsPFK was chosen using a more structural strategy by drawing a direct line between an active site located 22Å away from an allosteric site. Residue T158 lies within this direct path and is relatively equally distant from both sites. An alanine residue was chosen as the chimeric residue based on the results of the reverse mutation studied in *Thermus thermophilus* PFK (*54*). Here the A158T mutation in this particular species of PFK was found to actually enhance the coupling of the weaker regulated form of PFK. For BsPFK an alanine at this position will represent the last residue to be examined.

Materials and Methods

All the chemical reagents for protein purifications are identical to those described in the previous chapter of General Methods. Plasmid pBR322 was used for site-directed mutagenesis performed using the QuikChange Mutagenesis Kit. Mutagenesis primers were synthesized by Integrated DNA Technology (IDT):

G184C, 5'GTCGTCGTCGTCAAATTTCCCGGGTGTC3'

D59N, 5'ATATTCGACGTCGACCTACTACTACGTG3'

T158A, 5'TGGCAGTACCTTAGGCCATACATGACTGA3'

The altered plasmids were purified using Qiagen mini preps and sequenced by IDT. Plasmids with the desired mutations were then transformed into RL257 cells for protein purification. Once protein concentrations were determined via BCA, the hybrid

strategy was implemented according to the general protocol described in Chapter II. Each of the three potential allosteric residues was setup to form a hybrid with each of the four individual heterotropic interactions.

Once the hybrids were formed and isolated, the binding and coupling parameters were determined using the kinetic assay and linked-function analysis described in Chapter II. For all $K_{0.5}$ measurements, the data were then corrected by equation,

$$K_{0.5}\ corrected = \frac{K_{0.5}1|1}{K_{0.5}\ 1|0} \tag{3-1}$$

for any inhibitory effect on F6P binding from the low affinity PEP binding sites of the hybrid. This correction needs a new hybrid construct to measure any effect the mutated allosteric sites may have on the F6P binding to the one native site as shown in Figure 3-1.

The sum of the four individual interactions is compared to the total heterotropic effects of the enzyme. BsPFK has both heterotropic communication and PEP homotropic communication. In order to measure the total heterotropic effects without any PEP homotropic effects a new hybrid is constructed as shown in Figure 3-2. The coupling parameter measured with this construct is an average of one heterotropic interaction therefore:

$$Q_{4|1} = \frac{1}{4}Q_{4|4} \tag{3-2}$$

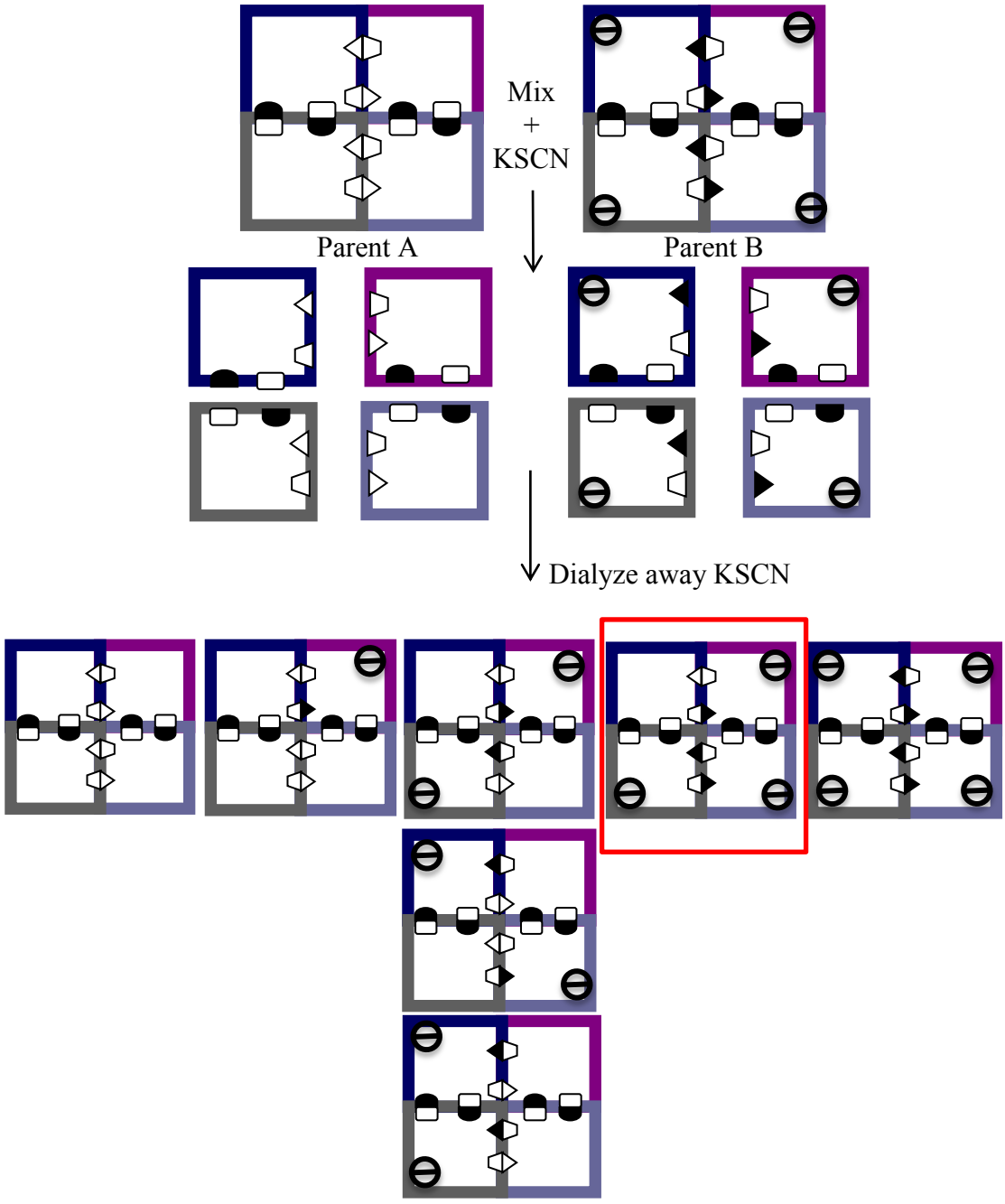

Figure 3-1 Hybrid Strategy for the Isolation of 1|0 Control. Parent A has the same allosteric site mutations as Parent B. Parent B has the active and allosteric site mutations corresponding to 1|1 interaction. The hybrid species highlighted in red is isolated and measured.

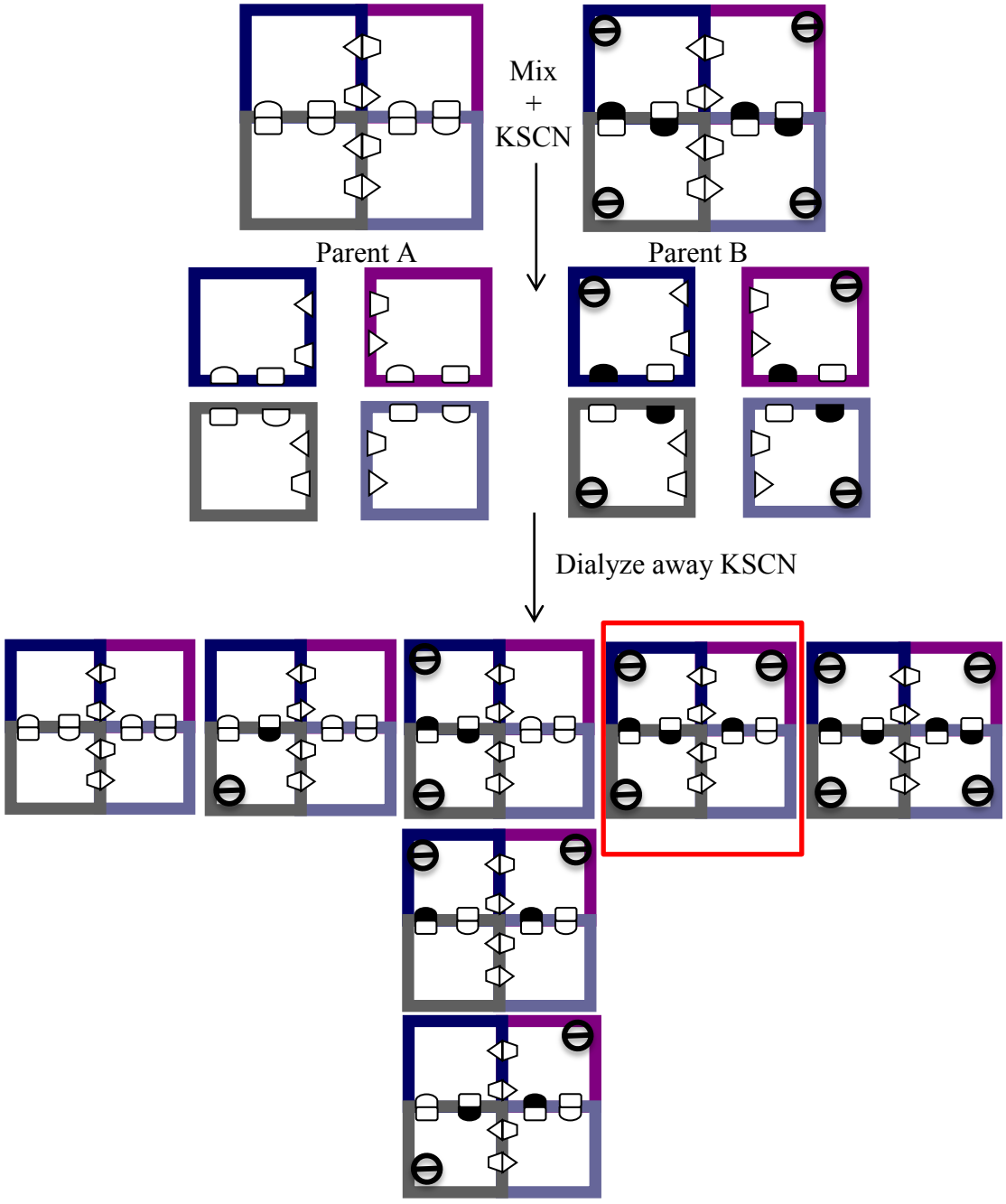

Figure 3-2 Hybrid Strategy for the Isolation of the 4|1 Control. Parent A contains all native active sites and all four native allosteric sites. Parent B contains mutated allosteric sties and all four native active sites. The hybrid species highlighted in red is the species isolated and measured.

Results and Discussion

Three residues for BsPFK were selected and characterized. Residue 184 is located along the 32Å interaction, residue 59 interacts with the effector bound to the 45Å/30Å interaction, and residue 158 lies along the 22Å interaction as shown in Figure 3-3. For all three residues, F6P titrations were performed at increasing concentrations of PEP as seen in Figure 3-4. The coupling parameter was then determined for all three residues using equation 2-3. Compared to the wild-type form of the enzyme, residue 184 when mutated to a cysteine showed the greatest decrease in the enzyme's coupling over 6-fold. Residue 59 when changed to an asparagine diminished the coupling of BsPFK by almost 6 fold and residue 158 when changed to an alanine decreased the overall coupling over 4-fold as seen in Figure 3-4 and Table 3-1. For all three residues, when mutated to a residue from a lesser inhibited species, the coupling for the BsPFK tetramer decreases indicating that each of these residues is important for the allosteric coupling between F6P and PEP as shown in Figure 3-5. The next step is to determine which specific heterotropic interactions are affected by each perturbation using the hybrid strategy.

Aspartic Acid 59

The asparagine mutation was then introduced at the 59 position of the enzyme into all the individual heterotropic interactions. The coupling parameters were then quantified using the initial velocity experiments for all four interactions as shown in

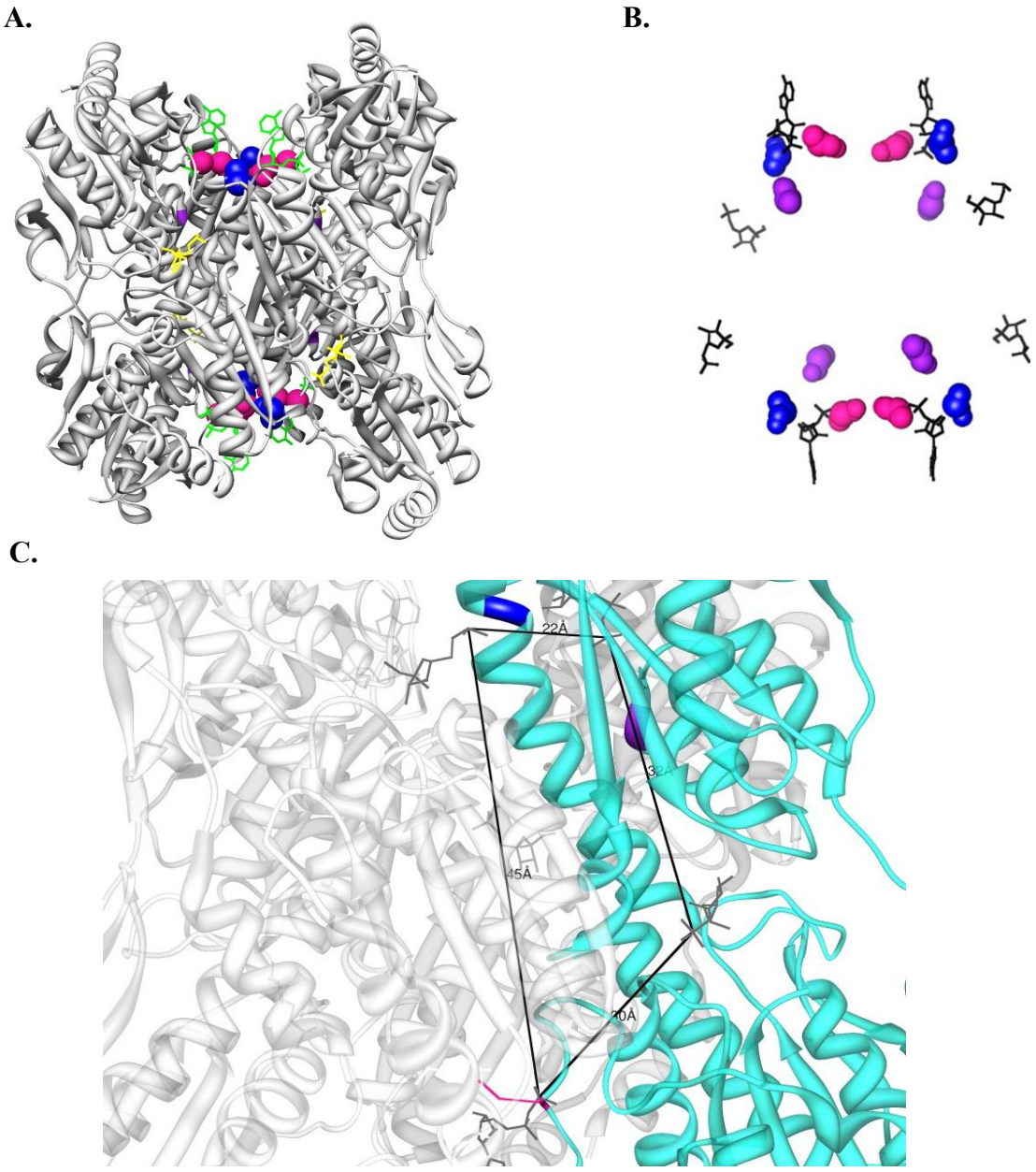

Figure 3-3 BsPFK Crystal Structure. A. Ligands F6P and ADP are shown bound to the active and allosteric sites in yellow and green respectively. Residues 59, 184, and 158 are highlighted in pink, purple, and blue respectively. B. Residues 59, 184, and 158 are shown with respect to the location of bound 4 ADP molecules and 4 F6P molecules shown in black. C. The native monomer in the hybrid strategy of BsPFK is shown in cyan. All four unique heterotropic interactions are outlined according to distance between the active site and its paired allosteric site. The three residues are highlighted as in the previous figures.

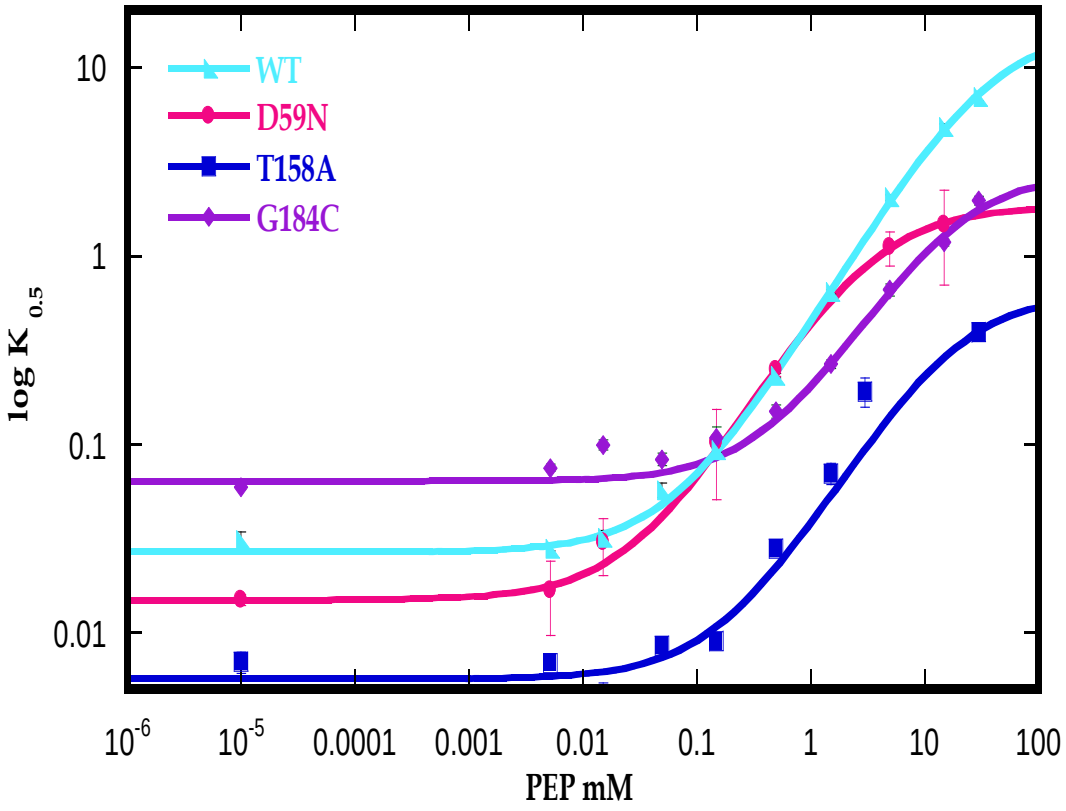

Figure 3-4 Kinetic Analysis of F6P Binding Affinity as a Function of PEP Concentration. WT BsPFK is shown in blue. D59N is shown in pink, G184C is shown in purple, and T158A is shown in blue. Experiments were completed at 25°C and pH 8. The data were fit to equation 2-3 to obtain the thermodynamic parameters shown in the table below.

	WT	D59N	T158A	G184C
$\mathbf{K}^{o}_{ia}$ (mM)	0.031 ± 2	0.0149±0.00096	0.017 ± 0.0005	0.0813± 0.0035
$\mathbf{K}^{o}_{ix}$ (mM)	0.093 ± 6	0.0258 ± 0.0033	0.098 ± 0.004	0.2381± 0.0172
$\mathbf{Q}_{ax}$	0.0021±0.0003	0.0115 ± 0.0026	0.009 ± 0.0003	0.0149± 0.0019

Table 3-1 Thermodynamic Parameters for the Inhibition of BsPFK

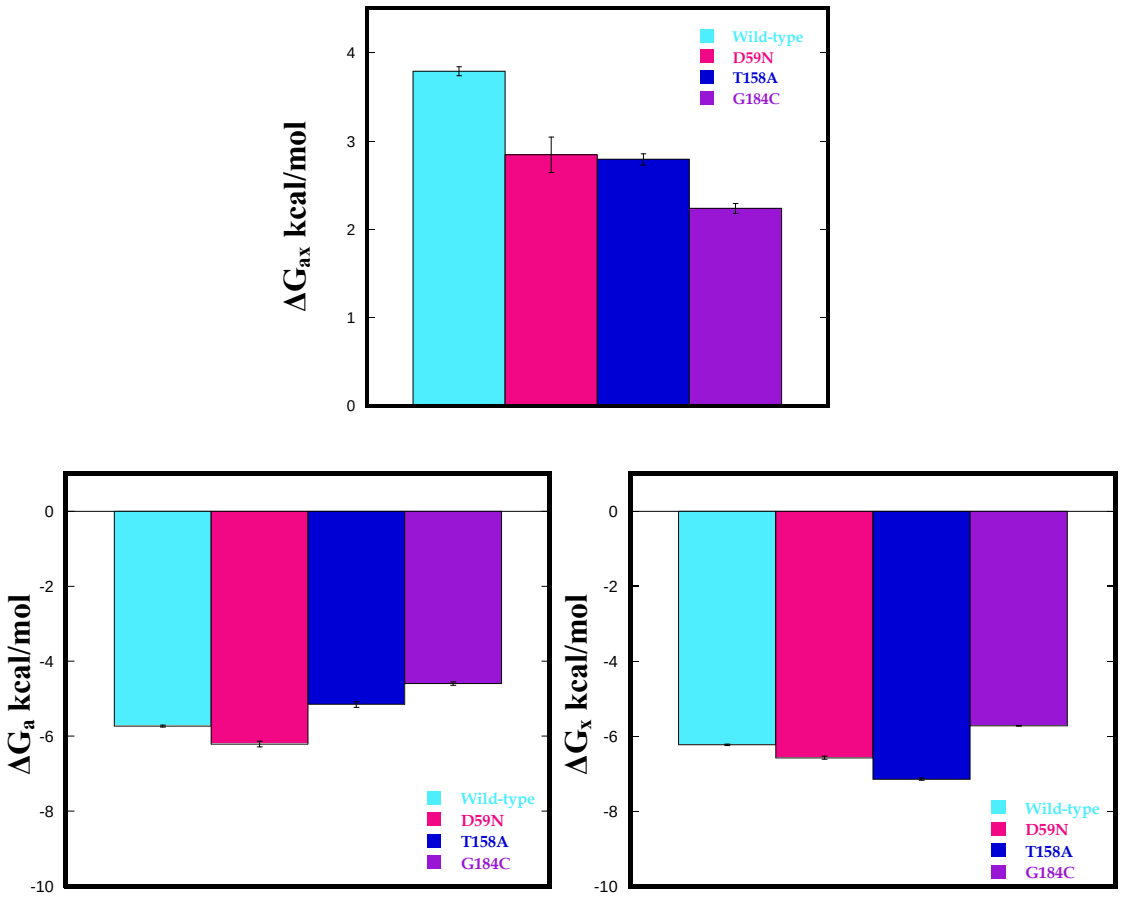

Figure 3-5 Coupling Free Energies and Binding Free Energies of BsPFK Variants. The coupling free energy for BsPFK was calculated using equation 1-5. (A) Coupling Free Energy of BsPFK WT, D59N, T158A, and G184C. (B) Binding Free Energies for F6P. (C) Binding Free Energies for PEP. Data were collected at 25°C and pH 8.

Figure 3-6. In the hybrid construct the mutated allosteric sites can still bind the inhibitor at high concentrations. The binding of this inhibitor can affect the binding of substrate to the single native active site. To correct for this influence, a 1|0 control was constructed as shown in Figure 3-1 to measure any inhibition from the mutated sites. To correct for this influence at each PEP concentration, a $K_{1/2}$ corrected value is calculated as a ratio of the $K_{1/2}$ calculated value from the hybrid construct with one native active site and one native allosteric site over the $K_{1/2}$ calculated value from the hybrid construct with 1 native active site and no native allosteric sites as shown in equation 3-1. The corrected values for the binding affinity for substrate in the presence of increasing concentrations of the inhibitor were then used to calculate a precise coupling parameter between a single active site and a single allosteric site. The coupling free energies for each of the four interactions including the perturbation were then calculated using equation 1-5. When compared to the wild-type heterotropic interactions, residue 59 shows a great decrease in the 22Å interaction as shown in Figures 3-7. However, in similar experiments with the isolated heterotropic EcPFK interactions, this residue decreased the coupling for the 22Å and 30Å interaction, enhanced the coupling in the 32Å, and had no effect on the coupling of the 45Å interaction. In BsPFK, residue 59 had no effect on the remaining three heterotropic interactions as shown in Figure 3-8 for the 32Å interaction, Figure 3-9 for the 30Å interaction, and Figure 3-10 for the 45Å interaction.

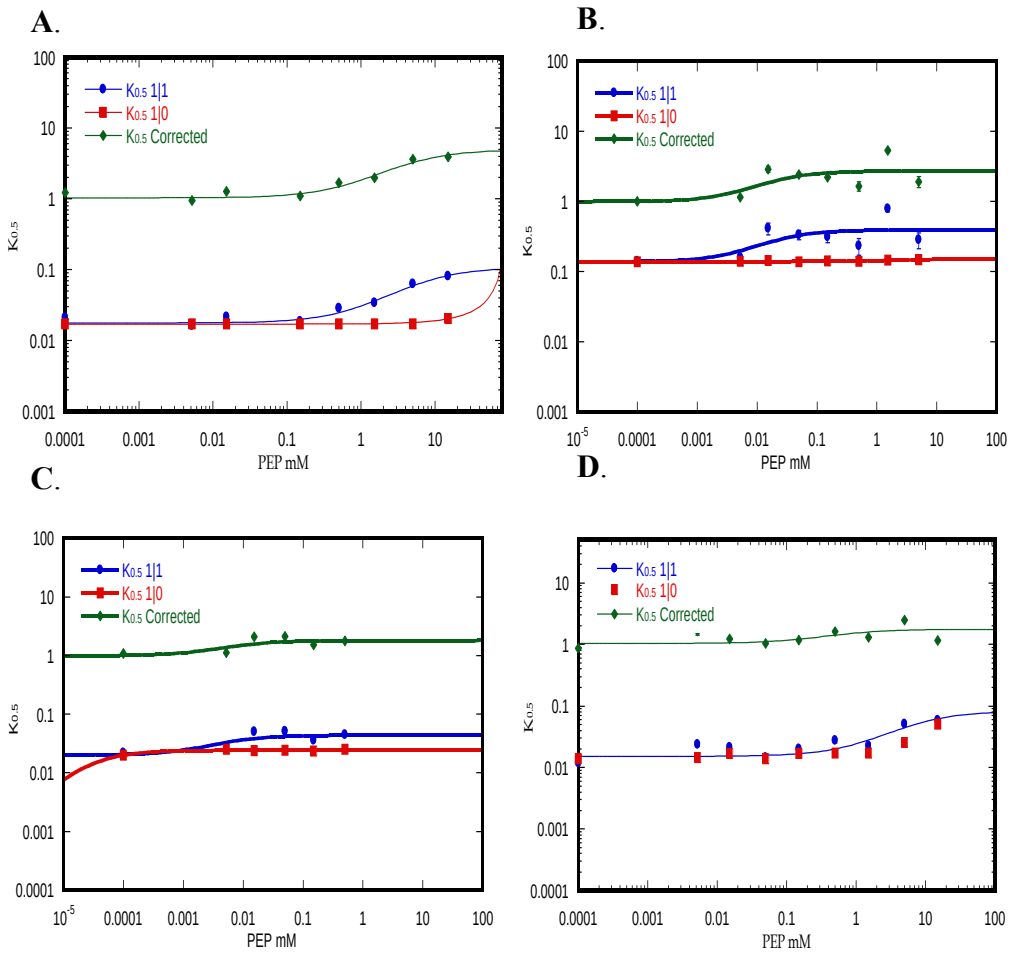

Figure 3-6 Change in the Apparent Dissociation Constants for Substrate as a Function of Effector Concentration Due to D59N **A**. 22Å interaction including the1|1 and the 1|0 experiments **B**. 32Å interaction including the 1|1 and 1|0 experiments **C.** 30Å interaction including the 1|1 and 1|0 experiments, **D**. 45Å interaction including the 1|1 and the 1|0 experiments.

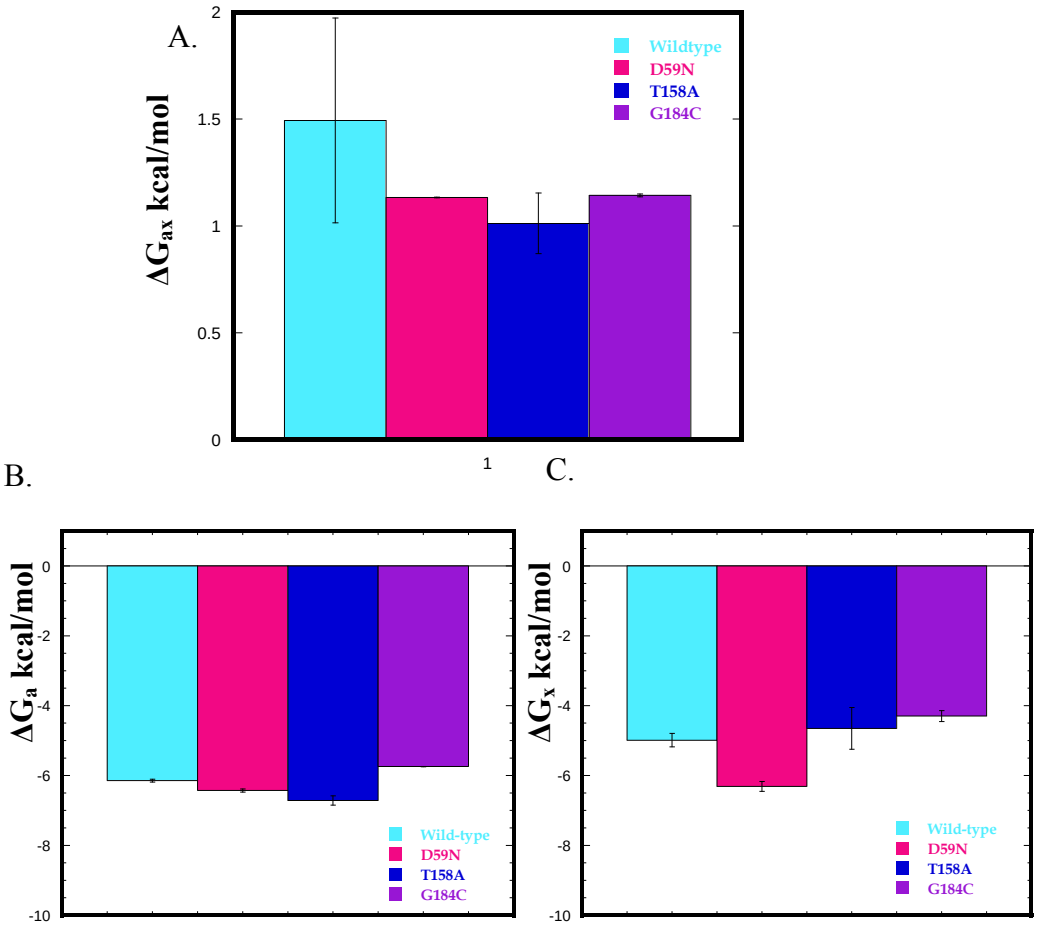

Figure 3-7. 22Å Coupling Free Energies and Binding Free Energies of BsPFK Variants. The coupling free energy for BsPFK was calculated using equation 1-5. (A) Coupling Free Energy of BsPFK WT, D59N, T158A, and G184C. (B) Binding Free Energies for F6P. (C) Binding Free Energies for PEP. Data were collected at 25°C and pH 8.

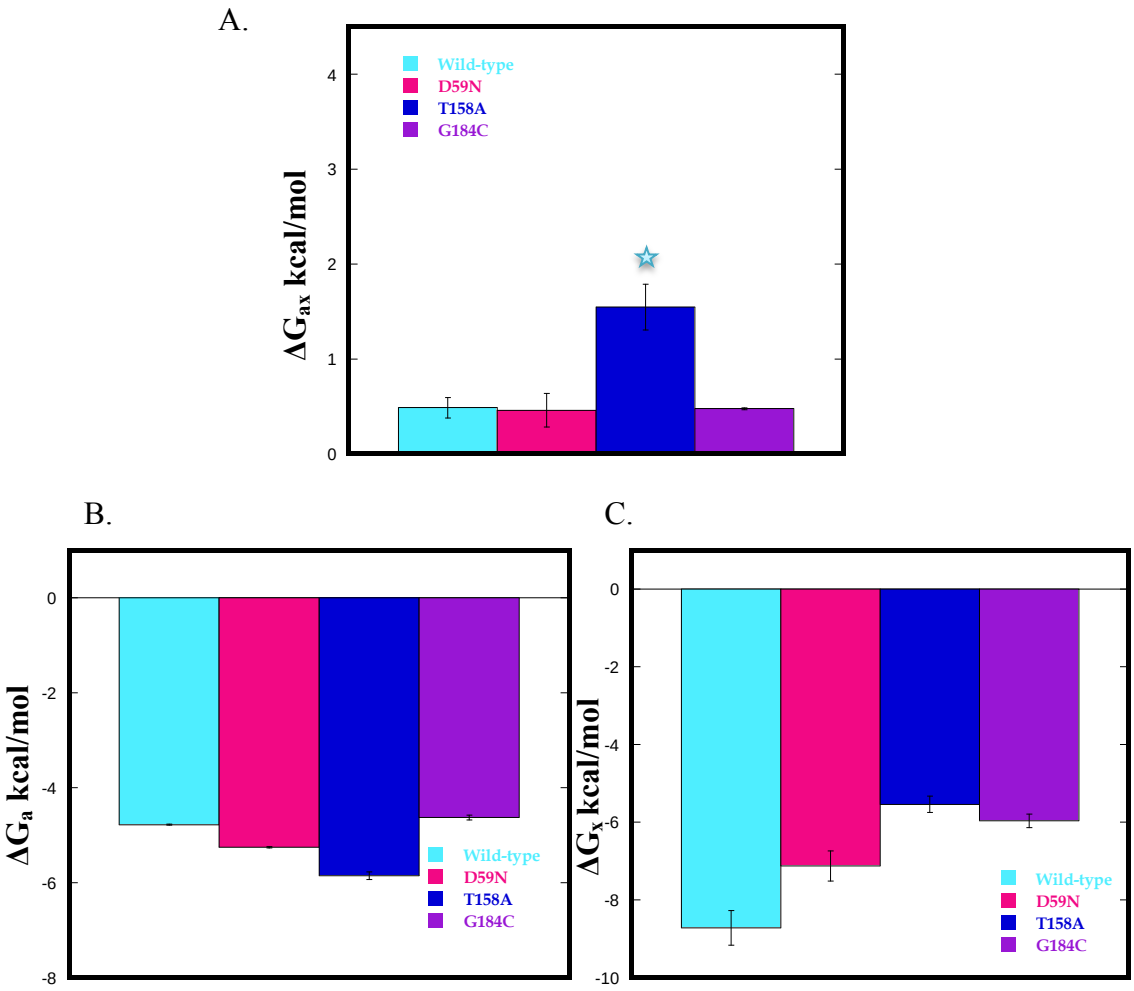

Figure 3-8. 32Å Coupling Free Energies and Binding Free Energies of BsPFK Variants. The coupling free energy for BsPFK was calculated using equation 1-5. (A) Coupling Free Energy of BsPFK WT, D59N, T158A (* uncorrected), and G184C. (B) Binding Free Energies for F6P. (C) Binding Free Energies for PEP. Data were collected at 25°C and pH 8.

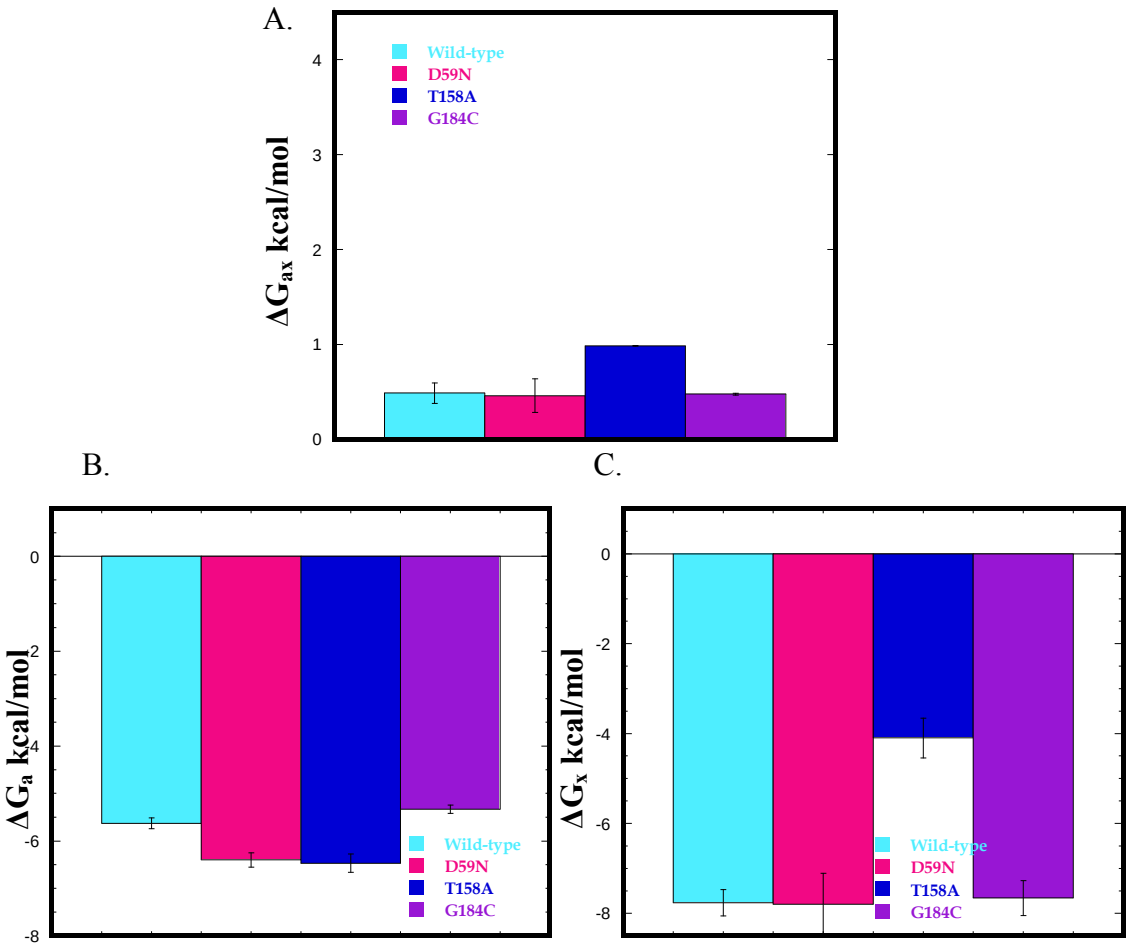

Figure 3-9 30Å Coupling Free Energies and Binding Free Energies of BsPFK Variants. The coupling free energy for BsPFK was calculated using equation 1-5. (A) Coupling Free Energy of BsPFK WT, D59N, T158A, and G184C. (B) Binding Free Energies for F6P. (C) Binding Free Energies for PEP. Data were collected at 25°C and pH 8.

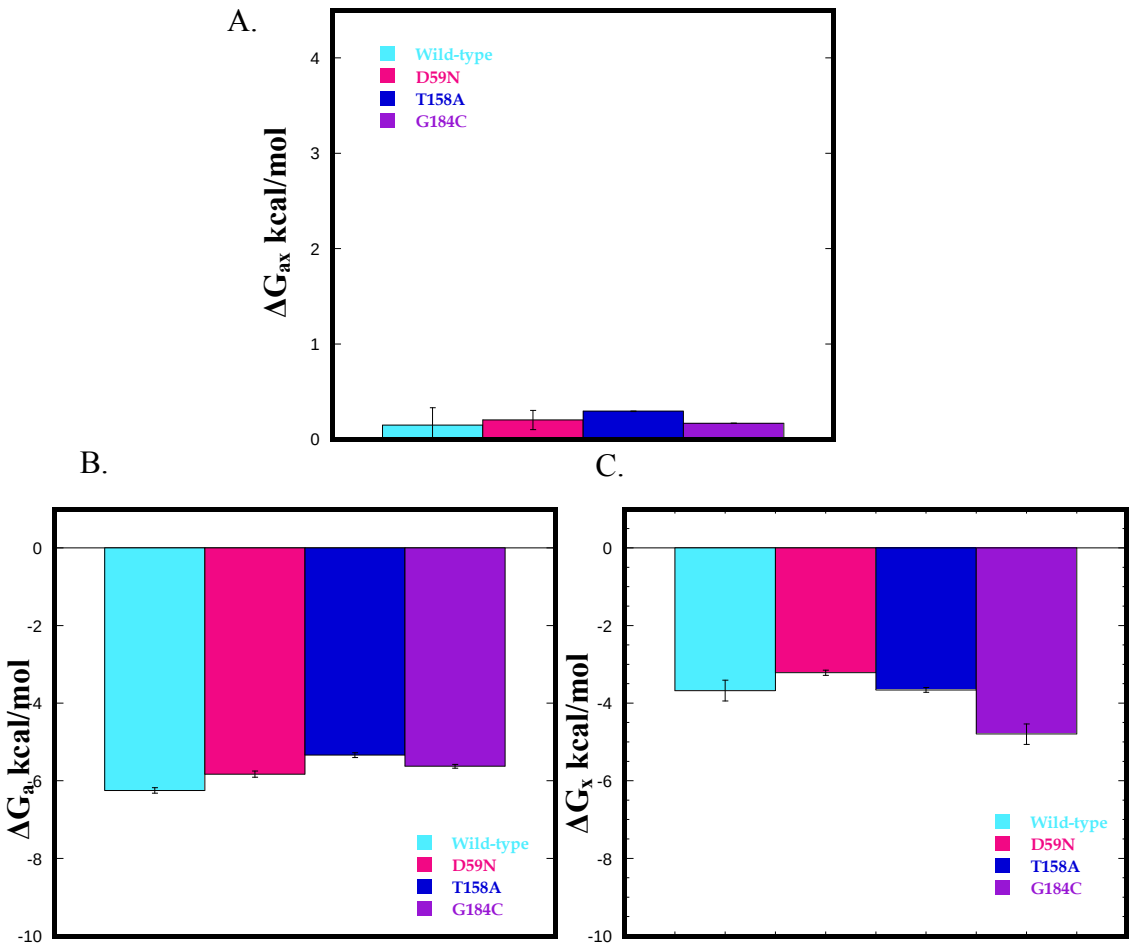

Figure 3-10. 45Å Coupling Free Energies and Binding Free Energies of BsPFK Variants. The coupling free energy for BsPFK was calculated using equation 1-5. (A) Coupling Free Energy of BsPFK WT, D59N, T158A, and G184C. (B) Binding Free Energies for F6P. (C) Binding Free Energies for PEP. Data were collected at 25°C and pH 8.

Threonine 158 to Alanine

The alanine mutation was introduced at the 158 position of the enzyme into all the individual heterotropic interactions. The coupling parameters were then quantified using the initial velocity experiments for all four interactions as shown in Figure 3-11. With the exception of the 32Å hybrid construct, similar 1|0 controls were completed to account for any inhibitory affect the mutated allosteric sites may have on the binding of substrate to the native active site as described in the previous paragraph. T158A has a significant role in diminishing the coupling of the 22Å interaction as indicated in Figure 3-7. This residue lies between the active and allosteric site as shown in Figure 3-3 parts (b) and (c). It increases coupling in the 30Å and has no effect on the 45Å interaction as displayed in Figure 3-9 and 3-10 respectively. The extent of perturbation concerning the 32Å interaction was found to be inconclusive as shown with an asterisk in Figure 3-8 due to the instability of the hybrid construct for the 1|0 control needed to calculate the corrected values for substrate binding affinity. The threonine at this position has been shown to be of great significance in a lesser inhibited phosphofructokinase from *Thermus thermophilus*. In the tetrameric form of the enzyme, the alanine at position 158 was mutated to a threonine. The modest coupling free energy value for the enzyme was enhanced over 1 kcal/mol with this single mutation and nearly an additional 1 kcal/mol when combined with the asparagine at position 59 mutated to an aspartic acid (*54*).

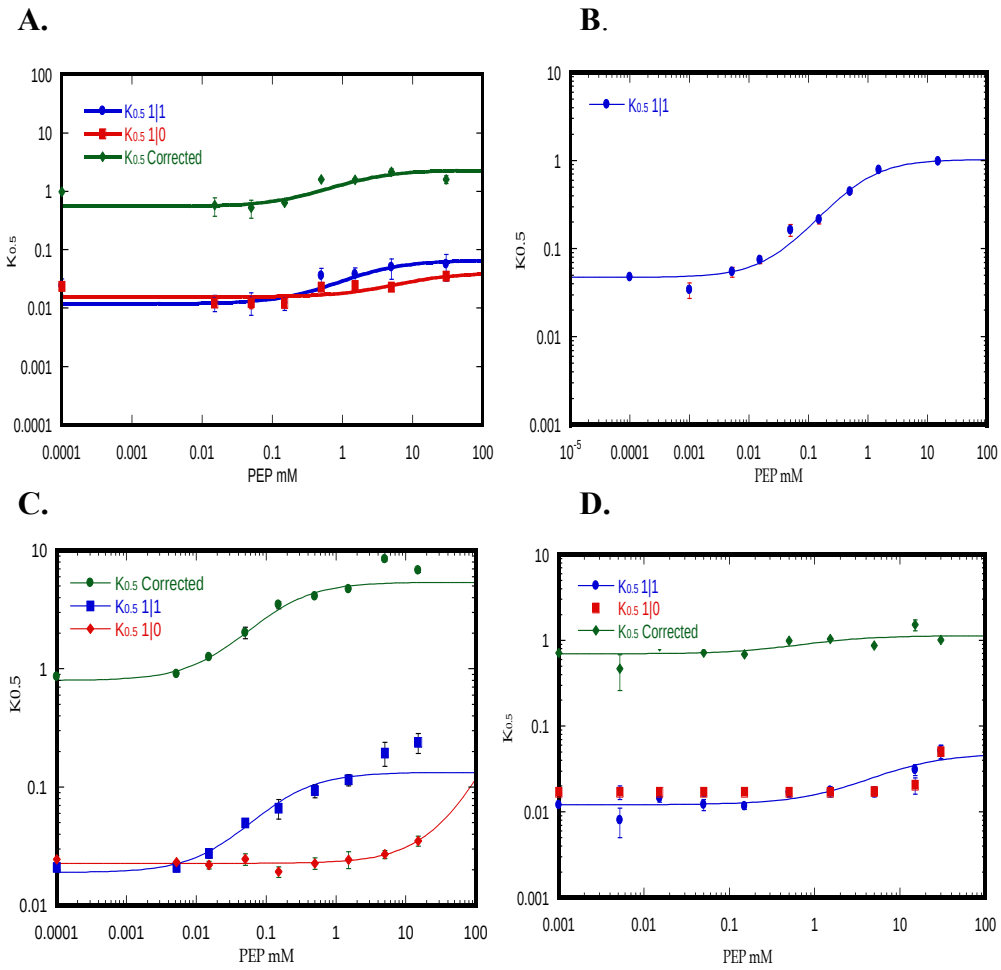

Figure 3-11 Change in the Apparent Dissociation Constants for Substrate as a Function of Effector Concentration Due to T158A **A**. 22Å interaction including the1|1 and the 1|0 experiments **B**. 32Å interaction including the 1|1 experiment **C.** 30Å interaction including the 1|1 and 1|0 experiments, **D**. 45Å interaction including the 1|1 and the 1|0 experiments.

Glycine 184 Mutated to a Cysteine

A cysteine mutation was also introduced at the 184 position of the enzyme into all the individual heterotropic interactions. The coupling parameters were then quantified using the initial velocity experiments for all four interactions as shown in Figure 3-12, including the proper 1|0 controls for each interaction. When comparing the three residues to the wild-type 22Å interaction, residue 184 showed the greatest reduction in coupling as shown in Figure 3-7. The mutation did not have any effect, however on the coupling of the 32Å interaction as seen in Figure 3-10 even though it is located in close proximity between the two native sites as shown in Figure 3-3. In addition, residue G184 does not play a significant role in either the 30Å or 45Å interaction as shown in Figure 3-9 and Figure 3-10, respectively. G184 was previously shown to play a role in the coupling of the 22Å interaction for EcPFK (*53*). To validate the significance for EcPFK, the side chain was also changed to threonine and a valine, yet the diminishment in the coupling between the two ligands was similar to the cysteine alteration, establishing the importance of G184 in the signaling of the 22Å interaction for both EcPFK and BsPFK.

The Allosteric Impact of Each Residue Is Confined to One Subunit

The impact on the four single heterotropic interactions as a result of each single mutation can be summed up and compared to the total heterotropic communication of the enzyme similar to the wild-type heterotropic interactions as shown in Figure 1-9. As described in Chapter I, the wild-type BsPFK enzyme contains both homotropic and

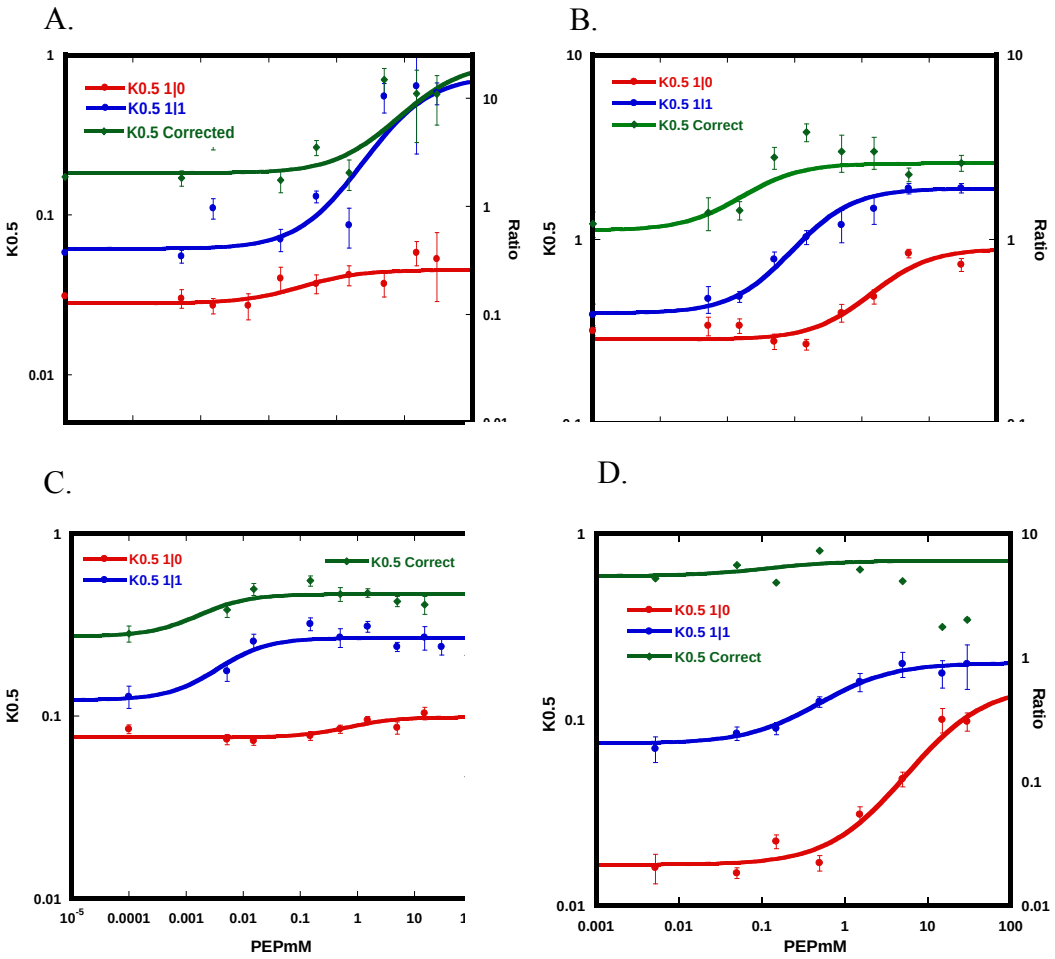

Figure 3-12 Change in the Apparent Dissociation Constants for Substrate as a Function of Effector Concentration Due to G184C **A**. 22Å interaction including the1|1 and the 1|0 experiments **B**. 32Å interaction including the 1|1 and 1|0 experiments **C.** 30Å interaction including the 1|1 and 1|0 experiments, **D**. 45Å interaction including the 1|1 and the 1|0 experiments.

heterotropic communication pathways. A special hybrid construct, known as a 4|1 hybrid, is used to measure only the heterotropic communication of the enzyme since it contains 4 native active sites and only one native allosteric site as depicted in Figure 3-2. As shown in Figures 3-13, the impact of the T158A mutation on the four individual heterotropic interactions are summed up in the right half of the figure and are compared to the impact of the T158A mutation on the total heterotropic communication of the enzyme. Figure 3-14 shows the influence of the G184C mutation on the four individual heterotropic interactions. They are summed up in the right half of the figure and are compared to the impact of the G184C mutation on the total heterotropic communication for BsPFK. Figure 3-15 shows the sum of the changes in coupling of the four individual interactions as a result of the D59N mutation. This summation is compared to the total diminishment in heterotropic coupling for the D59N variant. Since the summation for each variant does not exceed the respective 4|1 control, it can be concluded that the alterations in allosteric communication can be accounted for within the single subunit, meaning there are few inter-subunit effects as a result of the mutation. The summation from the T158A perturbation includes the uncorrected value from the 32Å interaction thereby surpassing the limit of its respective 4|1 control.

In conclusion, residues D59, T158, and G184 have been identified to likely play a significant role in the allosteric communication of BsPFK. All three of the residues seemed to effect the communication of the 22Å interaction indicating an indirect transmission of communication for this particular pathway due to the dispersal of these residues throughout the subunit. Past predictions have implicated other residues near the

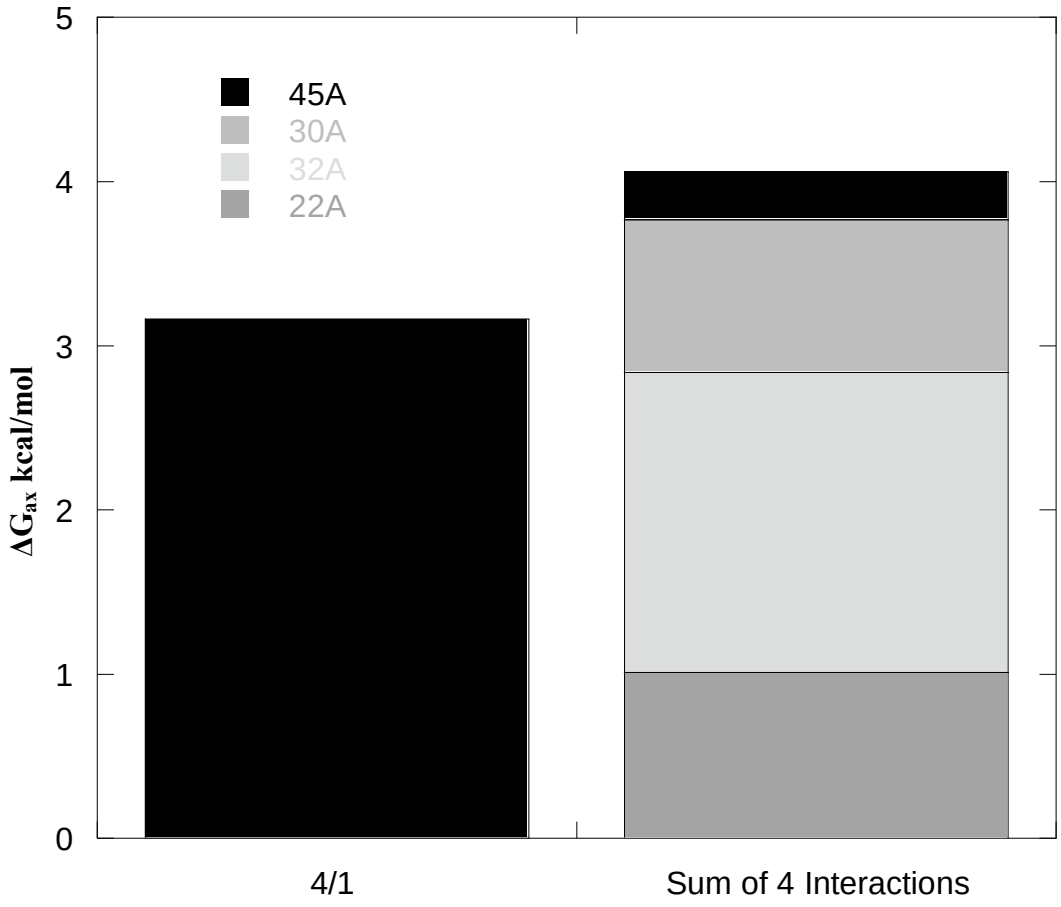

Figure 3-13 Coupling Free Energies of BsPFK T158A Heterotropic Control vs Summation of Heterotropic Interactions. The coupling free energy for BsPFK was calculated using equation 1-5. Data were collected at 25°C and pH 8.

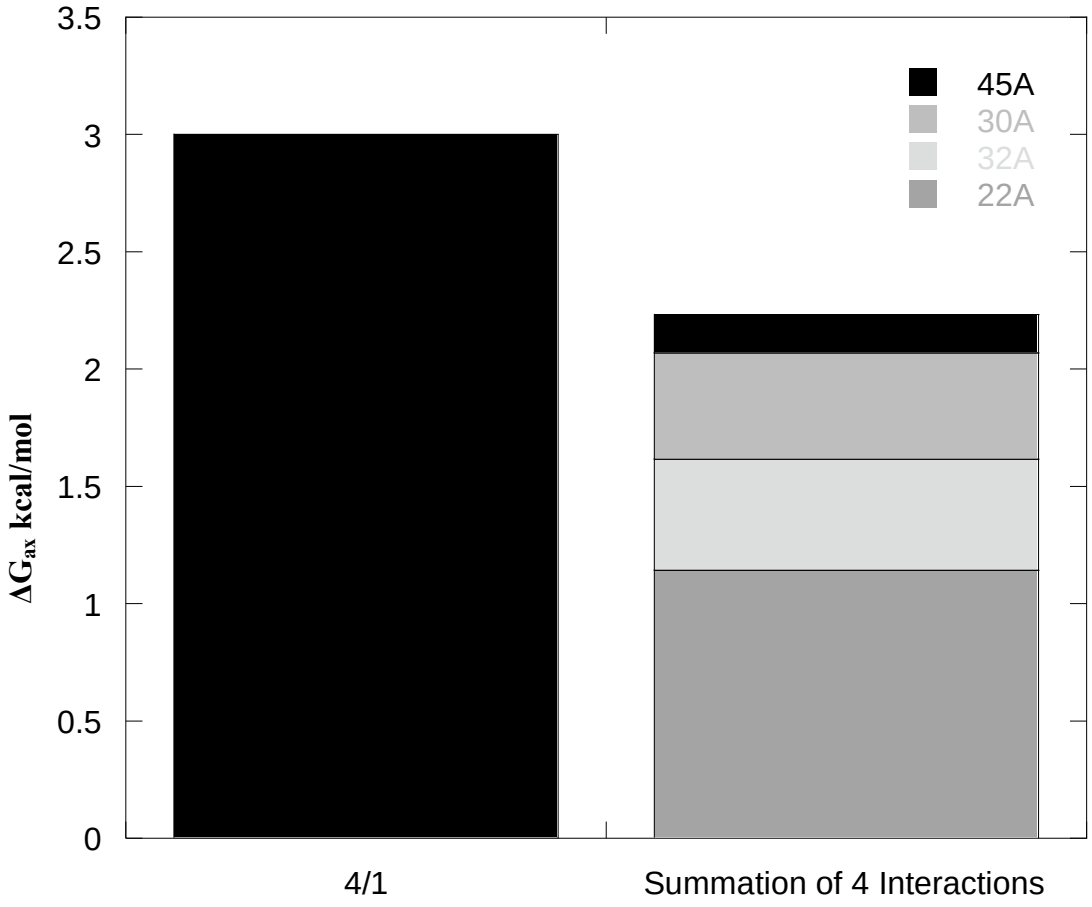

Figure 3-14 Coupling Free Energies of BsPFK G184C Heterotropic Control vs Summation of Heterotropic Interactions. The coupling free energy for BsPFK was calculated using equation 1-5. Data were collected at 25°C and pH 8.

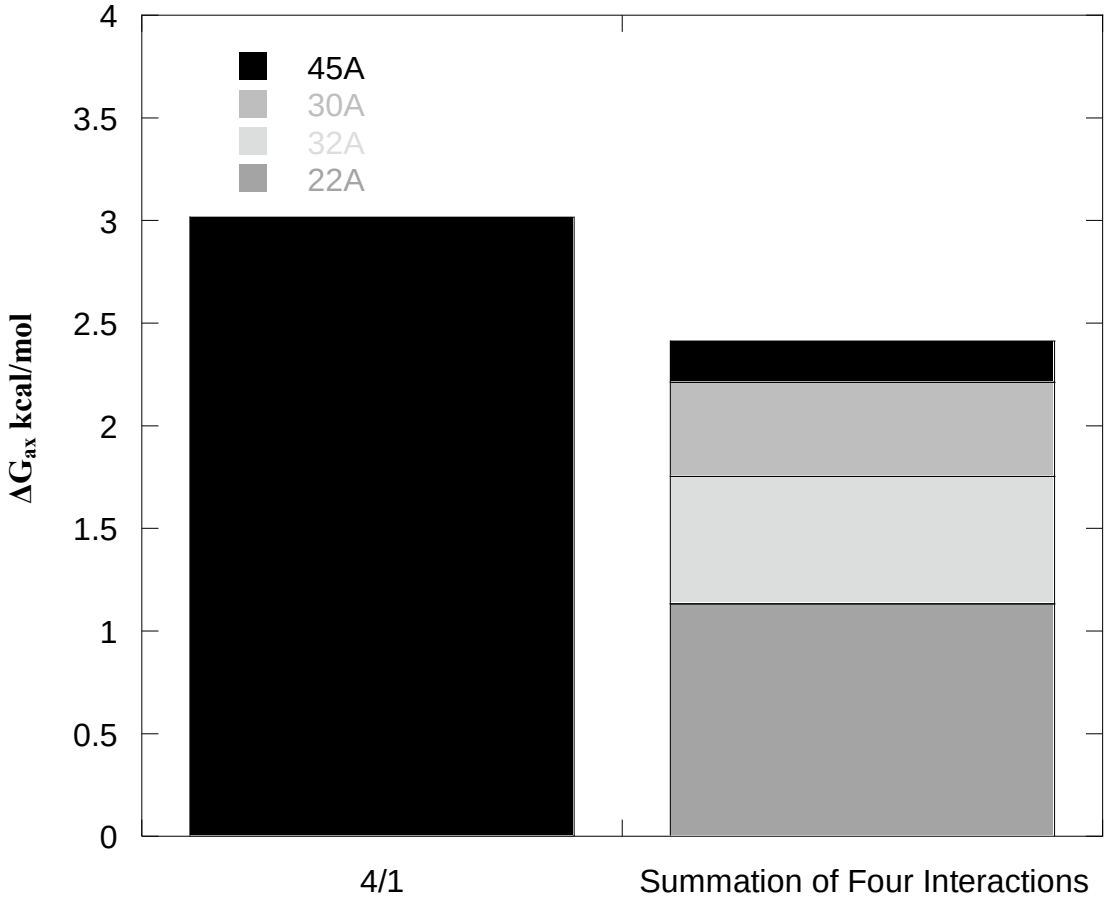

Figure 3-15 Coupling Free Energies of BsPFK D59N Heterotropic Control vs Summation of Heterotropic Interactions. The coupling free energy for BsPFK was calculated using equation 1-5. Data were collected at 25°C and pH 8.

active site and a structural quaternary shift within the enzyme responsible for the transmission of the allosteric signal (*21*). When directly measured, however, these predictions were shown to be false (*25, 55*). Current studies utilizing the hybrid strategy with a thermodynamic linked function analysis enables the identification of new residues whose magnitude of influence on a single interaction from the 28 potential interactions can be measured directly. Future experiments are needed to find residues that affect the other three unique lines of heterotropic communication and to also assess their degree of independence from each other.

CHAPTER IV

ILLUMINATING DYNAMIC CHANGES ASSOCIATED WITH HETEROTROPIC ALLOSTERIC COMMUNICATION IN PHOSPHOFRUCTOKINASE FROM *BACILLUS STEAROTHERMOPHILUS*

Introduction

Upon ligand binding, phosphofructokinase from *Bacillus stearothermophilus* (BsPFK) undergoes both conformational and dynamic changes throughout its rigid structure. Ligands such as fructose 6-phosphate (F6P) bind to four identical sites along the active site interface and phospho(*enol*)pyruvate (PEP) binds to four identical sites located along the allosteric site interface. When distinguishing the nature and the extent of the allosteric effect between F6P and PEP, all possible ligation states of the enzyme are considered with respect to the two ligands: BsPFK, BsPFK-F6P, PEP-BsPFK, and PEP-BsPFK-F6P.

Experimentally, the effect PEP has on the binding of F6P to the enzyme can be quantified in terms of Q_{ax}, the coupling constant defined as a ratio of thermodynamic dissociation constants of F6P (A) and PEP (X):

$$Q_{ax} = \frac{K^{\circ}_{ia}}{K^{\infty}_{ia}} = \frac{K^{\circ}_{ix}}{K^{\infty}_{ix}} \tag{4-1}$$

where K°_{ia} and K^{∞}_{ia} are the substrate dissociation constants in the absence and saturating presence of effector respectively. Parameters K°_{ix} and K^{∞}_{ix} are the effector dissociation constants in the absence and saturating presence of substrate respectively. With simple substitutions in this equation, the coupling constant can serve as an equilibrium constant between the four species in a disproportionation reaction:

$$XE + EA \overset{Q_{ax}}{\longleftrightarrow} E + XEA \tag{4-2a}$$

$$PEP - BsPFK + BsPFK - F6P \overset{Q_{ax}}{\longleftrightarrow} BsPFK + PEP - BsPFK - F6P \tag{4-2b}$$

where the left side of the reaction includes the two binary complexes and the right side includes free enzyme and the ternary complex. The PEP-BsPFK species (XE) denotes the inhibitor bound to the enzyme's allosteric sites and the BsPFK-F6P species (EA) is defined as substrate bound to the active sites of the enzyme. The BsPFK (E) is the free enzyme species with no ligands present and the PEP-BsPFK-F6P species (XEA) contains inhibitor bound to the allosteric sites and F6P bound to the active sites. For this reaction, the standard free energy can either be defined in terms of the equilibrium constant or its enthalpy and entropy parameters:

$$\Delta G_{ax} = -RT\ln(Q_{ax}) = \Delta H_{ax} - T\Delta S_{ax} \tag{4-3}$$

$$+3.67\ \text{kcal/mol} = -RT\ln(0.004) = (-10\text{kcal/mol}) - (-14\text{kcal/mol}) \tag{4-4}$$

where R equals the gas constant, T is the absolute temperature in Kelvin. The standard free energy ΔG, referred to in this case as coupling free energy ΔG_{ax} (*31, 32*), has a positive value of 3.5 kcal/mol at 25°C, pH 8.0, indicative of an unfavorable reaction due to inhibition. By measuring the coupling constant at various temperatures, van't Hoff analysis revealed the coupling enthalpy and coupling entropy values (equation 4-4) (*27*). It is made evident here that the sign and value for coupling free energy, ΔG_{ax}, is established by the dominating coupling entropy value. In other words, the coupling entropy value is what distinguishes PEP as an inhibitor rather than a molecule that facilitates or has no effect on the binding of F6P to the enzyme. In an effort to ascertain the molecular basis for PEP as an inhibitor, one must first return to the four enzyme

species depicted in equation 4-2b and their differences that ultimately generate the thermodynamic values of ΔH and ΔS as shown in equation 4-4.

In general, most allosteric models have attributed their regulation in binding by the obvious changes in structure. However, in 1984 Cooper and Dryden suggested that the allosteric signal could be induced by changes in the protein dynamics upon ligand binding. They propose a model where this dynamic form of allostery is entropy-driven. Since it has previously been established that the entropy parameter is what classifies PEP as an inhibitor and this enzyme reaction is defined by four enzyme species, one can use the dynamic differences of the four enzyme species to focus on the enzyme's entropy characteristics in hopes to find new insight into the allosteric properties of BsPFK. In addition, the linearity in the data used for van't Hoff analysis of PEP coupling as a function of temperature suggests minimal changes in heat capacity associated with solvation differences between free ligand and the enzyme species. Thus, it can be suggested that the origins of the coupling entropy is the dynamic differences of the four enzyme species upon ligand binding.

One approach capable of detecting these changes in dynamics is fluorescence spectroscopy. Using an intrinsic fluorophore in the form of a tryptophan side-chain has previously been shown to be sensitive to the dynamic changes that occur around the immediate environment for EcPFK (*29*). One limitation to this approach with respect to BsPFK is the native tryptophan in each subunit has been shown to be only weakly responsive to the enzyme's state of ligation due to its location within a hydrophobic core. Nevertheless, phenylalanine and tyrosine residues can serve as targets for

conservative tryptophan-shift mutations. By single residue point-mutations, a phenylalanine or tyrosine residue is mutated to a tryptophan and the native tryptophan is subsequently mutated to the corresponding phenylalanine or tyrosine residue. With the use of this approach, three local regions have previously been shown to be responsive to ligand binding and were studied by fluorescent techniques (*56-58*)

This chapter attempts to correlate the four enzyme species and their conformational dynamic contribution to the coupling entropy parameter by measuring changes in internal motions within the vicinity of the fluorophore upon ligand binding. The strategy of using tryptophan-shift mutations is combined with the hybrid strategy for isolating individual heterotropic interactions. Specifically, a single tryptophan-shift mutant is strategically isolated in conjunction with the native 22Å interaction, the interaction with the highest contribution to the overall coupling of the enzyme. Sixteen targets throughout the subunit exist and half of them are characterized in this study by steady-state and time-resolved fluorescent measurements. The analysis from the measurements of motion could suggest specific regions that may aid in establishing the nature and magnitude of the 22Å interaction dominated by entropy.

Materials and Methods

Materials

All the chemical reagents used in buffers, protein purifications, *in vitro* hybrid strategy, and fluorescence assays are listed and described in Chapter II.

Mutagenesis

Tryptophan-shift mutants were previously constructed using the Altered Sites II Mutagenesis System (Michelle's dissertation & Rotation students). Plasmid preps were purified using kits from Qiagen, Inc. (Valencia CA). DNA sequencing to confirm each mutation was performed using the BigDye kit of ABI (Foster City, CA). For the 22Å parent, mutating the native tryptophan to a tyrosine was accomplished using Quickchange Site-directed Mutagenesis system from Stratagene. All oligonucleotides applied in this study were previously purchased from Integrated DNA Technologies (IDT).

Purification and in vitro Hybrid Formation

For the following purification and preparation of hybrids, Parent A will be described using one tryptophan example, W179 as seen in Figure 4-1. Parent B is the 22Å heterotropic interaction including the K90E/K91E charge tag mutations, R211E/K213E allosteric site mutations, the R162E active site mutation, plus the W179Y tryptophan-minus mutation. The purification and hybrid strategy of Parent A and Parent B followed the steps as previously described in Chapter II. Once the 1:3 hybrid species was isolated for each individual tryptophan-shift mutant, the four enzyme species were generated.

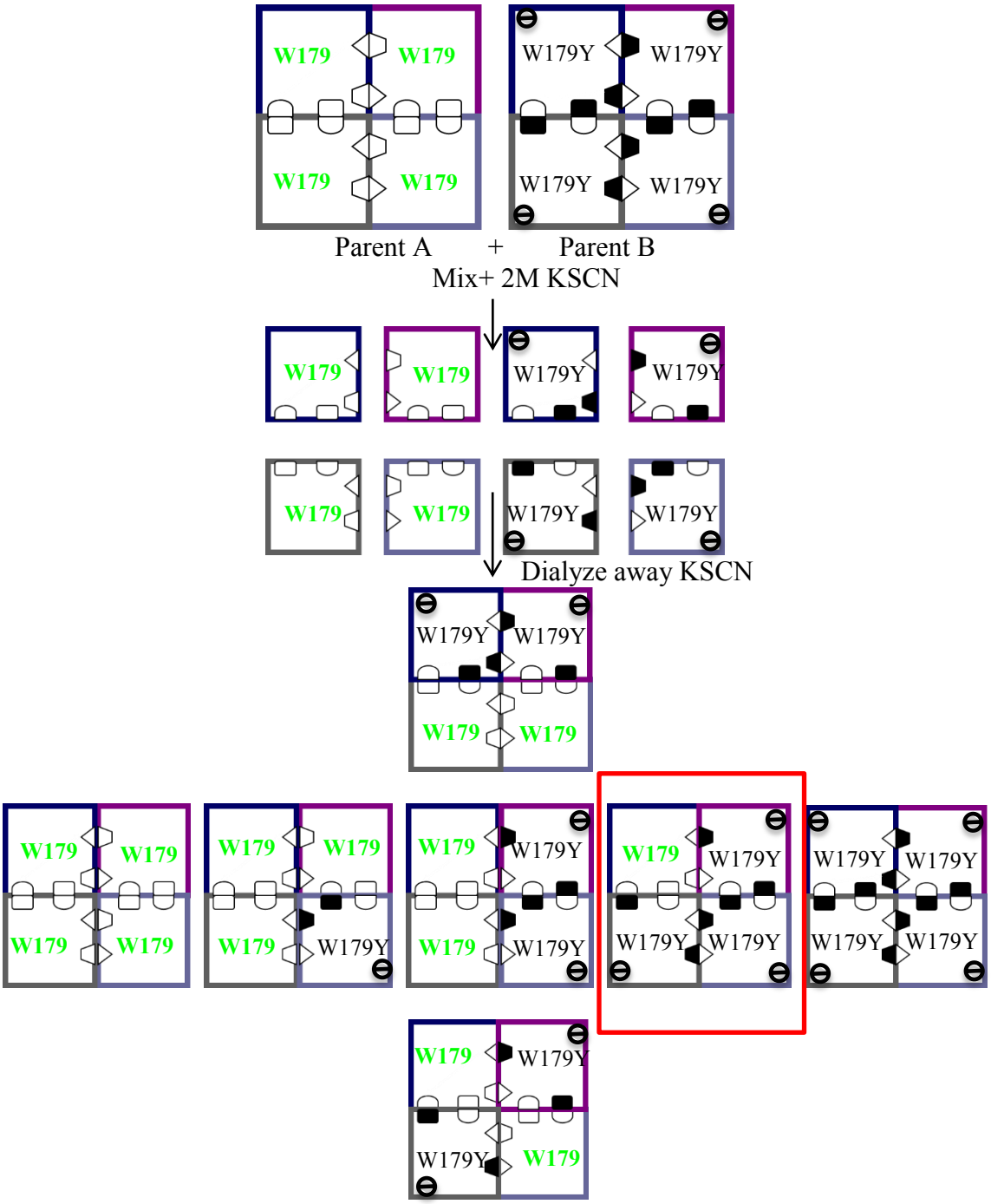

Figure 4-1 Hybrid Strategy to Isolate 22Å Interaction with a Single Tryptophan. The established protocol is modified by placing the tryptophan-shift mutant with parent A and a W179Y mutation with parent B.

Generation of Enzyme species

To generate the PEP-BsPFK species, 3mM PEP was added to BsPFK. For the generation of the substrate bound complex, 0.5mM F6P was added to BsPFK. The tertiary complex was mixed with 5mM F6P and 28mM PEP to generate PEP-BsPFK-F6P. Based on the ligand dissociation constants, less than 5% of other species were present.

Steady-state Fluorescence Measurements

Steady-state anisotropy measurements of a single tryptophan in a hybrid sample were performed on and ISS KOALA Model fluorometer using a 300-watt xenon arc lamp as the excitation source and the monochromator set to select light at 300nm. The light was passed through a Glan-Taylor vertical polarizer and the emission was collected for each sample through a 2mm thick Schott WG 335nm cut-on filter and a Glan-Thompson polarizer. All samples were measured in a buffer of 50 mM EPPS-KOH pH 8.0, 10 mM MgCl2, 100 mM KCl, and 0.1 mM EDTA, with a buffer blank correction.

Frequency-Domain Fluorescence Measurements

Measurements for frequency-domain fluorometry were performed on an ISS K2 multi-frequency fluorometer with a 300nm Light Emitting Diode (LED) as the light source. Modulation frequencies were produced using a Marconi 2022A Synthesizer. Since the LED light source is not vertically polarized, the modulated emission was passed through a 2mm thick WG Schott 345nm cut-on filter and a Glan-Thompson polarizer oriented at 35.3° to the vertical axis to avoid polarization artifacts (Spencer and Weber 1970). With a lifetime of 2.85 ns, NATA (N-acetyl-tryptophanamide, phosphate

buffer pH 7.0, Kodak) served as a reference sample for the 12 excitation frequencies used to obtain the phase shift and modulation data for each ligation state of the enzyme (lackowicz and gryczynski, 1991). Data was analyzed with ISS Software.

Results and Discussion

Characterization of Tryptophan Mutants

A single monomer of the protein contains sixteen phenylalanine and tyrosine residues, however only eight were targeted for tryptophan-shift mutations in this study as shown in Figure 4-2. Each individual target was mutated to a tryptophan to serve as the single fluorescent probe monitored in the steady-state and time-resolved measurements, with their respective distances from the 22Å active site and allosteric site shown in Table 4-1. Therefore, parent A consists of eight different resulting proteins: F230W/W179Y, Y164/W179Y, F240W/W179Y, F139W/W179Y, Y196W/W179Y, Y41W/W179Y, Y69W/W179Y, and Y311W/W179Y. Parent B stays constant in mutation with each hybrid formation and is commonly referred to as the 22Å Trp minus heterotropic interaction: R162E/R211E/K213E/K90E/K91E/W179Y. Both parents were expressed in *E.coli*, the same bacterial system as wild-type, and were purified according to the same protocol. The steady-state kinetic parameters with F6P and PEP as ligands were characterized for each parent A form and are listed in Table 4-2.

Steady-state Fluorescence Experiments

The steady-state experiments included measuring the environmental change detected by a tryptophan's side chain in the absence, and presence of each ligand added

individually and simultaneously. These measurements are repeated with each new location for the fluorophore within the subunit. The changes in anisotropy of each ligation state are graphed with respect to free enzyme in Figure 4-2A, B, and C. These changes are assumed to originate from the movement of the intrinsic fluorophore submerged within the large protein since the addition of small ligands do not alter the overall tumbling of PFK (24, 29). The environment sampled around each tryptophan-shift mutant varies in their response in the presence of ligands signifying a specific response dependent upon the location of the fluorophore.

Overall, the magnitude of anisotropy changes when compared to free enzyme are not as large as seen previously with EcPFK (53), however these changes measured for BsPFK are repeatable and vary depending on the location of the fluorophore. Any anisotropy changes greater than 0.004 were considered significant and are seen in Figure 4-3. The largest changes in anisotropy compared to free enzyme are seen when the inhibitor, PEP, is bound. Positions W164, W240, and W230 showed anisotropy changes above or below 0.01. When F6P is bound to BsPFK, the largest changes in anisotropy are seen at positions W41, W240, and W312. The binding of both ligands gives positions W139, Y196, and W230 the greatest change reaching above or below 0.005. rigidity with an increase in the rotational correlation time of W240 with 0.4 ns. The

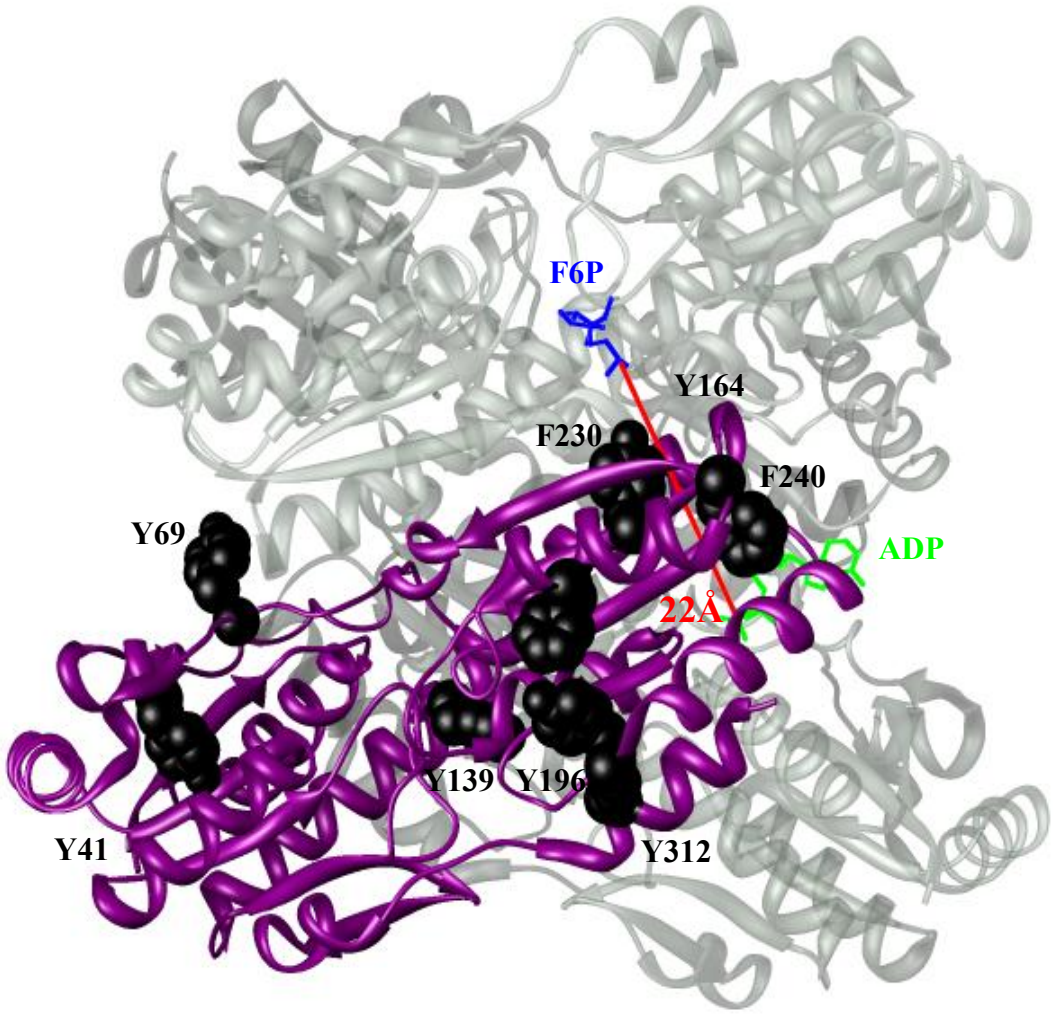

Figure 4-2 The Eight Tryptophan-Shift Mutations with Respect to the 22Å Interaction. Tryptophan-shift mutations shown in black include Y164, Y196, F240, Y139, Y312, Y69, F230, and Y41. The 22Å interaction is between F6P shown in blue and PEP (shown here as ADP) in green.

Tryptophan-Shift Mutation	Distance From 22Å Active Site	Distance from 22Å Allosteric Site
W164	6Å	16Å
W312	28Å	17Å
W41	45Å	43Å
W230	23Å	22Å
W240	18Å	16Å
W139	30Å	20Å
W69	39Å	43Å
W196	26Å	24Å

Table 4-1 Distance of Each Tryptophan-Shift Mutant from the 22Å Active and Allosteric Site. The distance from the side chain of each residue was measured to the native active site and native allosteric site.

Hybrid Protein	$K°_{ia}$ mM	$K°_{ix}$ mM	Q_{ax}
W179	0.031±0.002	0.22±0.07	0.08±0.02
W230	0.071±0.009	0.023±0.009	.056±.018
W240	0.007±0.001	0.116±0.045	.010±.004
W41	0.011±0.002	0.021±0.004	0.021±.002
W69	0.019±0.003	0.156±0.06	0.059±0.02
W196	0.009±.0009	0.14±0.063	0.0815±.04
W139	0.028±0.001	0.20±0.05	0.076±0.03
W312	0.018±0.007	0.13±0.012	0.064±0.011
W164	0.0069±.0009	0.276±0.008	0.028±0.0085

Table 4-2 Kinetic Parameters for the Tryptophan-Shift Mutants. The binding affinities and coupling constants were measured for F6P and PEP for each mutant.

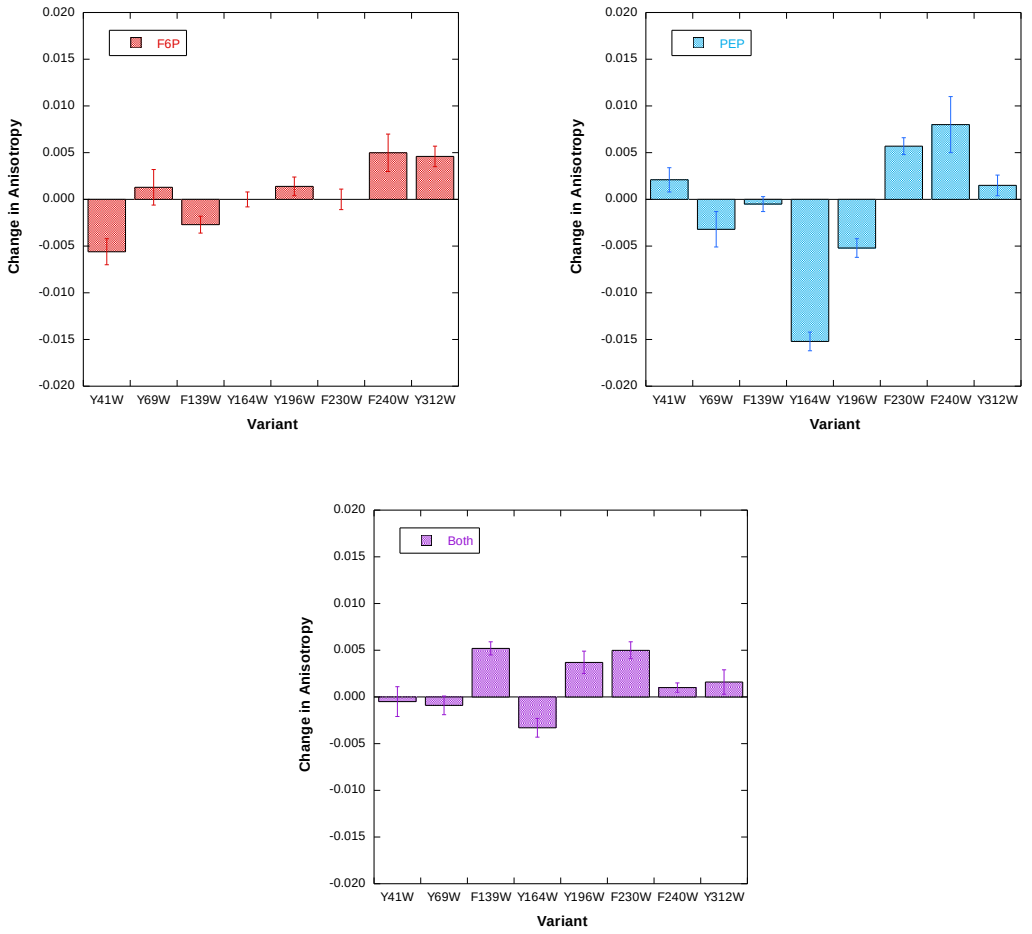

Figure 4-3 Changes in Anisotropy for Each Species. For each tryptophan-shift mutant, the changes in anisotropy of the fluorophore with respect to free enzyme is shown in red for F6P species, blue for PEP species, and purple for the PEP/F6P species.

Frequency Domain Lifetime Measurements

Changes in the anisotropy (r) measurements can originate from changes in motion (φ), either becoming more or less flexible within the region of the fluorophore, or from changes in the lifetime (τ) from the original value (r_0) of the fluorophore within the excited state as shown in the Perrin equation (*59*):

$$r = \frac{r_0}{1+(\tau/\varphi)} \tag{4-5}$$

In order to determine the lifetime influence of the anisotropy changes measured, the frequency domain method (*60*) was used to measure the lifetime of the fluorophore in its distinctive environment for each tryptophan-shift mutation. Changes in the phase and modulation of the emission from a single tryptophan were measured as a function of the frequency of the modulated excitation. For each 22Å construct, the phase and modulation were measured at each frequency in the absence of ligand, in the presence of substrate, in the presence of inhibitor, and in the presence of both substrate and inhibitor. All data were fit to various models and based upon the X^2 values, the best fit for each data set was a model containing a Lorentzian distribution plus a discrete exponential decay (*61-63*). For the 22Å interaction of BsPFK, the lifetime of each tryptophan-shift mutant is best described using two components. The first component ranged from 4-6 ns and includes the fractional contribution to the total fluorescence, $\boldsymbol{f_1}$ of the continuous distribution of lifetimes as defined by a central lifetime $\boldsymbol{\tau_1}$, the center point of the distribution, and the width $\boldsymbol{W}$, the extent of the distribution. The second component averaged 0.5ns and includes the fractional contribution 1to the total fluorescence, $\boldsymbol{f_2}$ of

the discrete exponential decay, τ_2. This second component varied only slightly. With respect to free enzyme, the changes in lifetime for all tryptophan-shift mutations are shown in Figure 4-4. In response to substrate binding the largest change in the lifetime of tryptophan is W164 with a decrease of 0.4ns. With the inhibitor bound, both W41 and W230 display an increase in fluorescence lifetime of 0.5 ns and W164 exhibited the largest change with a decrease in the fluorescence lifetime by 1 ns. When both ligands are bound, W230 and W196 increased in lifetime up to 0.5 ns while, W41, W164, and W240 all contained a decreased lifetime of 0.5 ns.

Calculation of Rotational Correlation Times

Once the lifetime values were determined for each state of ligation, the rotational correlation times were calculated to determine the time constant of motion and are shown with respect to free enzyme in Figure 4-5. In the evaluation of the data, the shape of the enzyme is assumed as a sphere. It is also assumed that any changes seen in the calculations are due to the rotational correlation time of the tryptophan, not the protein. When compared to free enzyme, increases in rotational correlation times signify the tryptophan is detecting a more rigid environment upon ligand binding. However, decreases in rotational correlation times signify a more flexible local environment as detected by the fluorophore.

In examining the protein binding to substrate, W164 showed the largest increase in flexibility with a decrease in rotational correlation time of 0.5 ns and a slight increase in rigidity with an increase in the rotational correlation time of W240 with 0.4 ns. The

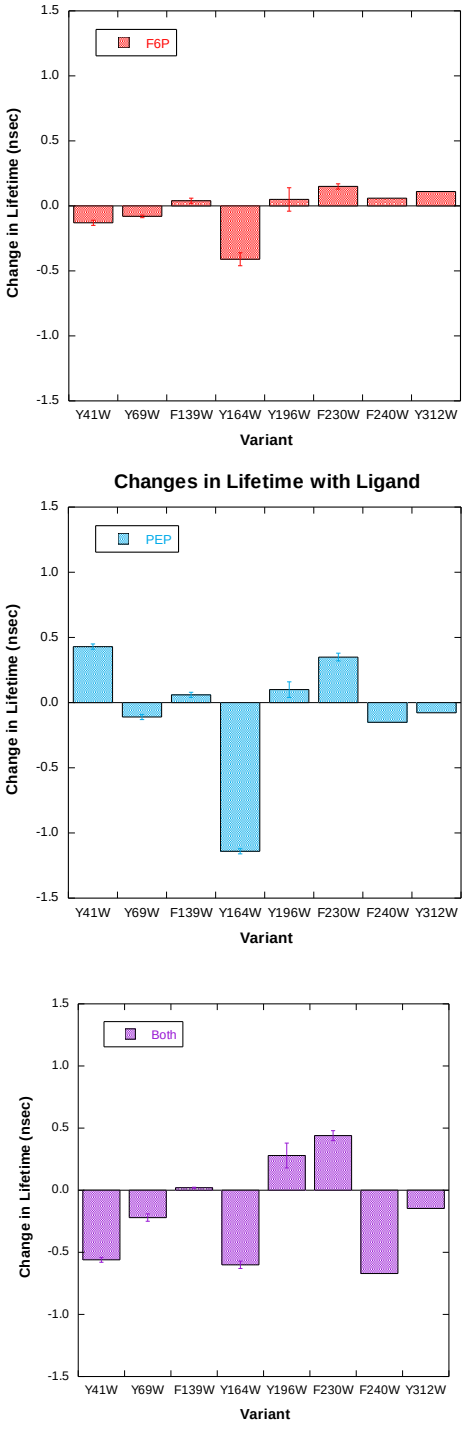

Figure 4-4 Changes in Lifetime for Each Species. For each tryptophan-shift mutant, the changes in the lifetime of the fluorophore with respect to free enzyme is shown in red for F6P species, blue for PEP species, and purple for the PEP/F6P species.

inhibitor bound structure exhibited the highest magnitude of change with decreases in the rotational correlation times of 3 ns around W164 and 2 ns at W240. W196 also decreased in its rotational correlation time, however to only 1 ns. Increases in structure rigidity occur at W230 with an increase in rotational correlation time of 2 ns. These findings are summarized structurally in Figure 4-6.

To distinguish changes in dynamics necessary for the allosteric regulation of BsPFK, it was essential to first define the dynamic properties in terms of motion for each ligation state of the enzyme as shown in equation 4-2. Now, the structural changes in terms of motion within the enzyme can be related to the energetics of allosteric coupling between the two ligands by elaborating on ΔG_{ax} as described previously (*64*):

$$\mathrm{PEP} - \mathrm{BsPFK} + \mathrm{BsPFK} - \mathrm{F6P} \overset{\Delta G_{ax}}{\longleftrightarrow} \mathrm{BsPFK} + \mathrm{PEP} - \mathrm{BsPFK} - \mathrm{F6P} \qquad (4\text{-}6)$$

where the equilibrium constant, Q_{ax} is replaced by the coupling free energy value ΔG_{ax} that it defines. Furthermore in reevaluating the disproportionation equilibrium equation, it is the contrast of the summation of chemical potentials of the left side of the equation versus the summation of the right side that determines the value of $\Delta G_{ax.}$ The coupling free energy value can further be described in terms of the coupling free energy of the products minus the coupling free energy of the reactants (*55*):

$$\Delta G_{ax} = (G_{XEA} + G_E) - (G_{EA} + G_{XE}) \qquad (4\text{-}7)$$

To simplify the equation in terms of free enzyme, subtracting the G_E term from both sides of the equation gives a simple rearrangement:

$$\Delta G_{ax} = \delta G_{XEA} - (\delta G_{EA} + \delta G_{XE}) \qquad (4\text{-}8)$$

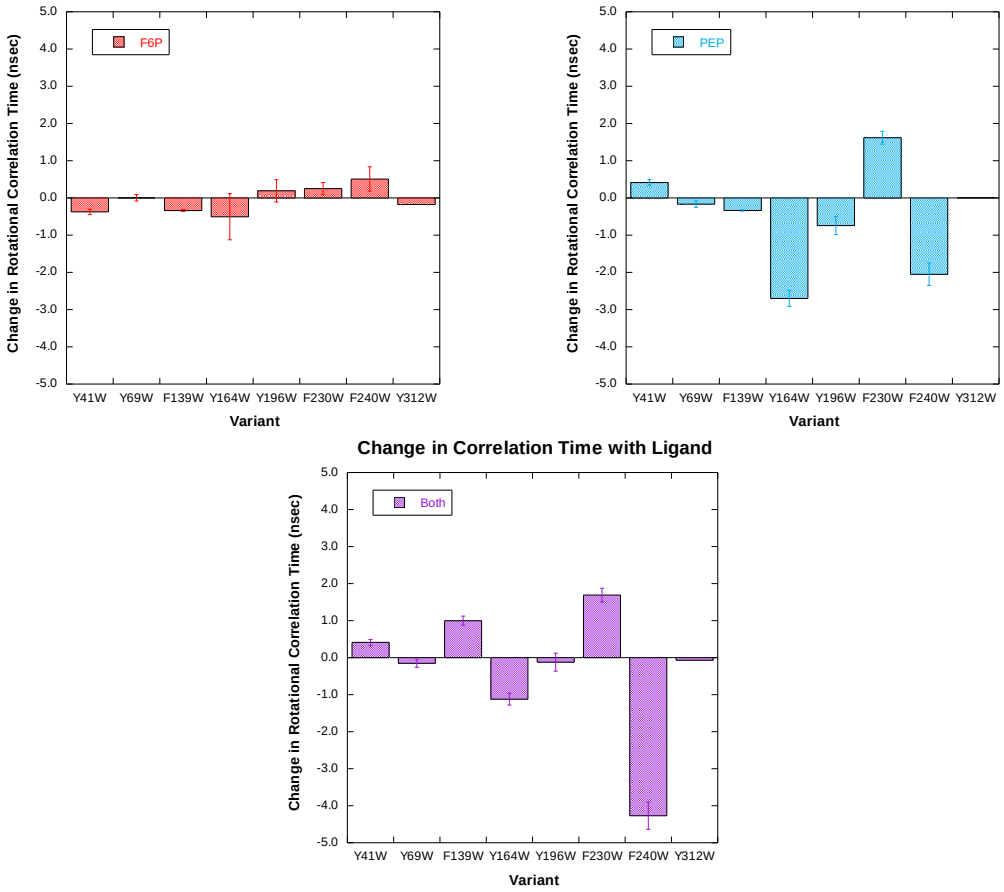

Figure 4-5 Changes in the Rotational Correlation Times of Each Species. For each tryptophan-shift mutant, F6P species are shown in red, PEP species are shown in blue, and the PEP/F6P species is shown in purple.

F6P

PEP

F6P/PEP

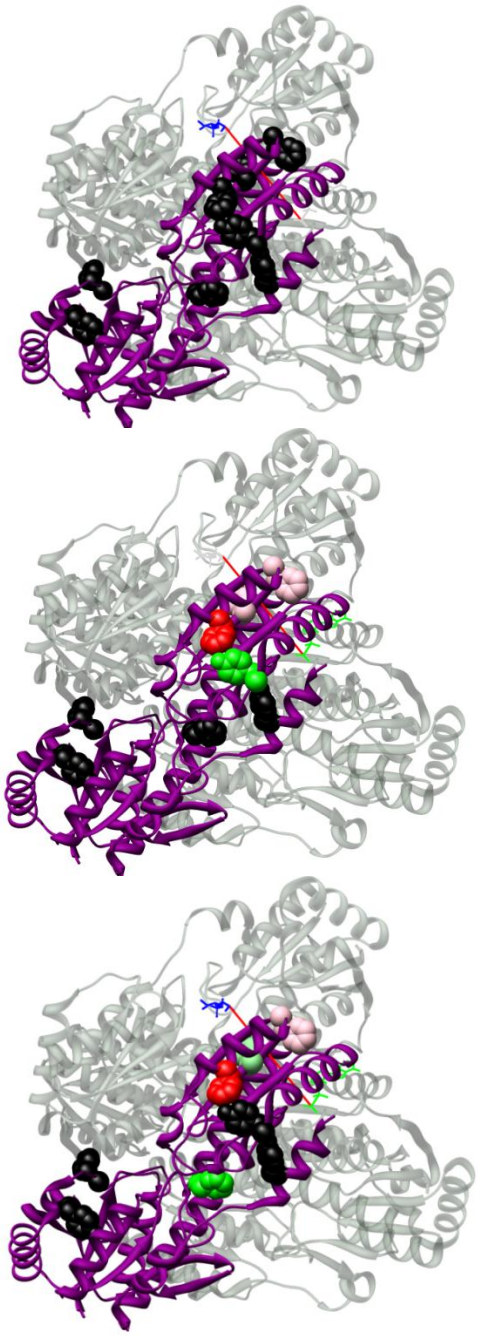

Figure 4-6 Structural Changes in Rotational Correlation Times. Residues with changes above or below 1 ns is indicated by a green or lime green color respectively. Residues with changes above or below 2 ns are indicated by a red or pink color respectively.

where the lower case delta δ signifies the differences with respect to the free energy value of the free enzyme species. The value of δG_{XEA} is equal to the difference in the formation of XEA to free enzyme so any perturbation in the free energy created when both A and X bind simultaneously to the enzyme is accounted for in this component.

When this value is equal to the summation of the perturbations that occur when the ligands bind individually, ΔG_{ax} equals zero, and by definition there is no allosteric effect. Rather, inhibition or activation occurs when these values are not equal to each other. The same can be said for coupling enthalpy and coupling entropy:

$$\Delta H_{ax} = \delta H_{XEA} - (\delta H_{EA} + \delta H_{XE}) \quad (4\text{-}9)$$

$$\Delta S_{ax} = \delta S_{XEA} - (\delta S_{EA} + \delta S_{XE}) \quad (4\text{-}10)$$

As previously mentioned, the coupling entropy in this study, favors the formation of ligands binding individually to the enzyme thus defining PEP as an inhibitor. Since structural perturbations in the form of motion can be attributed to this coupling entropy of the system, the rotational correlation times of each species were reexamined in Figure 4-7 to find local regions within the enzyme that may be part of the allosteric pathway in BsPFK. These regions of interest can be found by comparing the differences in rotational correlation times when the ligands bind simultaneously to the enzyme versus the summation of rotational correlation times when the ligands bind individually. Positions W312, W196, W41, and W69 show no substantial changes in their rotational correlation times. Position W230 shows significant changes in rotational correlation times within each species however, the ternary complex seems able to accommodate the perturbations brought on by the ligands at this location. Position W139 may have a role

in the allosteric pathway of the 22Å interaction, but the response is not strong enough in magnitude to regard this location as noteworthy. Positions W164 and W240 possessed the greatest differences in the comparison of rotational correlation times between the ternary complex and the summation of the binary complexes. These two positions are also in close proximity to the linear pathway between the 22Å active site and allosteric site as seen in Table 4-1.

To assess the direct influence the side chains of residue 164, 196, and 240 have on the allosteric communication of the 22Å interaction, site-directed mutagenesis was used to perturb the communication pathway between the two native sites. An alanine residue was introduced as a strategy to increase the flexibility of the side chain and thus an increase in communication. In addition, a proline residue was introduced to decrease the flexibility of the side chain, thus restricting the allosteric pathway. The coupling constant was measured for each of these individual modifications including residue 196, which showed little contribution in the communication between the two binding sites. These values were then compared to the coupling constant of the wild-type 22Å interaction, as shown in Figure 4-8. The side chains play a marginally significant but suggestive role in the direct coupling of the active and allosteric site within the single interaction.

In summary, the hybrid strategy was originally developed to isolate and experimentally characterize one heterotropic interaction from the sixteen heterotropic interactions present in BsPFK. Of the four unique heterotropic interactions, each possess their own coupling free energy influence with the 22Å interaction providing the

greatest influence to the overall inhibition to the enzyme. In addition, the hybrid method has successfully allowed the relocation of a single tryptophan to known proximities from this isolated 22Å interaction within the same subunit. Further studies can be completed with the three remaining heterotropic interactions and the uncharacterized eight tryptophan-shift mutations. Upon the addition of ligand, side-chain dynamics of the single tryptophan should reveal the nature of the local structural perturbations that occur in response to the mutual communication shared between an allosteric site 22 angstroms away from its coupled active site. With the use of the Perrin equation, these structural perturbations are characterized in the calculated rotational correlation time of the fluorophore in an attempt to gain insight on the origin of the entropic effect needed for allostery. In order for these dynamic measurements to be related to allostery, a coupling entropy difference must be measured for the effect of both ligands binding simultaneously compared to the summation of the influence when measured separately. Of all the locations sampled within the subunit, the analysis from the rotational correlation time data suggest that residues Y164 and F240 are in a dynamic area important in establishing the nature and magnitude necessary for the allosteric communication of the 22Å interaction as shown in Figure 4-9. It has previously been shown that solvent effects and changes in heat capacity do not play a major role in the input of entropy to this system (*29, 65*). In 1984, Cooper and Dryden proposed on the basis of theoretical calculations that changes in the dynamics of the protein are capable of driving an allosteric effect that may not be apparent in crystal structure comparisons (*66*).

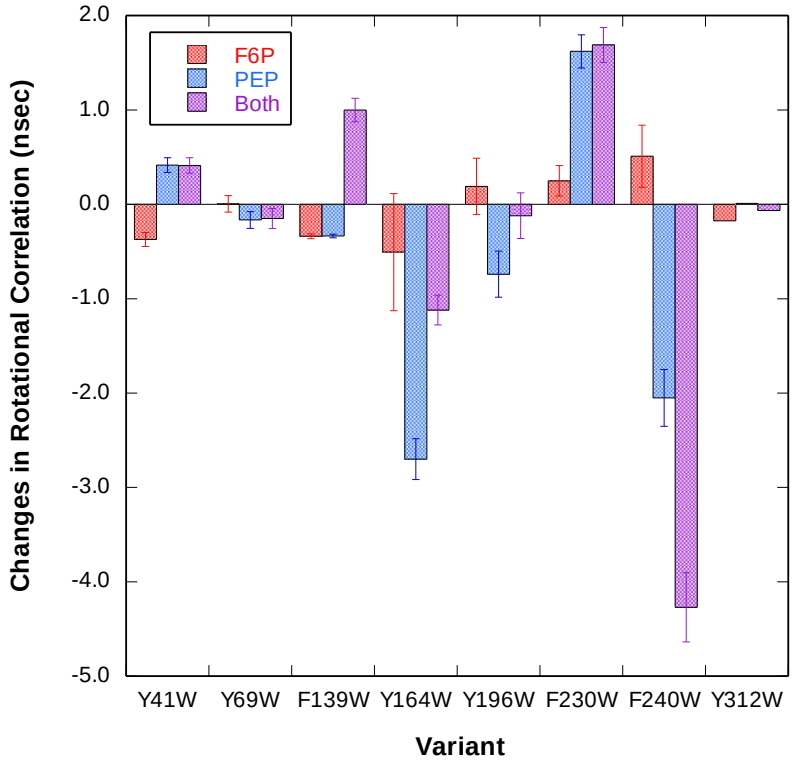

Figure 4-7 Changes in the Rotational Correlation Times of Each Fluorophore with Respect to Free Enzyme. The species shown with each variant are the rotational correlation times with F6P present, with PEP present, and with both F6P and PEP present.

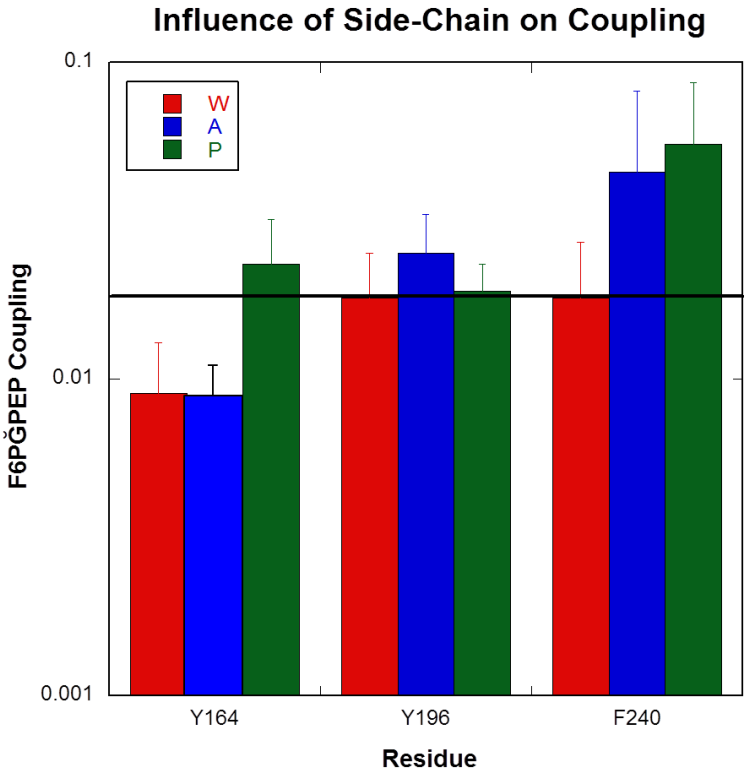

Figure 4-8 Coupling Constants Measured for Three Residues. With the use of mutagenesis, the coupling parameters were measured with a tryptophan, alanine, and a proline at each position. The black solid line represents coupling constant for the wild-type 22Å interaction.

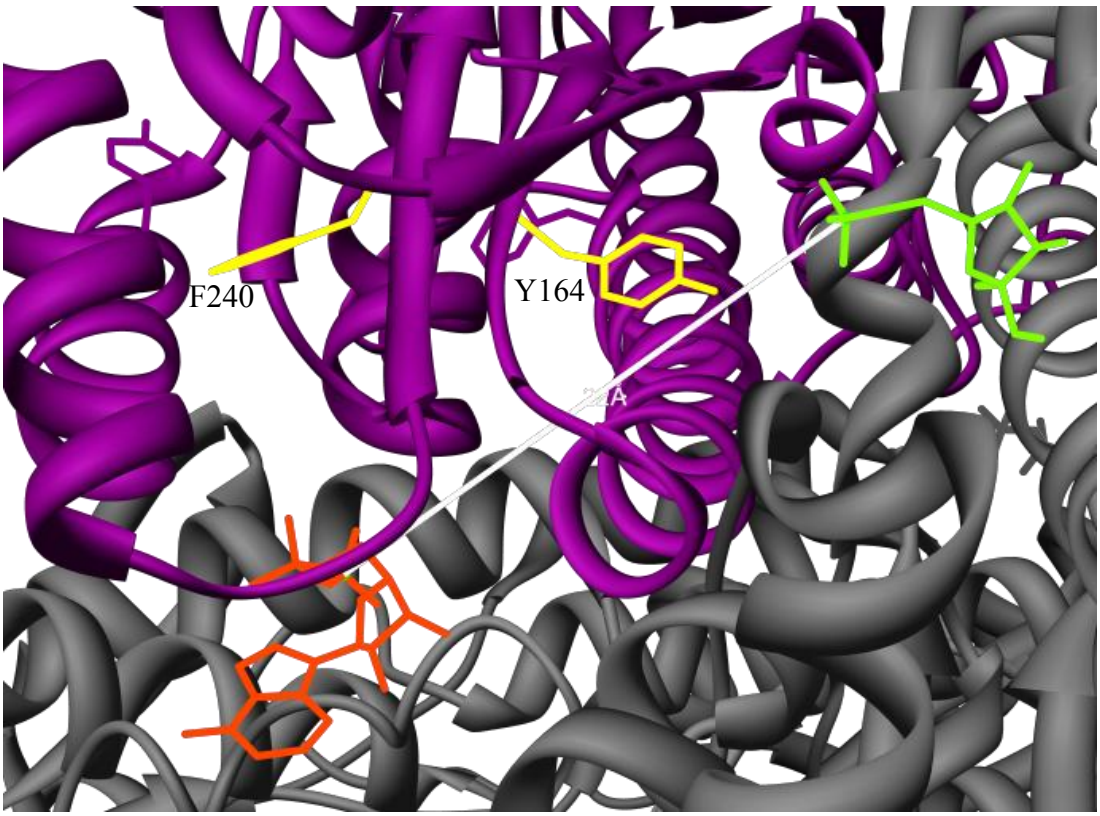

Figure 4-9 Position of Y164 and F240 with Respect to the 22Å Interaction. Residue 164 is 6Å away from F6P shown in lime green and 16Å away from PEP shown in red. Residue F240 is 18Å away from F6P and 16Å from PEP.

Therefore, the four protein species should have the ability to interconvert between various configurational states (*65*). The next step would be to further characterize these two residues and further probe the surrounding area to measure the degree of flexibility of the side chain in terms amplitude and discriminating the global motion of the protein from the local motion of the fluorophore with dynamic anisotropy measurements.

CHAPTER V

SUMMARY

The oligomeric form and multiple binding sites of PFK result in an intricate network of allosteric communication. However, we can take advantage of the fact that the four subunits are identical, the four active sites are identical, the four allosteric sites are identical, and each subunit contains half a binding site that is only rendered fully functional when the enzyme is in its tetramer form. And since considering all four enzyme species is critical to understanding the allosteric behavior of the enzyme, the hybrid strategy allows for all forms to be examined since the allosteric inhibition of the single interactions are not as strongly inhibited as in the wild-type form of the enzyme. Using these characteristics, two hybrid strategies have been developed for BsPFK and EcPFK. Van't Hoff analysis for both enzyme forms has concluded that the allosteric communication for BsPFK is entropy-dominated however for EcPFK is enthalpy-dominated. Previously for both species, the hybrid strategy has been implemented to measure the individual contribution for each of the single heterotropic interactions to the overall inhibition of the enzyme (*39, 42*). For each of the enzymes, the distribution pattern from each of the single heterotropic interactions differs implying that these two species possess alternate pathways for transmitting the inhibitory signal.

The next step is to outline these two pathways by finding regions or residues that play a role in the transmission of the inhibitory signal. Multiple sequence alignment of various PFKs and their structural comparisons have led to the characterization of residues G184, T158, and D59 as described in Chapter III. G184 may have a role in the

allosteric regulation for both EcPFK and BsPFK in the 22Å interaction in terms of inhibition, and the 30Å interaction in terms of activation for *E. coli* PFK. D59 is a residue that has important implications in various PFK species like *Thermus thermophilus* PFK, which does not possess as strong a coupling similar to BsPFK and EcPFK. For TtPFK, the residue at position 59 upon mutation to an aspartate, a strong enhancement in allosteric coupling is observed. Also, D59 in EcPFK dramatically decreases the allosteric coupling in the 22Å interaction similar to BsPFK, however it affects the 30Å and 45Å interactions. Residue T158 has been shown to enhance coupling in *T. thermophilus* when the alanine at position 158 is reverted to a threonine. Of the three candidates for BsPFK, T158 has a strong effect on the 22Å interaction further implicating its importance in the enzyme's regulation.

To explore regions of the enzyme that could play a role in the communication of the 22Å pathway using the hybrid strategy as described in Chapter IV, eight phenylalanines and tryptophans distributed throughout a single subunit were targeted for tryptophan-shift mutants. Since configurational entropy is a part of the many components of the total entropy of the system, we can examine changes in protein dynamics upon ligand binding. With the elimination of any changes due to solvent effects, we can assume that any change due to allostery as seen with the addition of ligand(s) can be due to the changes in the dynamics between the species. We can also use equation 4-10 to differentiate between general changes of the system and the changes due to an allosteric effect. Upon this type of analysis, we were able to

distinguish two important residues that showed dynamic changes due to allostery, Y164 and F240. Using site-directed mutagenesis, their direct role in the allosteric communication of the 22Å interaction was found to be slight but suggestive. Upon examining the local environment of these two tryptophan-shift mutants, a series of residues from three subunits form a continuous chain of hydrogen bonds from one active site to an allosteric site as shown in Figure 5-1. The distance between the sites is 22Å away and is the interaction that was isolated using the hybrid strategy in Chapter IV. Initially, it seems contradictory to examine the dynamic changes between the four enzyme species to help us locate allosteric regions within the enzyme to only have it lead us to a chain of hydrogen bonds connected from one active site to an allosteric site. However, it the identity of the residues involved that is interesting. From subunit 1, residue 59 begins the chain with the backbone interacting with the allosteric ligand and its side chain interacts with R154 from subunit two.

Residue 59 plays an important role in four of the PFK species studied in the Reinhart lab. It has been shown to be important for PEP binding in both LbPFK and TtPFK when changed to the aspartate residue as in BsPFK and EcPFK. As mentioned earlier, D59 has been shown in Chapter III to be important for allosteric coupling in BsPFK, TtPFK (when changed to an aspartate N59D), and EcPFK. Residue R154 then in turn, interacts with T158 when no ligands bound. However, in the presence of ADP and F6P, residue H215 forms a hydrogen bond with T158. The histidine at position 215

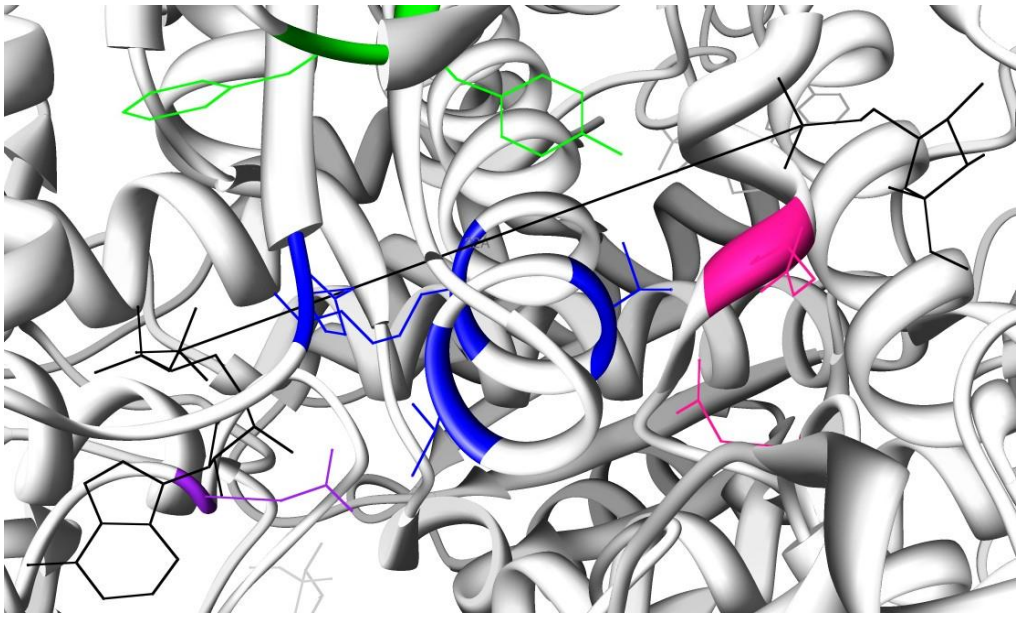

Figure 5-1 Residues that Draw a Direct Pathway from Active Site to Allosteric Site in BsPFK. As shown in a black is the 22Å difference between F6P and ADP also shown in black. Residues from right to left include D59 from the first subunit shown in purple. From a second subunit include H215, T158, and T156 as shown in blue. The third subunit includes R252 and D12 as highlighted in pink.

has previously been shown to be necessary for enhancement of coupling in TtPFK to the same extent of the coupling exhibited in BsPFK by combining it with the alterations at position 59 and 158 of the TtPFK enzyme form (*54*).

As a reminder, T158 has been shown to be necessary for TtPFK to reach an allosteric coupling comparable to the level of BsPFK with the reverse mutation A158T introduced in the tetrameric form of TtPFK. T158 is also important for allosteric coupling as previously shown in Chapter III with T158A in BsPFK.

When the inhibitor is present, H215 now interacts with 100% PFK conserved residue T156 and due to T158 undergoing a large displacement with the unwinding of its helix it now interacts with 100% conserved D12 from the third subunit (*55*). Residue 252 also from the third subunit has been shown to be important for substrate binding and interacts with F6P (*38, 39*). In summary, every residue in this hydrogen chain has previously been characterized in BsPFK and shown to be important for the overall communication pathways for BsPFK except residue 154. Thus the tryptophan side chain of both trp-shift mutants F240 and Y164 may be sensitive to this network that includes the residues suggested to be important for allostery. Extreme changes in dynamics directly in this region using new tryptophan-shift mutations should be seen if this were to be confirmed. It is still not understood the involvement of G184 in this pathway, thus more experiments are needed to define its involvement.

Overall the utilization of the hybrid strategy has enabled the initial identification of potential residues needed for the transmission of an inhibitory signal using 28 possible routes of communication within phosphofructokinase from Bacillus stearothermophilus.

The linked-function approach gives us an initial screening process for residues that interrupt this network of communication that allows the enzyme to compensate for the simultaneous binding of two ligands. The hybrid forms of the enzyme can then be used to quantify the extent of this disruption on a single heterotropic interaction. In a combination of using the hybrid strategy with site-directed mutagenesis and tryptophan-shift mutations, specific residues within the subunit can now be characterized for the extent of their respective involvement in the communication of an isolated interaction. In regard to the 22Å unique interaction, three residues have been identified in the participation of the exclusive inhibitory communication between the active site and allosteric site that makeup the pathway. Unlike EcPFK, these residues do not affect the communication of the other three unique heterotropic pathways for BsPFK. This gives an insight to the degree of independence for the main contributor in the regulation of BsPFK. Overall, the mapping of these residues suggests a distinct entropy-driven pathway for BsPFK when compared to the other species of phosphofructokinase. These findings are also contradictory to previous models proposed for the enzyme phosphofructokinase. These findings hope to inspire establishing a new model to better characterize the behavioral properties of this regulation.

REFERENCES

1. Monod, J., Wyman, J., and Changeux, J. P. (1965) On the nature of allosteric transition: a plausible model, *Journal of Molecular Biology 12*, 88-118.

2. Koshland, D. E., Nemethy, G., and Filmer, D. (1966) Comparison of experimental binding data and theoretical models in proteins containing subunits, *Biochemistry 5*, 365-385.

3. Grant, G. A., Xiao Lan, X., and Zhiqin, H. (2004) Quantitative Relationships of Site to site Interaction in *Escherichia coli* D-3-Phosphoglycerate Dehydrogenase Revealed by Asymmetric Hybrid Tetramers, *The Journal of Biological Chemistry 279*, 13452-13460.

4. Grant, G. A. (2011) Transient Kinetic Analysis of L-Serine Interaction with *Escherichia coli* D-3-Phosphoglycerate Dehydrogenase Containing Amino Acid Mutations in the Hinge Regions, *Biochemistry 50*, 2900-2906.

5. Lazdunski, M. (1972) Flip flop mechanisms and half-site enzymes, *Current Topics in Cellular Regulation 6*, 267-310.

6. Iwata, S., Kamata, K., Yoshida, S., Monow, T., and Ohta, T. (1994) T and R states in the crystals of bacterial L-lactate dehydrogenase reveal the mechanism for allosteric control, *Nature Structural & Molecular Biology 1(3)*, 176-185.

7. Fushinobu, S., Kamata, K., Iwata, S., Sakai, H., Ohta, T., and Matsuzawa, H. (1996) Allosteric Activation of L-Lactate Dehydrogenase Anaylyzed by Hybrid Enzymes with Effector-sensitive and -insensitive Subunits, *The Journal of Biological Chemistry 271*, 25611-25616.

8. Ackers, G. K., Doyle, M. L., Myers, D., and Daugherty, M. A. (1992) Molecular code of cooperativity in hemoglobin, *Science 255*, 54-63.

9. Huang, Y., Doyle, M. L., and Ackers, G. K. (1996) The Oxygen-Binding Intermediates of Human Hemoglobin: Evaluation of Their Contributions to Cooperativity Using Zinc-Containing Hybrids, *Biophysical Journal. 71*, 2094-2105.

10. Ackers, G. K., Holt, J. M., Huang, Y., Grinkova, Y., Klinger, A. L., and Denisov, I. (2000) Confirmation of a unique intra-dimer cooperativity in the human hemoglobin α1β1 half-oxygenated intermediate supports the symmetry rule model of allosteric regulation, *Proteins: Structure, Function, and Genetics 41*, 23-43.

11. Yonetani, T., Park, S., Tsuneshige, A., Imai, K., and Kanaori, K. (2002) Global allostery model of hemoglobin - Modulation of O-2 affinity, cooperativity, and Bohr effect by heterotropic allosteric effectors, *Journal of Biological Chemistry 277*, 34508-34520.

12. Ackers, G. K., Dalessio, P. M., Lew, G. H., Daugherty, M. A., and Holt, J. M. (2002) Single residue modification of only one dimer within the hemoglobin tetramer reveals autonomous dimer function, *Proceedings of the National Academy of Sciences 99*, 9777-9782.

13. Ackers, G. K., and Holt, J. M. (2006) Asymmetric Cooperativity in a Symmetric Tetramer: Human Hemoglobin, *Journal of Biological Chemistry 281*, 11441-11443.

14. Scott W. Nelson, Richard B. Honzatko, and Herbert J. Fromm. (2002) Hybrid Tetramers of Porcine Liver Fructose-1,6-bisphoshphatase Reveal Multiple Pathways of Allosteric Inhibition, *Journal of Biological Chemistry 277*, 15539-15545.

15. Hensley, P., and Schachman, H. K. (1979) Communication between dissimilar subunits in aspartate transcarbamoylase: Effect of inhibitor and activator on the conformation of the catalytic polypeptide chains, *Proceedings of the National Academy of Sciences 76*, 3732-3736.

16. Johnson, R. S., and Schachman, H. K. (1980) Propagation of conformational changes in Ni(II)-substituted aspartate transcarbamoylase: Effect of active-site ligands on the regulatory chains, *Proceedings of the National Academy of Sciences 77*, 1995-1999.

17. Yang, Y. R., and Schachman, H. K. (1980) Communication between catalytic subunits in hybrid aspartate transcarbamoylase molecules: Effect of ligand binding to active chains on the conformation of unliganded, inactive chains, *Proceedings of the National Academy of Sciences 77*, 5187-5191.

18. Lahue, R. S., and Schachman, H. K. (1986) Communication between polypeptide chains in aspartate transcarbamoylase, *Journal of Biological Chemistry 261*, 3079-3084.

19. Eisenstein, E., Han, M. S., Woo, T. S., Ritchey, J. M., Gibbons, I., Yang, Y. R., and Schachman, H. K. (1992) Negative complementation in aspartate transcarbamylase *Journal of BiologicalChemistry 267*, 22148-22155.

20. Sakash, J. B., and Kantrowitz, E. R. (2000) The contribution of individual interchain interactions to the stabilization of the T and R states of *Escherichia coli* aspartate transcarbamoylase, *Journal of Biological Chemistry 275*, 28701-28707.

21. Schirmer, T., and Evans, P. R. (1990) Structural basis of the allosteric behaviour of phosphofructokinase, *Nature 343*, 140-145.

22. Johnson, J. L., and Reinhart, G. D. (1992) MgATP and fructose-6-phosphate interactions with phosphofructokinase from *Escherichia coli*, *Biochemistry 31*, 11510-11518.

23. Johnson, J. L., and Reinhart, G. D. (1994a) Influence of MgADP on phosphofructokinase from *Escherichia coli*. Elucidation of coupling interactions with both substrates, *Biochemistry 33*, 2635-2643.

24. Johnson, J. L., and Reinhart, G. D. (1997) Failure of a two-state model to describe the influence of phosphoenolpyruvate of phosphofructokinase from *Escherichia coli*, *Biochemistry 36*, 12814-12822.

25. Kimmel, J. L., and Reinhart, G. D. (2000) Reevaluation of the accepted allosteric mechanism of phosphofructokinase from *Bacillus stearothermophilus*, *Proceedings of the National Academy of Sciences 97*, 3844-3849.

26. Tlapak-Simmons, V. L., and Reinhart, G. D. (1994) Comparison of the inhibition by phosphoenolpyruvate and phosphoglycolate of phosphofructokinase from *B. stearothermophilus*, *Archives of Biochemistry Biophysics 308*, 226-230.

27. Tlapak-Simmons, V. L., and Reinhart, G. D. (1998) Obfuscation of allosteric structure-function relationships by enthalpy-entropy compensation, *Biophyical Journal 75*, 1010-1015.

28. Riley-Lovinshimer, M. R., and Reinhart, G. D. (2001) Equilibrium Binding Studies of a Tryptophan-Shifted Mutant of Phosphofructokinase from *Bacillus stearothermophilus*, *Biochemistry 40*, 3002-3008.

29. Johnson, J. L., and Reinhart, G. D. (1994) Influence of substrates and MgADP on the time-resolved intrinsic fluorescence of phosphofructokinase from *Escherichia coli*. Correlation of tryptophan dynamics to coupling entropy, *Biochemistry 33*, 2644-2650.

30. Auzat, I., Le Bras, G., and Garel, J.-R. (1994) The cooperativity and allosteric inhibition of *Escherichia coli* phosphofructokinase depend on the interaction between threonine-125 and ATP, *Proceedings of the National Academy of Science 91*, 5242-5246.

31. Weber, G. (1972) Ligand binding and internal equilibrium in proteins, *Biochemistry 11*, 864-878.

32. Weber, G. (1975) Energetics of ligand binding to proteins, *Advances in Protein Chemistry 29*, 1-83.

33. Wyman, J. (1964) Linked functions and reciprocal effects in hemoglobin: a second look, *Advances in Protein Chemistry. 19*, 223-286.

34. Wyman, J. (1967) Allosteric linkage, *Journal of the American Chemical Society 89*, 2202-2218.

35. Reinhart, G. D. (1983) The Determination of Thermodynamic Allosteric Parameters of an Enzyme Undergoing Steady-State Turnover, *Archives of Biochemistry and Biophysics 224*, 389-401.

36. Reinhart, G. D. (1985) Influence of pH of the regulatory kinetics of rat liver phosphofructokinase: a thermodynamic linked-function analysis, *Biochemistry 24*, 7166-7172.

37. Reinhart, G. D., and Hartleip, S. B. (1986) Relationship between fructose 2,6-bisphosphate activation and magnesium ATP inhibition of rat liver phosphofructokinase at high pH. Kinetic evidence for individual binding sites linked by finite couplings, *Biochemistry 25*, 7308-7313.

38. Kimmel, J. L., and Reinhart, G. D. (2000) Isolation of an Individual Allosteric Interaction in Tetrameric Phosphofructokinase from *Bacillus stearothermophilus Proceedings of the National Academy of Science 97*, 3844-3849.

39. Ortigosa, A. D., Kimmel, J. L., and Reinhart, G. D. (2004) Disentangling the Web of Allosteric Communication in a Homotetramer: Heterotropic Inhibtion of Phosphofructokinase from *Bacillus stearothermophilus*, *Biochemistry 43*, 577-586.

40. Fenton, A. W., and Reinhart, G. D. (2004) Disentangling the Web of Allosteric Communication in a Homotetramer: Heterotropic Activation in Phosphofructokinase from *Escherichia coli*, *Biochemistry 43*, 14104-14110.

41. Fenton, A. W., and Reinhart, G. D. (2002) Isolation of a Single Activating Allosteric Interaction in Phosphofructokinase from *Escherichia coli, Biochemistry 41*, 13410-13416.

42. Fenton, A. W., and Reinhart, G. D. (2009) Disentangling the Web of Allosteric Communication in a Homotetramer: Heterotropic Inhibition in Phosphofructokinase from *Escherichia coli, Biochemistry 48,* 12323-12328.

43. French, B. A., Valdez, B. C., Younathan, E. S., and Chang, S. H. (1987) High-level expression of *Bacillus stearothermophilus* 6-phosphofructo-1-kinase in *Escherichia coli, Gene 59*, 279-283.

44. Lovingshimer, M. R., Siegele, D., and Reinhart, G. D. (2006) Construction of an inducible, pfkA and pfkB deficient strain of *Escherichia coli* for the expression and purification of phosphofructokinase from bacterial sources, *Protein Expression and Purification. 46*, 475-482.

45. Valdez, B. C., French, B. A., Younathan, E. S., and Chang, S. H. (1989) Site directed mutagenesis in Bacillus stearothermophilus fructose-6-phosphate 1-

kinase. Mutation at the substrate-binding site affects allosteric behavior, *Journal of Biological Chemistry 264*, 131-135.

46. Babul, J. (1978) Phosphofructokinase from *Escherichia coli*. Purification and characterization of the nonallosteric isozyme, *Journal of Biological Chemistry 253*, 4350-4355.

47. Kolartz, D., and Buc, H. (1982) Phosphofructokinase from *Escherichia coli, Methods in Enzymology 90*, 60-70.

48. Le Bras, G., Auzat, I., and Garel, J.-R. (1995) Tetramer-dimer equilibrium of phosphofructokinase and formation of hybrid tetramers, *Biochemistry 34*, 13203-13210.

49. Deville-Bonne, D., Le Bras, G., Teschner, W., and Garel, J.-R. (1989) Ordered disruption of subunit interfaces during stepwise reversible dissociation of *Escherichia coli* phosphofructokinase with KSCN, *Biochemistry 28*, 1917-1922.

50. Hill, A. V. (1910) A new mathematical treatment of changes of ionic concentration in muscle and nerve under the action of electric currents, with a theory as to their mode of excitation, *Journal of Physiology 40*, 190-224.

51. Reinhart, G. D. (1988) Linked-function origins of cooperativity in a symmetrical dimer, *Biophysical Chemistry. 30*, 159-172.

52. Paricharttanakul, N. M. (2004) Pathway to Allostery: Differential Routes for Allosteric Communication in Phosphofructokinase from Escherichia coli, Dissertation, Texas A&M University, College Station, TX.

53. Tie, C. (2008) Kinetics and Dynamics Study On the Allosteric Pathway of Phosphofructokinase from *Escherichia coli*, Dissertation, Texas A&M University, College Station, TX.

54. Shubina-McGresham, M. (2012) Characterization of the Allosteric Properties of *Thermus thermophilus* Phosphofructokinase and the Sources of Strong Inhibition Binding Affinity and Weak Inhibitory Response, Dissertation, Texas A&M University, College Station, TX.

55. Mosser, R. E. (2010) A Structural and Kinetic Study into the Role of the Quaternary Shift in *Bacillus Stearothermophilus* Phosphofructokinase, Dissertation, Texas A&M University, College Station, TX.

56. Lovingshimer, M. R., and Reinhart, G. D. (2001) Equilibrium Binding Studies of a Tryptohpan-Shifted Mutant of Phosphofructokinase from *Bacillus stearothermophilus*, *Biochemistry 40*, 3002-3008.

57. Lovingshimer, M. R., and Reinhart, G. D. (2002) Reverisible ligand induced dissociation shift of a tryptophan-shift mutant of phosphofructokinase from *Bacillus stearothermophilus*, *Biochemistry 41*, 12967-12974.

58. Lovingshimer, M. R., and Reinhart, G. D. (2005) Examination of MgATP binding in a tryptophan-shift mutant of phosphofructokinase from *Bacillus stearothermophilus Archives of Biochemistry and Biophysics 436*, 178-186.

59. Perrin, F. (1926) Polarization of light of fluorescence, average life of molecules in the excited state, *Journal de Phyique et Le Radium 7*, 390-401.

60. Gratton, E., DM, J., and Hall, R. (1984) Multifrequency phase and modulation fluorometry, *Annual Review of Biophysics and Bioengineering. 13*, 105-124.

61. Alcala, J., Gratton, E., and Prendergast, F. (1987) Resolvability of fluorescence lifetime distributions using phase and fluorometry *Biophysical Journal 51*, 587-596.

62. Alcala, J., Gratton, E., and Prendergast, F. (1987) Fluorescence lifetime distributions in proteins, *Biophysical Journal 51*, 597-604.

63. Alcala, J., Gratton, E., and Prendergast, F. (1987) Interpretation of Fluorescence decays in proteins using continuous lifetime distributions *Biophysical Journal 51*, 925-936.

64. Reinhart, G. D. (2004) Quantitative Analysis and Interpretation of Allosteric Behavior, *Methods in Enzymology 380*, 187-203.

65. Reinhart, G. D., Hartleip, S. B., and Symcox, M. (1989) Role of coupling entropy in establishing the nature and magnitude of allosteric response, *Proceedings in the National Academy of Sciences 86*, 4032-4036.

66. Cooper, A., and Dryden, D. T. F. (1984) Allostery without conformational change. A plausible model, *European Biophysics Journal 11*, 103-109.